November 2018

MODELING THE ABUNDANCE AND DISTRIBUTION OF TERRESTRIAL PLANTS THROUGH SPACE AND TIME

Caroline Curtis

MODELING THE ABUNDANCE AND DISTRIBUTION OF TERRESTRIAL PLANTS THROUGH SPACE AND TIME

A Dissertation Presented

by

CAROLINE A. CURTIS

Submitted to the Graduate School of the
University of Massachusetts Amherst in partial fulfillment
of the requirements for the degree of

DOCTOR OF PHILOSOPHY

September 2018

Graduate Program in Organismic and Evolutionary Biology

MODELING THE ABUNDANCE AND DISTRIBUTION OF TERRESTRIAL PLANTS THROUGH SPACE AND TIME

A Dissertation Presented

by

CAROLINE A. CURTIS

Approved as to style and content by:

_____
Bethany A. Bradley, Chair

_____
Jesse Bellemare, Member

_____
John T. Finn, Member

_____
Kristina A. Stinson, Member

_____
Paige S. Warren, Graduate Program Director
Organismic and Evolutionary Biology

_____
Patricia Wadsworth, Director
Interdepartmental Graduate Programs

ACKNOWLEDGMENTS

This research was made possible through the support of my advisor, committee members, peers, family and friends, and funding sources.

I am grateful to my advisor, Bethany Bradley who granted me creative freedom to follow my interests, then helped to refine my ideas into workable scientific enquiries. I am also thankful for her enormous effort in providing feedback on countless drafts of manuscripts and presentations.

My committee members, Jesse Bellemare, Jack Finn, and Kristina Stinson provided guidance and thoughtful advice on my various projects. More importantly, they reminded me to think outside the realm of each project and envision a broader impact for my research.

I am thankful to the OEB community and the Bradley lab members for their support and feedback throughout my time here.

Finally, I acknowledge the important role of my family and friends in supporting me in many ways as I worked toward completing this degree.

ABSTRACT

MODELING THE ABUNDANCE AND DISTRIBUTIONS OF TERRESTRIAL PLANTS THROUGH SPACE AND TIME

SEPTEMBER 2018

CAROLINE A. CURTIS, B.S., BRIDGEWATER STATE UNIVERSITY

M.S., FORT HAYS STATE UNIVERSITY

Ph.D., UNIVERSITY OF MASSACHUSETTS AMHERST

Directed by: Professor Bethany A. Bradley

The question of why species live where they do is a fundamental concept in ecology. If we can determine how biotic and abiotic factors control patterns of species presence and abundance, we can better manage populations facing threats. Anthropogenically-driven changes such as climate- and land-use change threaten ecosystems and species over regional to global scales. Therefore, there is a need to understand how species ranges will respond to these changes over large spatial and temporal extents. The need to quantify responses is even more pressing in the context of invasive species, which have the potential to exacerbate the negative processes affecting native ecosystems. I sought to address several questions related to species distributions and gain a better understanding of what determines where a species occurs.

Models of species presence are useful for identifying the spatial extent of climatically suitable habitat. However, presence-based models cannot be used to draw inferences about the abundance of the species and, therefore, cannot inform impact risk. I modeled presence and abundance of two widespread invasive plants (red brome (*Bromus rubens*) and African mustard (*Brassica tournefortii*)) in the southwest U.S.

under current and projected future climatic conditions. Suitability for *B. rubens* presence and high abundance are projected to expand by up to 65% and 64%, respectively, whereas suitability for *B. tournefortii* presence and high abundance expand by up to 29% and 28%, respectively. These results highlight the possibility of increased invasion pressure in the future.

Many tools have been developed for addressing questions associated with patterns of species occurrences. Among them are species distribution models (SDMs) which relate spatial or temporal occurrence data with environmental factors thought to determine a species' location. Large, pre-existing data sets are commonly used in SDMs, although it is often assumed that expert-based climatic tolerance data will better reflect a species' physiological constraints. This assumption had only been tested for few species and at local scales. To gain a general understanding of how well different data sets capture species climate niches, I compared climatic ranges derived from herbarium data to those from expert-based data for over 1,800 terrestrial plant species. Our results show that distribution records from herbaria provide more robust estimates of climatic tolerance, especially for widespread forbs and grasses.

Models of percent cover present a unique opportunity to make better informed management decisions and improve conservation prioritization. Big sagebrush (*Artemisia tridentata)* characterizes shrublands of the intermountain western U.S. and provides habitat for many obligate species. However, sagebrush is threatened by several forms of global change, including invasive species, land cover change, and climate change. Previous models of sagebrush focused on presence-only models which do not allow for inference about habitat quality. Therefore, we leveraged unique spatial percent

cover datasets to model potential sagebrush cover under current and future climate in the western U.S. We then used potential sagebrush cover to estimate habitat for five sagebrush-obligate species. Our results suggest that the potential future distributions of sagebrush obligate species will vary markedly. The pygmy rabbit (*Brachylagus idahoensis*), which has the highest percent sagebrush requirements, is projected to lose up to 91% of currently suitable habitat. In contrast, the Brewer's sparrow (*Spizella breweri*), which has the lowest sagebrush percent cover requirements, is projected to gain up to 26% of additional sagebrush habitat. These results identify regions most likely to support sagebrush and sagebrush obligate species in the context of climate change and can, therefore be used to quantify risks to species populations within their ranges.

Throughout the southern hemisphere, *Pinus* species are used in large plantations and, in many cases, have spread into the surrounding landscape and established invasive populations. In remote areas of southern Chile, the extent of plantations and invasion is unknown, although the threat of non-native populations is well documented. To address questions about the spatial extent and configuration of non-native pines in this region, we classified a Landsat image using coefficients from a time series model and used that classified image to quantify landscape patterns. Most invasive pine patches occur at low slopes and mid-range elevation, share boundaries with native forest patches, and occur within 500 m of other pine patches. These results suggest that: 1) areas with high relief and high or low elevation might be less prone to invasion; 2) invasion risk might be lower than assumed given the prevalence of invasion-resistant native forest; and 3) the landscape should be monitored for new invasion sites stemming from isolated pine patches.

My research spans study systems and geographic locations but addresses the central theme of defining the factors that control species distribution and abundance. My findings highlight the significance of modeling percent cover for quantifying impact risk or habitat suitability, the importance of understanding how model parameterization influences results, and the extension of using model results to understand landscape-scale patterns and processes.

TABLE OF CONTENTS

LIST OF TABLES

LIST OF FIGURES

CHAPTER 1

CLIMATE CHANGE MAY ALTER BOTH ESTABLISHMENT AND HIGH ABUNDANCE OF RED BROME AND AFRICAN MUSTARD IN THE SEMIARID SOUTHWEST UNITED STATES

Authors

Caroline A. Curtis[1] and Bethany A. Bradley[2]

Abstract

Nonnative, invasive plants are becoming increasingly widespread and abundant throughout the southwestern United States, leading to altered fire regimes and negative effects on native plant communities. Models of potential invasion are pertinent tools for informing regional management. However, most modeling studies have relied on occurrence data, which predict the potential for nonnative establishment only and can overestimate potential risk. We compiled locations of presence and high abundance for two problematic, invasive plants across the southwestern United States: red brome (*Bromus rubens*) and African mustard (*Brassica tournefortii*). Using an ensemble of five climate projections and two types of distribution model (MaxEnt and Bioclim), we modeled current and future climatic suitability for establishment of both species. We also used point locations of abundant infestations to model current and future climatic suitability for abundance (i.e., impact niche) of both species. Because interpretations of future ensemble models depend on the threshold used to delineate climatically suitable

[1]Graduate Program in Organismic and Evolutionary Biology, University of Massachusetts Amherst, Amherst, Massachusetts 01003
[2]Department of Environmental Conservation, University of Massachusetts Amherst, Amherst, Massachusetts 01003

from unsuitable areas, we applied a low threshold (1 model of 10) and a high threshold (6 or more models of 10). Using the more-conservative high threshold, suitability for *B. rubens* presence expands by 12%, but high abundance contracts by 42%, whereas suitability for *B. tournefortii* presence and high abundance contract by 34% and 56%, respectively. Based on the low threshold (worst-case scenario), suitability for *B. rubens* presence and high abundance are projected to expand by 65% and 64%, respectively, whereas suitability for *B. tournefortii* presence and high abundance expand by 29% and 28%, respectively. The difference between results obtained from the high and low thresholds is indicative of the variability in climate models for this region but can serve as indicators of best- and worst-case scenarios.

Management Implications

In the arid and semiarid regions of the southwestern United States, two nonnative, invasive plant species, red brome (*Bromus rubens*) and African mustard (*Brassica tournefortii*) occur at varying levels of abundance. Within the study region (i.e., the area from which presence and high abundance data were collected), bioclimate envelope models (BEMs) indicate current widespread climatic suitability for the presence of both species. However, central and northwest Arizona, southern Nevada, and Baja California, Mexico, are currently most climatically suitable for high abundance of *B. rubens*. Hot, dry regions of southern California are currently most climatically suitable for high abundance of *B. tournefortii*. Based on a high threshold (6 or more of 10 models project suitability), climatic suitability is projected to increase only for *B. rubens* presence (+12%), whereas climatic suitability for *B. tournefortii* presence could decrease (-34%). Similarly, climatic suitability for high abundance of *B. rubens* (-42%) and *B. tournefortii*

(-56%) could also decrease. For *B. tournefortii*, areas of contraction (i.e., projected loss of climatic suitability) appear in southern Arizona and California, and in Baja California and Sonora, Mexico. For high abundance of *B. rubens*, contraction is projected to occur along the southern edges of climatically suitable area, primarily in Arizona and Nevada. Climatic suitability for *B. tournefortii* is projected to contract mainly in western Nevada, southeastern California, and Baja California, Mexico. Based on an ensemble of future models and a low threshold (any 1 of 10 models projects suitability), climatic suitability for the presence of *B. rubens* and *B. tournefortii* could increase by up to 65% and 29%, respectively, by 2050. Climatic suitability for high abundance of *B. rubens* could expand northward into Nevada and Utah by up to 64%, indicating that these areas might be at an elevated risk for impact from this species in the future. Area suitable for *B. tournefortii* high abundance could expand by up to 28% by 2050 with slight increases in suitable area projected in southern Nevada, California, and Arizona. Efforts to minimize the impact of *B. rubens* and *B. tournefortii* would be more effective if focused on the areas identified as suitable for high abundance (rather than suitable for presence only) and likely to maintain or expand climatic habitat according to multiple projections.

Introduction

The spread of nonnative, invasive plants can alter landscapes and degrade native ecosystem function (Mack et al. 2000). An invasive plant colonizes or is introduced to a novel location, establishes a self-sustaining population, and spreads into surrounding, uncolonized ecosystems (Lockwood et al. 2013; Richardson et al. 2000). Invasive plants can decrease species richness of native plants and animals (Vitousek et al. 1996), alter nutrient availability (Ehrenfeld 2003), and contribute to changes in disturbance regimes

(Brooks et al. 2004). The recent, unprecedented increases in global temperature and changes in precipitation regimes predicted to occur during this century (Stocker et al. 2013) are likely to create novel environmental conditions and may increase opportunities for invasion by nonnative plant species (Bradley et al. 2010; Dukes and Mooney 1999). Spatially explicit invasion risk assessments (Peters and Lodge 2013; Rouget et al. 2002) could improve management by targeting high-risk areas for monitoring and control.

The greatest potential damage to an ecosystem occurs not only where a nonnative species can establish but also where it can spread and become abundant (Parker et al. 1999). Populations of species occur at varying levels of abundance across landscapes, influenced by biotic and abiotic conditions (Brown 1995). Areas where invasive plants reach high abundance have the greatest probability of detrimental ecosystem effects (Brooks et al. 2004; Parker et al. 1999). For example, in the arid and semiarid ecosystems that characterize the southwestern United States, isolated occurrences of invasive annual grasses, such as red brome (*Bromus rubens*), are unlikely to cause significant damage. However, high abundance of these plants can reduce native plant biomass (Brooks 2000) and increase fire frequency (Balch et al. 2013) because of continuous cover of fine fuels (Brooks 1999; D'Antonio and Vitousek 1992). Forecasting invasive plant abundance will increase our ability to manage regional invasions in a changing climate by identifying emerging areas of high risk for monitoring and control.

Bioclimatic envelope models (BEMs) have become an increasingly common tool for quantifying the relationship between occurrences of a species and regional-scale climate conditions. BEMs are used to estimate the geographic range of climatic

suitability and to understand how that range might shift as climate changes. However, although abundance is arguably more important for prioritizing management, most BEM studies have modeled suitability for invasive plant presence only because of the scarcity of abundance information across broad regions (see for examples Bradley 2013). Unfortunately, models based on invasive plant presence vastly overestimate potential abundance and associated impact (Bradley 2013).

Previous studies have argued that modeling the "impact niche" (Leibold 1995) or "damage niche" (McDonald et al. 2009) associated with locations of high abundance gives more realistic information about environmental effects than does modeling occurrences alone. For example, McDonald et al. (2009) used surveys of weed experts to identify states where cropping systems were highly affected by velvetleaf (*Abutilon theophrasti*) or johnsongrass (*Sorghum halepense)* and modeled the impact niche under current and future climate, based on these high-impact locations. Similarly, Bradley (2013) used surveys of invasive plant managers to identify locations with high invasive plant abundance to model the impact niche. In the absence of regional, continuous cover data (which are exceedingly rare for any species), point locations of high abundance can be used to model climatic conditions that describe the impact niche (Bradley 2013; Estes et al. 2013; McDonald et al. 2009), a subset of the total potential range.

Here, we used BEMs to project the current and potential future distributions of two of the most common and problematic, invasive species in the southwestern United States: *B. rubens* and African mustard (*Brassica tournefortii*). *Bromus rubens* is an invasive, annual grass, native to southern Europe, which was first recorded in the United States in the 1880s (Salo 2005). High abundance of *B. rubens* is most likely to occur

following average or above-average winter rainfall (Brooks 2000). When growing in high abundance, *B. rubens* is able to dominate available water and nitrogen (Brooks 2000) and reduce native plant biomass (Brooks 2000; Salo 2005).

Brassica tournefortii is an annual forb, native to the semiarid and arid regions of northern Africa and to the Mediterranean regions of southern Europe, and was first collected in the United States in 1927 (Minnich and Sanders 2000). *Brassica tournefortii* produces prolific seeds that germinate when conditions are favorable (Bangle et al. 2008). Following periods of high precipitation, *B. tournefortii* populations reach higher abundances than they do in years with low or average precipitation (Minnich and Sanders 2000). *B. tournefortii* seeds germinate earlier than seeds of native species, and plants can grow and monopolize resources before native species emerge (Minnich and Sanders 2000).

Invasion of both *B. rubens* and *B. tournefortii* is a concern because of alteration to regional fire cycles. Historically, large-scale fires in the desert regions of the southwestern United States were infrequent because of the scarcity of fine fuels and the patchy native vegetation cover (Brooks and Pyke 2001). The addition of nonnative annuals increases aboveground biomass and the continuity of fine fuels among native plants (Brooks 1999). Invasions of alien species that produce prolific biomass lead to a "grass–fire cycle" that has been identified in many ecosystems globally (Brooks et al. 2004; D'Antonio and Vitousek 1992). In areas in which they reach high abundances, *B. rubens* and *B. tournefortii* have the potential to increase fire frequency.

BEMs based on all locations of species presence and BEMs based on the subset of high abundance points were created to separately model suitability for presence and

suitability for high abundance. We applied the two BEMs to future climate-change scenarios based on five climate models to test how invasive species presence and high abundance are projected to change by 2050. Relative to current climate, we also identified locations of expanded risk (climatic suitability) of presence and high abundance.

Materials and Methods

Presence and High Abundance Data

Presence data for *B. rubens* and *B. tournefortii* were compiled from regional data sets (CalFlora; http://www.calflora.org/ and Cal-IPC http://www.cal-ipc.org/), surveys by managers with the Bureau of Land Management and the Mojave Desert Network Parks, records from local and regional biologists, and herbaria. These existing datasets were supplemented with two field surveys focused on roadsides only in southern Nevada, southern California, and Arizona (Appendix A). For both species, some abundance data were available from land managers and herbarium records as values of percent cover and from field surveys as qualitative descriptions of relative abundance at each site. Abundance data tended to be collected within more-restricted areas where each species is problematic and, therefore, are likely representative of climatic conditions in heavily invaded landscapes.

We transformed these data into two groups for each species: presence and high abundance. We classified locations as high abundance if the species had at least 10% cover, if the area was described qualitatively as having continuous ground cover (categorical rank data), or if the target species was observed in abundance (percent cover or rank data) beyond the road corridor. We included all available presence data,

including points with high abundance, in the presence data sets. Records for both species were restricted to the southwestern United States (i.e., the region from which *B. rubens* and *B. tournefortii* are problematic invaders). Therefore, we limited the extents of our study regions using a convex hull around the presence locations of each species. Absence data comparable in extent to the presence/high-abundance data were not available for either species. To remove duplicate entries and reduce sampling bias, we resampled each of the four data sets to include only one point per 2.5 arcmin climate-grid cell (see below). If more than one point within a grid cell had abundance data, we assumed that the grid cell was climatically suitable for the highest level of abundance, and the maximum abundance value was retained.

Even if comprehensively collected, invasive species distribution data might still underestimate climatic suitability because the species has not yet spread to the full range it could potentially invade (Araújo and Pearson 2005). High abundance points might further underestimate climatic suitability for abundance because species are less abundant following dry growing season conditions (Abatzoglou and Kolden 2011). Nonetheless, numerous studies have used an envelope-modeling approach to estimate potential range for invasive plants with the assumption that the distribution data reasonably approximate the climatic space in which the species could establish or become abundant (see for examples, Bradley 2013). The data compiled for this analysis extend across broad climatic gradients of the southwest region and, therefore, encompass a high proportion of available climate space, making this analysis consistent with other envelope-modeling studies. However, incomplete data could still lead to an underestimation of potential range for presence, high abundance, or both. Our results are also limited by the spatial

extent of our models. To improve model performance, we limited the models to the area enclosed by the presence locations of each species. It is possible that current or future climatic suitability could extend beyond these boundaries and allow the distributions of *B. rubens* and *B. tournefortii* to expand further than what we have shown. Therefore, these and all envelope models should be interpreted as having fairly high confidence that areas modeled at risk are indeed at risk, but lower confidence that areas modeled as not at risk are indeed not.

Climate Data

We obtained data representing global current and projected future climate from WorldClim (http://www.worldclim.org/) as interpolated climate surface layers of mean monthly temperature and precipitation at 2.5-min spatial resolution. Current climate data for the period of 1950 to 2000 are available through WordClim as interpolated layers of monthly averages of mean, minimum, and maximum monthly temperature and mean monthly precipitation (Hijmans et al. 2005).

We used future climate projections from five atmosphere–ocean general circulation models (AOGCMs) from the Fifth Intergovernmental Panel on Climate Change (IPCC) report that were downscaled using the WorldClim 1.4 current climate data as a baseline (Hijmans et al. 2005). We chose climate-model projections based on those that predicted Pacific Northwest temperature and precipitation with the lowest error (Rupp et al. 2013). We assumed that this accuracy also held for the southwest because no comparable assessment for the southwest region is currently available. We selected AOGCMs based on their performance as assessed by Rupp et al. (2013) and availability of relative concentration pathways (RCPs) in WorldClim. In the Fifth IPCC assessment

report, RCPs replace the previously used emissions scenarios (Nakicenovic and Swart 2000). We included AOGCM projections based on RCP4.5 and RCP8.5. RCP4.5 is the "medium-low" pathway in the Fifth IPCC report and is characterized by a stabilization of radiative forcing at 4.2 W m^{-2} by 2100, which corresponds to atmospheric CO2 concentrations of 650 ppmv. RCP8.5 is the "high" pathway and projects a stabilization of radiative forcing at 8.3 W m^{-2} by 2100, which corresponds to atmospheric CO2 concentrations of 900 ppmv (Stocker et al. 2013). Climate projections were based on five AOGCMs from the following modeling groups: National Center of Atmospheric Research, National Centre of Meteorological Research, Met Office Hadley Center, Atmosphere and Ocean Research Institute, National Institute for Environmental Studies, and Japan Agency for Marine-Earth Science and Technology, and Norwegian Climate Center.

We used four climate-variable predictors derived from the climate data: mean monthly temperature for the coldest (January) and warmest (July) months of the year and accumulated precipitation for two quarters (March, April, May; and June, July, August). Precipitation for the winter quarter (December, January, February) and fall quarter (September, October, November) were not included because they were highly correlated with other precipitation predictors within the study region and were the least important precipitation variables in MaxEnt models. These predictors were selected to encompass climatic conditions that likely influence both native and invasive species growth and reproduction. The timing and relative importance of climatic conditions that facilitate *B. tournefortii* growth are largely untested. *B. rubens* is thought to be limited by winter temperatures (Bykova and Sage 2012) and fall precipitation (Beatley 1966; Salo 2004).

Both species likely interact with native perennial species that respond to spring and summer (monsoonal) precipitation. By using climate data that covered the range of seasonal climate conditions in the study regions, we allow the model fit to define climate conditions that influence species distribution and high abundance.

Modeling Presence and Abundance under Current Climate Conditions

Many techniques for BEM (also referred to as species-distribution modeling, habitat-suitability modeling, or environmental-niche modeling) have been developed. BEMs are used to understand the relationship between the geographic location where species occur and the climatic conditions at those locations (Franklin 2009). A model of suitable climate can then be projected back into geographic space to identify the spatial extents of the potential for invasive plant establishment or abundance. Suitable climate conditions can also be projected spatially based on the geographic distribution of future climate associated with climate change. For *B. rubens* and *B. tournefortii*, we used two BEM methods (MaxEnt and Bioclim) to predict the current and future geographic distributions of presence and high abundance.

We used MaxEnt (Version 3.3.3k), an implementation of maximum entropy modeling (Phillips et al. 2006), to model climatic suitability for the two coverage groups: presence and high abundance. MaxEnt relies on presence-only data, but generates pseudoabsences drawn from the study area to construct probabilistic relationships between climate and species distribution. Pseudoabsence points drawn from too far afield from occurrences can lead to underestimates of climatic habitat, whereas pseudoabsences too close and not distinct from occurrences can lead to overestimates of climatic habitat (VanDerWal et al. 2009). To include climate conditions with enough

difference from occurrences to define suitability, but also where the species' could plausibly have been introduced, we selected pseudoabsence points in MaxEnt within a convex hull around each species' occurrences. To account for uneven sampling of occurrence points (Kramer-Schadt et al. 2013), we included a bias file for each of the species based on the presence of National Parks and distance to roads. Each MaxEnt model was evaluated by performing a 10-fold cross-validation (the default setting) to evaluate model fit. MaxEnt creates a different function for each climatic predictor variable related to the suitability of climate conditions for species presence based on data for the locations in which the species has been detected. This process generates a spatial model with continuous values associated with climatic suitability for occurrence. We transformed this continuous model into a binary suitable/unsuitable map based on a threshold value that encompassed 95% of the location points. Using this threshold assumes that the species' status at almost all of the locations was correctly identified, which is consistent with a goal of broadly characterizing invasion risk.

To reduce potential bias introduced by using a single BEM, we also created Bioclim models of climatic suitability for *B. rubens* and *B. tournefortii*. Bioclim identifies thresholds for each climatic predictor that encompass the distribution data (Busby 1991; Pearson and Dawson 2003). We used ArcGIS 10.1 (ESRI,Redlands, CA 92373) to extract the values of the four climate variables to all the known locations and then calculated climatic limits that encompassed 95% of the distribution data set. This threshold was created by excluding the climate values associated with the upper and lower 2.5% of presence or high abundance points. We calculated Bioclim climatic suitability as areas identified as suitable by all four climate layers. The MaxEnt and

Bioclim results were combined to quantify the spatial extent of climatic suitability in either model.

We evaluated MaxEnt model performance based on the area under the curve (AUC) values, which are widely applied to determine agreement between predicted species distributions and occurrence records (Fielding and Bell 1997; Pearson et al. 2006; Thuiller 2003). AUC values are based on the receiver operating curve (ROC), which plots the rate of true-positive predictions (sensitivity) against false-positive predictions (specificity) with values ranging from 0.5 (no better than random) to 1 (perfect model prediction). For all models, we also calculated true-skill statistic (TSS). TSS (Allouche et al. 2006) provides a measure of the accuracy of presence–absence predictions based on calculations of sensitivity (proportion of true positives) and specificity (proportion of true absences). Values range from +1 to -1, with zero indicating model performance no better than expected by chance. These statistics are typically used to evaluate the accuracy of landcover maps not projected-suitability models. Therefore, TSS values typically used to define good map accuracy are not applicable to suitability modeling because BEM projections aim to model climatic suitability for invasion, not the current distribution of invasive species.

Modeling Presence and Abundance under Future Climate Conditions

After establishing the climate conditions suitable for *B. rubens* and *B. tournefortii* based on current climate, we projected those conditions onto future climate models using the same thresholds used to describe current climatic suitability. We repeated this process for the five AOGCM projections.

We created ensemble models of future presence and high abundance of *B. rubens* and *B. tournefortii* by summing all of the binary climatic suitability maps (i.e., those created by MaxEnt and Bioclim for each AOGCM) to create models ranging from zero (unsuitable in all models) to 10 (suitable in all models). Combining models of suitability made with multiple BEMs and AOGCMs (Araújo and New 2007) reduces the effect of any single model or scenario, and the degree of model overlap provides a measure of confidence associated with model agreement. For example, there is less uncertainty about the future climatic suitability for presence or high abundance of areas that are projected to be suitable by a greater number of AOGCMs (greater model agreement). We created separate ensemble models for the two relative concentration pathways.

To identify climatic suitability for invasion by *B. rubens* and *B. tournefortii* in the future, we created maps of range shift that show areas of future expansion, maintenance, and contraction. We simplified this analysis by considering any area projected to have suitable climate conditions currently by either MaxEnt or Bioclim as suitable. We created two sets of range shift maps by applying a low and a high threshold for identifying suitability. The low threshold provided a very liberal interpretation of the data in which areas projected to be suitable by any one of the 10 models in the ensemble were considered suitable. The high threshold provided a more conservative interpretation in which suitable areas had to be projected as suitable by 6 or more of the 10 models in the ensemble. We compared current and future suitability to measure the spatial extent of projected contraction and the maintenance and expansion of invasion risk by 2050 within the study region defined for each species.

Results and Discussion

Distribution Data

The spatial locations of high abundance, low abundance, and presence with unknown abundance are shown in Figure 1-1. At the 2.5 arcminute resolution, we compiled 3,303 occurrences of *B. rubens* and 1,855 occurrences of *B. tournefortii*. Within these datasets, we identified 110 locations of highly abundant *B. rubens* and 218 locations of highly abundant *B. tournefortii*. Further information on the data sources is presented in Appendix A.

Current Climatic Suitability for Invasion

Current climatic suitability for *B. rubens* and *B. tournefortii* presence extends throughout the study region, consistent with known location points (Figure 1-2A). Suitable climate for *B. rubens* high abundance is currently limited to relatively small areas of southern California, Nevada, and Utah and a larger region of central and northwestern Arizona (Figure 1-2B). Suitable climate for *B. tournefortii* high abundance occurs primarily in southern California (Figure 1-2B). Based on the AUC statistic for MaxEnt models and True skill statistics (TSS) for all models, the projected models performed better than expected by random chance (Table 1-1). The smaller suitable range for high abundance (relative to presence) for both species supports previous findings that models of potential establishment overestimate potential impact (Bradley 2013).

Based on the MaxEnt models, different climate conditions influence species presence vs. high abundance. For both *B. rubens* and *B. tournefortii*, temperature was by far the strongest predictor of presence (minimum temperature for *B. rubens* and

maximum temperature for *B. tournefortii*). For *B. rubens* this result suggests that freezing tolerance may limit the species' survival over winter, which is consistent with experimental studies (Bykova and Sage 2012). For, *B. tournefortii*, this result suggests that the species effectively establishes under hot conditions, which is consistent with its measured heat tolerance (Suazo et al. 2012).

In contrast, minimum temperature and spring precipitation were both strong predictors of abundance for *B. rubens* and summer precipitation was the strongest predictor of abundance for *B. tournefortii*. Both invasive species are likely to better compete against native species (e.g., (Barrows et al. 2009) and have stronger population growth (Beatley 1974, Salo 2004) under wetter conditions. Thus, while temperatures limit the overall range, precipitation may be more influential for invader abundance.

Future Range Shifts with Climate Change

Projections of future climatic suitability for *B. rubens* and *B. tournefortii* presence and abundance under the RCP4.5 emissions pathway are shown in Figure 1-2C and D, respectively. The model projections based on RCP4.5 vs. RCP8.5 were similar both in overall magnitude of calculated range shift as well as spatial pattern. For simplicity, we present results from RCP4.5 in the main text and present the same results for RCP8.5 in Appendix B. An analysis of future climate conditions indicates that they are climatically similar to current conditions. That is, we are not extrapolating model fits into novel climate conditions (Appendix C), which would increase uncertainty in model projections if it were the case.

Most models agreed that large areas will be suitable for *B. rubens* presence in the future (Figure 1-2C). Future suitability for *B. rubens* abundance is projected to be

greatest in northwest Arizona, southwest Nevada, and Baja California, Mexico based on ensemble model overlap (Figure 1-2D). Based on the high threshold (six or more models projecting suitability), climatic suitability for *B. rubens* presence could expand by 12% along the northern edge of the currently suitable range (Figure 1-3A; Table 1-2). However, contraction along the southern edge is also predicted, with areas primarily in Arizona becoming unsuitable. Using the more inclusive low threshold (one or more models projecting suitability), climatic suitability for *B. rubens* presence could expand northward up to 65% (Figure 1-3B). In the model projections, northward expansion is primarily driven by warming temperatures, which is consistent with experimentally derived limitations. (Bykova and Sage 2012) show that *B. rubens* is sensitive to freezing temperatures and is not as cold tolerant as the related species *Bromus tectorum*.

High abundance of *B. rubens* based on the high threshold could decrease by 42% (Table 1-2; Figure 1-3C). However, using the more inclusive low threshold, climatic suitability for high abundance could expand northwards by as much as 64% (Figure 1-3D). The large differences in potential future range illustrate uncertainty associated with both differences between BEMs and climate projections as well as the importance of choosing a threshold for delineating suitable from unsuitable. Areas of expansion in southern Nevada, northwestern Arizona, and Baja California, Mexico show the highest model agreement (Figure 1-2). Therefore, these areas might see a shift towards high abundance of *B. rubens* with climate change. Interestingly, *B. rubens* is already present throughout southern Nevada, making it likely that populations will not be limited by propagules and could expand rapidly once climate conditions become suitable.

The future presence model of *B. tournefortii* shows high model agreement in southern California and Nevada, and throughout much of Arizona (Figure 1-2C). Future climatic suitability for *B. tournefortii* is projected by most models to occur in southern California (Figure 1-2D). Based on the high threshold (six or more models projecting suitability), climate conditions suitable for *B. tournefortii* presence are projected to decrease by 34% overall, with areas in southern California, eastern Nevada, and Mexico becoming unsuitable (Table 1-2; Figure 1-3A). Using the more inclusive low threshold (one or more models projecting suitability), climatic suitability for *B. tournefortii* could expand up to 29% (Figure 1-3B).

In contrast, climatic suitability for high abundance of *B. tournefortii* is projected to decrease by 56% (Table 1-2; Figure 1-3C). Using the inclusive low threshold, climatic suitability for high abundance expands by 28% (Figure 1-3D). The difference between these two projections can primarily be attributed to how MaxEnt vs. Bioclim interpret high temperatures for *B. tournefortii* (Appendix D). Bioclim identifies a high temperature threshold, above which conditions become unsuitable, while MaxEnt considers all high temperatures suitable. Although *B. tournefortii* has a broad tolerance for warm temperatures (Suazo et al. 2012), it is not clear whether it is approaching its high temperature limit within its current range. Further experimental analyses are required to enable better interpretation of the model results.

Suitable Area

Interpretations of future ensemble models strongly depends on how suitable area is differentiated from unsuitable area. The overall spatial extent of climatic suitability varies depending on the choice of an acceptable threshold for identifying climatic

suitability (Figure 1-4). Areas of high model overlap have lower uncertainty. Despite differences in climate changes projected by these AOGCMs (Rupp et al. 2013), areas of high overlap maintain climatic suitability. For prioritizing management and control efforts, higher overlap is a better bet than lower overlap for identifying the most likely areas with future invasion risk (Figure 1-2). However, even areas with low overlap could still maintain or expand risk if under-sampled distribution data cause models to underpredict climatic suitability. We suggest that locations of expansion, particularly using the high threshold (Figure 1-3A-C) are likely to be at the highest risk, but contraction using the same high threshold may be over-predicted.

Conclusions

It is currently unknown whether the impact niche of invasive plants will respond to climate change in a similar direction and magnitude as the overall range. Based on the low threshold of model overlap, climatic suitability for presence and high abundance for *B. rubens* and *B. tournefortii* are projected to shift in a similar magnitude and direction under climate change. However, based on the high threshold of model overlap, climatic suitability for presence and high abundance are projected to vary considerably in magnitude and direction under climate change. Differences between shifts in modeled establishment niche and impact niche between the species highlight the need for considering both presence and high abundance in models of invasion risk. Overall, high abundance of nonnative, invasive plant species threatens native plant species and has the potential to alter ecosystem function (e.g., increased fire threat in areas with high abundance of *B. rubens* and *B. tournefortii*). Given the importance of understanding

where the greatest threat is likely to occur, future analysis of range shifts for invasive plants should include suitability for high abundance where possible.

The relatively sparse amount of abundance data in this study highlights the need for a different focus in field data collection. Presence data are useful, but information on the relative abundance of invasive species, even qualitative information, is more directly related to their potential ecological effects (Bradley 2013; Leibold 1995; McDonald et al. 2009; Parker et al. 1999). Continuous cover data collected across broad climatic or latitudinal gradients would provide the most accurate representation of community composition at each location and would allow for more-comprehensive models of the response of species to climate change. In lieu of time-intensive continuous cover data, qualitative descriptions or cover ranks, such as those used here, can be used for identifying the impact niche of an invasive species.

Current models of the distributions of presence and abundance can be used to guide data collection by identifying areas projected to be climatically suitable but not previously sampled. They can also help to identify those regions with the greatest risk of impact from invasion, assuming that abundance and impact are positively correlated (Parker et al. 1999). Future research is needed to quantify whether and how abundance relates to impact, thereby enabling managers to use regional models to better target management action. Nonetheless, potential for an abundant infestation is likely to be of greater concern than potential for presence only and focusing management in areas with current and future climatic suitability for abundance is a good approach for mitigating future invasions.

Acknowledgments

We thank L Pelech and L. Zachmann for collecting and compiling distribution data sets. Thanks also to S. Abella, J. Cipra, K. Kain, C. Norman, the National Park Service Mojave Desert Network Inventory & Monitoring Program, the NPS National Vegetation Mapping Program, C. Powell and the California Invasive Plant Council (Cal-IPC) mapping team for contributing additional distribution datasets. This research was supported by the Department of Defense through the Strategic Environmental Research and Development Program (SERDP) grant number RC-1722 and by Cooperative Agreement H8C07080001 between the National Park Service and University of California, Davis.

Tables

Table 1-1. Model validation based on current projections.

Model validation indicates agreement between the projected distribution and observations for each species for the current projections. Statistics were calculated for models based on presence data (P) and high-abundance data (HA). The true skill statistic (TSS) measures the map accuracy of presence–absence predictions and ranges in value from +1 to -1, with +1 indicating perfect model agreement and 0 indicating performance no better than expected by random chance. The area under the receiver operating curve (AUC) measures overall model accuracy and ranges from 0 to 1 with 0.5 indicating no better than random. AUC can only be calculated for models with continuous predictions of suitability (MaxEnt in this case).

	B. rubens		*B. tournefortii*		*B. rubens*		*B. tournefortii*	
	MaxEnt				Bioclim			
	P	HA	P	HA	P	HA	P	HA
TSS	0.50	0.76	0.39	0.75	0.54	0.66	0.56	0.79
Mean test AUC (st dev)	0.752 (0.008)	0.914 (0.037)	0.752 (0.020)	0.909 (0.017)	NA	NA	NA	NA

Table 1-2. Projected increases in distribution size (km^2 x 1000) within the study areas based on the low (one or more model projecting climatic suitability) and high (six or more models projecting climatic suitability) thresholds under future climate conditions for RCP4.5.

			Low Threshold		High Threshold	
			Area	% Change	Area	% Change
B. rubens	Presence	Current	736		736	
		Future	1219	65	826	12
	High abundance	Current	475		475	
		Future	780	64	273	-42
B. tournefortii	Presence	Current	410		410	
		Future	531	29	270	-34
	High abundance	Current	135		135	
		Future	173	28	59	-56

Figures

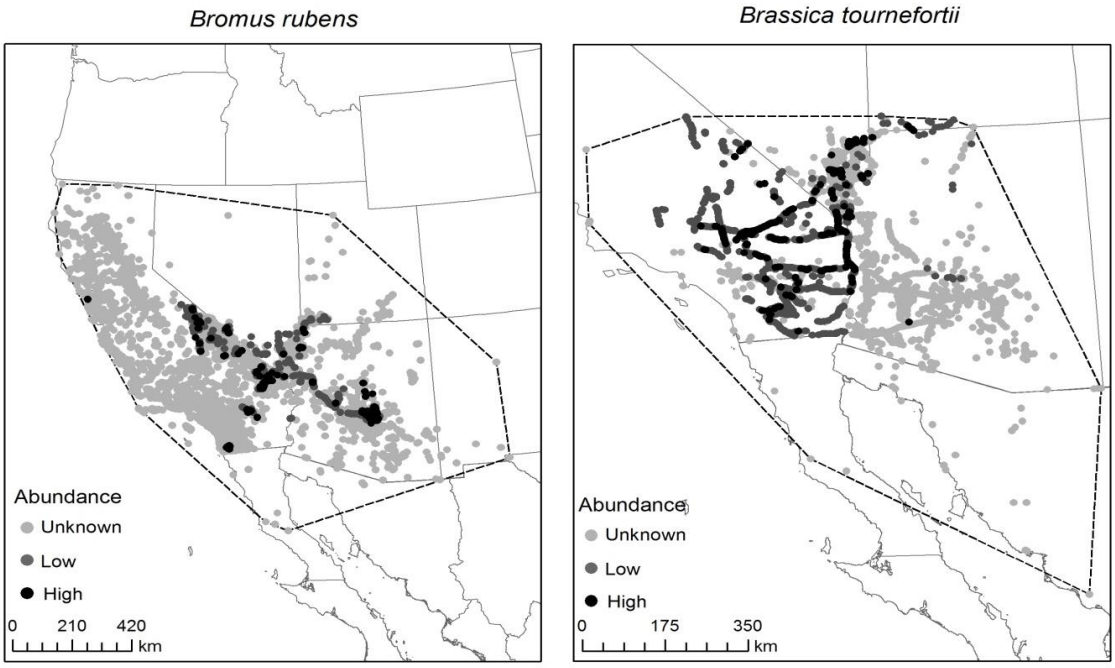

Figure 1-1. Spatial locations of data collection for each species.

We classified locations as high abundance if the species was recorded as having least 10% cover, was described as having continuous ground cover, or was observed in abundance beyond the road corridor. Points are shown as low abundance if they do not meet these criteria but have some description of abundance associated with them. Points lacking a description of abundance level are considered unknown. At the 2.5 arcminute resolution, we compiled 110 high abundance occurrences for *B. rubens* and 218 for *B. tournefortii*. 243 points were classified as low abundance for *B. rubens* and 565 for *B. tournefortii*. Unknown abundance was found for 2,950 *B. rubens* points and 1,072 *B. tournefortii* points.

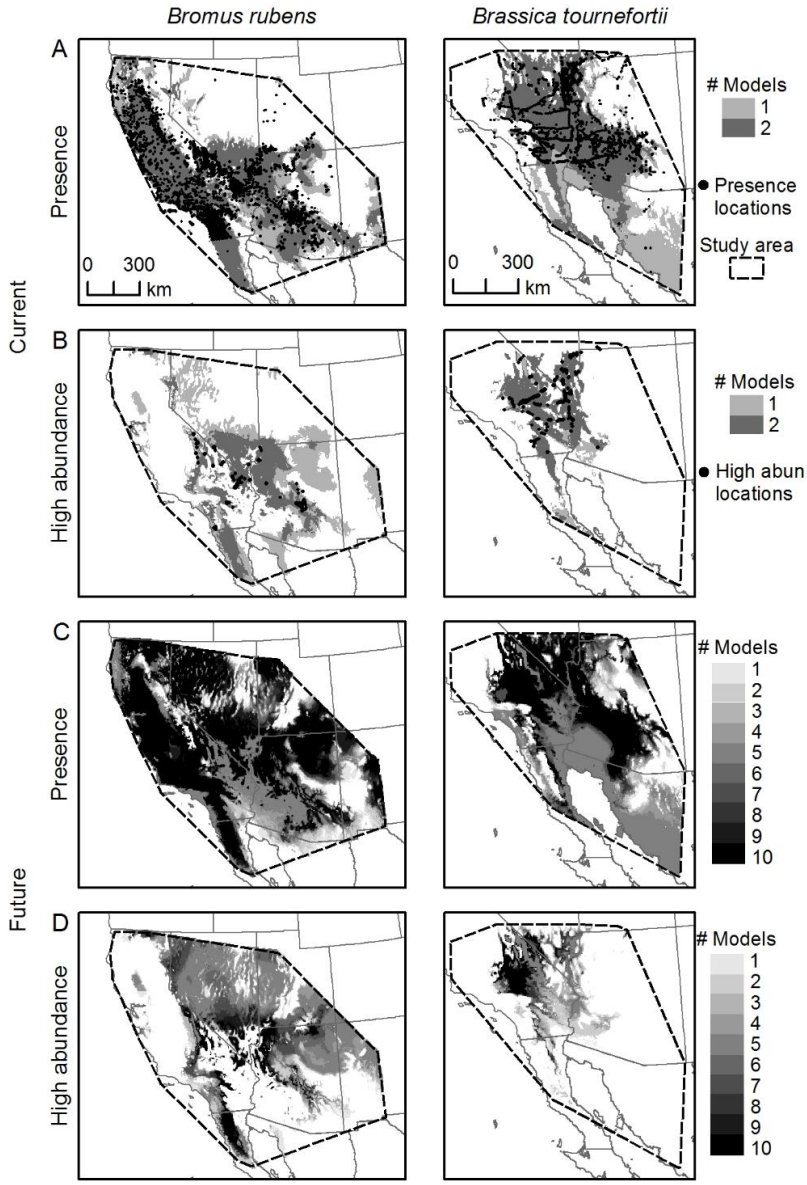

Figure 1-2. Species distribution models for *Bromus rubens* and *Brassica tournefortii*. Point locations indicate where (A) presence and (B) high abundance data were collected. The predicted current climatic suitability for (A) presence and (B) high abundance include the MaxEnt and Bioclim projections and encompass 95% of the original distribution data. Future ensemble models are based on RCP4.5. The future-ensemble models for (C) presence and (D) high abundance were created by combining

the projections of 10 models: two bioclimate envelope models and five Atmosphere–Ocean General Circulation models. Values indicate how many of the 10 models projected climatic suitability.

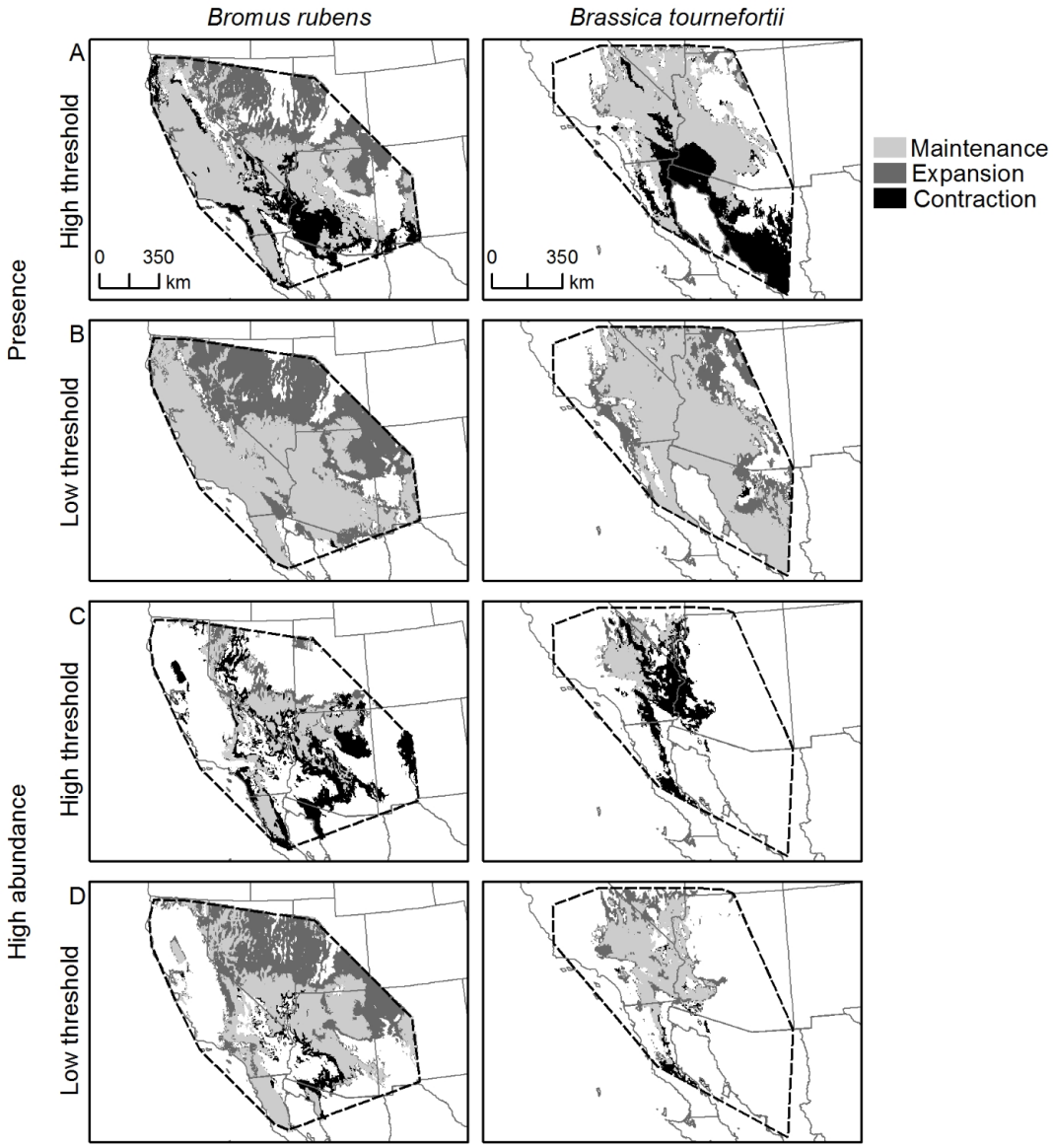

Figure 1-3. Distribution models showing maintenance, expansion, and contraction of suitable climate under future climate conditions for RCP4.5.

Maintenance indicates that a location was climatically suitable both under current and future climate conditions. Expansion indicates that a location was climatically suitable under future, but not current climatic conditions. Contraction indicates that a

location was climatically suitable under current, but not future climatic conditions. The high-threshold models (A and C) are based on a more conservative view of future climatic suitability, where six or more models must agree for a location to be included as future potential habitat. Low-threshold models (B and D) include all areas where at least one future model indicates suitable habitat.

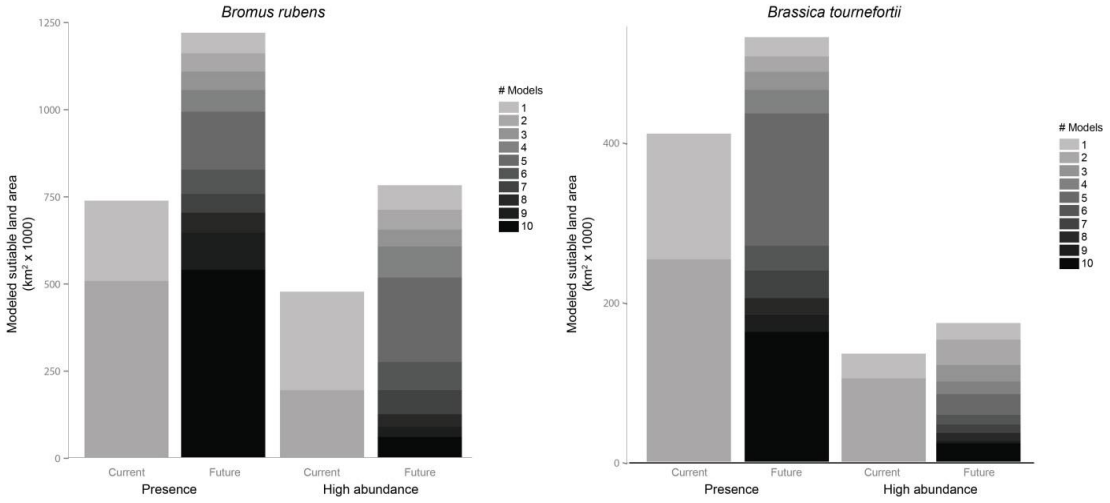

Figure 1-4. Predicted suitable land area for the target species currently and by 2050 under RCP4.5. Darker gray indicates higher ensemble model overlap.

CHAPTER 2

PLANT DISTRIBUTION DATA SHOW BROADER CLIMATIC LIMITS THAN EXPERT BASED CLIMATIC TOLERANCE ESTIMATES

Authors

Caroline A. Curtis[1] and Bethany A. Bradley[2]

Abstract

Although increasingly sophisticated environmental measures are being applied to species distributions models, the focus remains on using climatic data to provide estimates of habitat suitability. Climatic tolerance estimates based on expert knowledge are available for a wide range of plants via the USDA PLANTS database. We aim to test how climatic tolerance inferred from plant distribution records relates to tolerance estimated by experts. Further, we use this information to identify circumstances when species distributions are more likely to approximate climatic tolerance. We compiled expert knowledge estimates of minimum and maximum precipitation and minimum temperature tolerance for over 1800 conservation plant species from the `plant characteristics' information in the USDA PLANTS database. We derived climatic tolerance from distribution data downloaded from the Global Biodiversity and Information Facility (GBIF) and corresponding climate from WorldClim. We compared expert-derived climatic tolerance to empirical estimates to find the difference between their inferred climate niches (ΔCN), and tested whether ΔCN was influenced by growth

[1]Graduate Program in Organismic and Evolutionary Biology, University of Massachusetts Amherst, Amherst, Massachusetts 01003
[2]Department of Environmental Conservation, University of Massachusetts Amherst, Amherst, Massachusetts 01003

form or range size. Climate niches calculated from distribution data were significantly broader than expert based tolerance estimates (Mann-Whitney ρ values $<< 0.001$). The average plant could tolerate 24 mm lower minimum precipitation, 14 mm higher maximum precipitation, and 7° C lower minimum temperatures based on distribution data relative to expert-based tolerance estimates. Species with larger ranges had greater ΔCN for minimum precipitation and minimum temperature. For maximum precipitation and minimum temperature, forbs and grasses tended to have larger ΔCN while grasses and trees had larger ΔCN for minimum precipitation. Our results show that distribution data are consistently broader than USDA PLANTS experts' knowledge and likely provide more robust estimates of climatic tolerance, especially for widespread forbs and grasses. These findings suggest that widely available expert-based climatic tolerance estimates underrepresent species' fundamental niche and likely fail to capture the realized niche.

Introduction

Understanding the factors that define species niches has long been a central theme in ecology, beginning with Joseph Grinnell's initial description of the niche as an ecological space sufficient for the survival of a single species (Grinnell 1914). Interest in the ecological niche was further developed by G. E. Hutchinson, who refined the niche concept by separating the fundamental niche (the multidimensional environmental conditions in which a population could exist) from the realized niche (the biotic and abiotic conditions in which a species actually does exist) (Hutchinson 1957). In the decades following Hutchinson's statements, there began the development of research focused on modeling species distributions and disentangling the factors that define the

fundamental and realized niches (e.g. Roughgarden 1972, Colwell and Fuentes 1975). Recently, more sophisticated techniques have been applied to defining a species' niche (Soberón 2007) and species distribution models (SDMs) have become increasingly useful tools for identifying a species' habitat, projecting distribution changes in response to climate (Thomas et al. 2004), and mapping habitat areas of importance for biodiversity conservation (Araújo et al. 2004, 2011) and those at risk from environmental threats (Thuiller et al. 2005).

However, SDMs parameterized from species distributions are likely to underestimate climatic tolerance because species are not in climatic equilibrium (i.e., they are not present in all climatically suitable locations (Hutchinson 1957)) and/or distribution data are unevenly collected and reported, thereby underrepresenting the total distribution (Yesson et al. 2007). Some of the earliest works on SDMs highlighted the need to consider species occurrences outside the natural range (Booth et al. 2015). In doing so, SDMs will more closely approximate the fundamental niche, allowing researchers to draw more accurate conclusions about the potential for range shifts in response to climate change. Underestimating the climatic niche, which may be the result of parameterizing models with a subset of a species' range, causes models to miss suitable climatic space under current and future conditions, potentially exaggerating habitat loss and associated risk to species.

Several lines of evidence suggest that species distributions underestimate climatic tolerance. For example, studies comparing niche space in the native and non-native ranges have often shown that non-native occurrences expand the climatic niche (i.e. show a lack of niche conservatism) (Broennimann et al. 2007, Gallagher et al. 2010, Early and

Sax 2014, Li et al. 2014). Other studies have found that regional distributions are heavily influenced by factors other than climate including dispersal barriers (Davis et al. 1998, Svenning and Skov 2004, Bradley et al. 2015, Bosci et al. 2016), introduction history (Strubbe et al. 2013) and biotic interactions (Davis et al. 1998, Torchin et al. 2003, Tingley et al. 2014). Collectively, these influences on species realized niches cause distributions to underestimate climatic tolerance. Therefore, correlative models, which typically rely on climatic tolerance derived from species distributions, might be of limited utility for projecting suitable habitat in future or novel environmental conditions because they lack the causal information that can be derived from functional traits included in mechanistic models (Helmuth et al. 2005).

One potential solution is to avoid the problems inherent in species distribution data by building SDMs based on alternative climatic tolerance data such as experimentally gathered physiological tolerance data (Helmuth 2009, Kearney and Porter 2009, Kearney et al. 2010a, Evans et al. 2015) or expert-based estimates of growth requirements. Spatial models based on physiological tolerance information for a species are more likely to identify the fundamental niche, or all conditions where a species can survive, rather than the smaller realized niche based on where the species currently exists geographically. In one example, Buckley et al. (2010) parameterized spatial models for the eastern fence lizard (*Sceloporus undulatus*) in the USA based on empirically measured foraging energetics, biophysical thresholds, and demography along with downscaled climate data to project suitable habitat under current and future climate conditions. In another example, critical maximum thermal thresholds were measured experimentally for forest-dwelling ant species and used to model response to warming

across a latitudinal gradient (Diamond et al. 2012). The mechanistic approach has also been used to model the dispersal and population growth potential for the invasive cane toad in Australia (Kearney et al. 2008).

However, measuring physiological tolerance limits requires time intensive field- and/or lab-based sampling and, as a result, those data are only available for a few well-studied taxa. Similarly, expert-opinion data are typically limited to crops, ornamental species or those used in conservation and restoration. The USDA PLANTS database provides standardized information primarily designed to support land conservation activities and consists of estimates of climatic tolerance for approximately 2,500 plant species and cultivars in its `characteristics' data. These data are based on expert knowledge rather than experimental manipulations and are, therefore, considered estimates of the range of conditions under which the species can survive. However, given that this database is among the first large-scale compilation of freely available, easily accessible plant climatic tolerance estimates, it provides an appealing alternative to species distribution data. The USDA PLANTS database is also a primary source for some plant traits, including temperature tolerance and precipitation requirement, archived in the TRY database (https://www.try-db.org; (Kattge et al. 2011)). TRY is an important repository for plant trait data which includes over 1,000 traits and 100,000 plant species (Kattge et al. 2011) and reported estimates of climatic tolerance could easily be interpreted as `fundamental' growth requirements. Moreover, climatic tolerance estimates from USDA PLANTS are used to select species for conservation and restoration of ecosystems across the U.S. Thus, it is important to understand how well

these expert-derived climatic tolerances perform in terms of capturing suitable climatic limits relative to species' distributions.

Here, we compare climatic niches inferred from two commonly used data sets: the USDA PLANTS database, and herbarium records from the Global Biodiversity Information Facility (GBIF). Observations available on GBIF represent both species' native distribution as well as records outside of the native range (e.g., accidental movement or purposeful plantings of species). Therefore, these data provide useful insight about species' climatic tolerance. For example, the climatic niche of commercial Eucalypt species was better approximated by integrating global GBIF records with native range data from the Atlas of Living Australia (ALA) (Booth 2014) and the extinction risk for over 7.000 woody plant species was modeled from compiled GBIF, Forest Inventory and Analysis (FIA) and permanent sampling plot data (Zhang et al. 2016). We calculated a comparative niche value (hereafter ΔCN) for each species as the difference between climatic niche defined by expert-based climatic tolerance estimates and those derived from climate conditions associated with distribution data. First, we ask how climatic niches calculated from expert-based climatic tolerance estimates compare to those calculated from distribution data. Second, we ask whether range size influences ΔCN and lastly, we ask whether species growth form influences ΔCN.

Methods

Expert-Based Climatic Tolerance Data

The USDA PLANTS database provides detailed information about the traits and growth requirements of approximately 2,500 vascular plants in their `characteristics' data. Included in these characteristics data are estimates of species' tolerance to absolute (i.e.

record) minimum temperature (for perennial species and annual species with dominant growing seasons in fall, winter, and spring), and minimum and maximum precipitation tolerance (for all species). Climatic tolerance is estimated based on expert knowledge of historical and current species ranges within the USA and associated historical climate conditions. We downloaded the characteristics data, including growth form, for all species for which minimum temperature, and/ or minimum and maximum precipitation were available and refer to these data hereafter as climatic tolerance estimates.

Herbarium Records

We searched the Global Biodiversity Information Facility (GBIF) for all species with climatic tolerance estimates using the rgbif package for R (Chamberlain et al. 2015) and downloaded all georeferenced records. Because the climatic tolerance estimates are based on expert knowledge of tolerance within the USA, we created a USA distribution dataset by restricting the records for each species to the coterminous USA, Hawaii, and Alaska (hereafter, USA herbarium). We excluded species with five or fewer records from the analyses. Taxonomic discrepancies between the USDA PLANTS database and the GBIF records were resolved using the Integrated Taxonomic Information System (ITIS, http://www.itis.gov). In cases where a single species was reported by two names (i.e., one name was identified as a synonym of the other using ITIS), the taxonomy given by the USDA PLANTS database was retained. Data representing current climate (1950-2000) were obtained from WorldClim (http://worldclim.org) as interpolated climate surface layers at 10 arc-minute (approximately 18.5 km at the equator) spatial resolution (Hijmans et al. 2005) and extracted to herbarium records. WorldClim data were used to encompass both the coterminous USA as well as Hawaii and Alaska. For each species,

we used the climate data associated with occurrence records to calculate the 95th percentile of minimum temperature and minimum and maximum precipitation. We present the 95th percentile to avoid biasing our calculations due to inaccurate outliers in the distribution dataset, although we also calculated results associated with absolute minimum and maximum values (Appendix E). We calculated range size based on the area within a convex hull surrounding the occurrence records for each species.

Climate Corrections and Comparisons

The climatic tolerance estimates are based on extreme values of each climate variable (e.g., absolute minimum temperature) while the WorldClim dataset is based on temporal averages from 1950-2000. In order to make the datasets comparable, we transformed the average values into extreme values based on linear corrections using climate time series available for the US.

Minimum precipitation climatic tolerance estimates are reported as the cumulative annual precipitation that occurs 20% of the time at the driest weather station (i.e. the annual precipitation value corresponding to the 20^{th} percentile over a multi-year period). In the WorldClim dataset, precipitation is recorded as cumulative monthly precipitation averaged over the time period of 1950-2000. We adjusted the WorldClim results to make them more directly comparable to the climatic tolerance estimates of minimum precipitation by calculating climate transformations based on time series of PRISM climate interpolations (Daly et al. 2002). PRISM data are available as time series of monthly precipitation from 1981-2013 for the continental US. We used these time series to calculate the 20^{th} percentile of annual precipitation and compared these data to the

PRISM average annual precipitation using 50,000 random points in the continental US to calculate and apply linear gain and offset corrections.

Maximum precipitation climatic tolerance estimates are reported as the mean annual precipitation at the wettest weather station in the species' range as defined by expert knowledge. As the two measures are both based on average precipitation, we considered them comparable and did not apply a climate transformation to the WorldClim maximum precipitation results.

Minimum temperature climatic tolerance estimates are reported as either the lowest recorded temperature from the historical range or the lowest January temperature recorded from weather stations within the current range. WorldClim monthly minimum temperature is calculated as the mean monthly temperature minus half of the monthly temperature range (Hijmans et al. 2005). These data are then temporally averaged (1950-2000) to estimate minimum temperature. To adjust the WorldClim results for minimum temperature and make them comparable to the climatic tolerance estimates, we calculated a climate transformation based on time series of weather station climate records (Menne et al. 2012). We compiled a time series (1950-2000) of daily January minimum temperature from over 80 weather stations throughout the USA (Appendix F). From daily temperature data, we calculated the absolute lowest January minimum temperature and the 1950-2000 average January minimum temperature from which the linear gain and offset corrections were calculated and applied to the WorldClim data. We capped the minimum temperature at -60° C, which approximates the coldest temperatures measured in the USA.

Analyses

We used Mann-Whitney-Wilcoxon tests to compare the climate niches derived from the climatic tolerance estimates and the herbarium records. We calculated ΔCN for each species and each of the three climate variables (maximum precipitation, corrected minimum precipitation, and corrected minimum temperature). For consistent visual comparison, ΔCN was calculated for all climate variables such that positive values indicate a broader climatic niche measured from the herbarium data. We used linear regressions to test for a relationship between species range size and the magnitude of ΔCN for each climate variable. We used Kruskal-Wallis tests and post-hoc Kruskal Nemenyi tests to determine if ΔCN varied by growth form.

Results

From the USDA PLANTS database, minimum and maximum precipitation data were available for 2,053 species and minimum temperature data were available for 2,080 species (excluding summer annuals). Forbs/herbs and trees were the most common growth form in the data comprising 28% and 27% of the species, respectively. Grasses (23%) and shrubs (19%) were also well represented while vines represented only 3% of the species in the dataset. Of those species with climatic tolerance estimates for minimum and maximum precipitation, and minimum temperature, six or more GBIF herbarium records within the USA were available for 1,860 and 1,870 species, respectively. Mann-Whitney-Wilcoxon tests showed that the distribution of climatic niches measured from the climatic tolerance estimates and herbarium records are significantly different for minimum precipitation ($W = 1991976$, ρ -value $<< 0.001$),

minimum temperature (W = 1993790, ρ -value << 0.001), and maximum precipitation (W = 1523031, ρ -value = 0.04) (Figure 2-1).

For all climate variables, we measured a broader climate niche from the herbarium records than from the climatic tolerance estimates. Minimum and maximum precipitation values derived from herbarium records were broader (i.e. lower minimum and higher maximum) than climatic tolerance estimates for 71% and 52% of species, respectively (Figure 2-1A and 2-1B). The mean minimum and maximum precipitation values from the herbarium records were 110 mm (median: 72 mm) lower and 24 mm (median: 13 mm) higher than climatic tolerance estimates, respectively. Similarly, 74% of species had lower minimum temperature recorded from the herbarium records than from the climatic tolerance data (Figure 2-1C), with a mean difference of 7° C (median 4.5° C). For only one growth form was this general trend not supported. ΔCN values for maximum precipitation were generally negative for trees, with the climate niche inferred from climatic tolerance estimate larger by an average of 300 mm. When all U.S. distribution data were considered (not just the 95th percentile), the pattern was even more pronounced, with the vast majority of species showing a broader climate niche from herbarium records (Appendix E).

Species range size was significantly positively related to ΔCN for minimum precipitation (df = 1779, ρ -value << 0.001; Figure 2-2A) and minimum temperature (df = 1783, ρ -value << 0.001; Figure 2-2B). In other words, for species with larger ranges, there was a greater difference between the two datasets (with herbarium records consistently broader) than for species with smaller ranges. Although there was a slight

positive trend between range size and ΔCN for maximum precipitation, the trend was not significant (df = 1779, ρ -value = 0.606, Figure 2-2C).

We found that ΔCN differed by growth form for minimum precipitation (KW X2 = 79, df = 4, ρ << 0.001), maximum precipitation (KW X2 = 35, df = 4, ρ << 0.001), and minimum temperature (KW X2 = 133, df = 4, ρ << 0.001) (Figure 2-3A-C). Because of the small number of vine species, we excluded vines from the growth form analyses. Grasses and/or forbs tended to have the broadest range size as well as the largest ΔCN values, with herbarium records consistently broader than climatic tolerance estimates. In contrast, trees and shrubs tended to have narrower ranges and smaller (although still positive) ΔCN values. In only one case was this general trend not supported. ΔCN values for maximum precipitation were negative for trees, with the climate niche inferred from climatic tolerance estimates larger by an average of 300 mm. We also found that range size differed by growth form (KW X2 = 79, df = 4, ρ -value << 0.001) (Figure 2-3D).

Discussion

Understanding the extent to which commonly used data sources approximate species' fundamental niche is an important step toward creating realistic predictions of suitable habitat. Distribution data are likely to underestimate the fundamental niche because species ranges are not in climatic equilibrium (Hutchinson 1957). Distributions are limited not only by climate conditions, but also by dispersal barriers, introduction history and biotic interactions (e.g. Strubbe et al. 2013, Early and Sax 2014, Tingley et al. 2014, Bradley et al. 2015). These concerns have prompted proposals to use alternative estimates of climatic tolerance in lieu of distribution data when parameterizing spatial

models (Kearney and Porter 2009, Cuddington et al. 2013, Evans et al. 2015), assuming that expert knowledge or lab-based measurements will provide a broader approximation of climatic tolerance. However, our results show that distribution data in the US describe a consistently broader climatic niche than climatic tolerance estimates available for over 1800 plants (Figure 2-1).

Distribution data suggest a broader climatic tolerance for all three of the climate variables tested and the magnitude of the difference was substantial. Distribution data suggest that the average plant can withstand an extreme minimum temperature 7° C lower than estimated by experts. These records also infer lower drought tolerance (20^{th} percentile of annual precipitation) of 24 mm. Moreover, these results are based on a conservative approach of using the 95^{th} percentile of minimum and maximum precipitation and minimum temperature for each species. The results are even more pronounced (15° C lower minimum temperature, 250 mm lower drought tolerance) if we use a less conservative approach and include all distribution data in the analyses (Appendix E).

The one exception to this trend is ΔCN measured for maximum precipitation among tree species. One possible explanation for this inconsistent result is that, for a few species with distributions in areas of high precipitation, an extreme value of maximum precipitation was reported in the USDA PLANTS characteristics. For example, white mangrove (*Laguncularia racemosa*) has a maximum precipitation ΔCN value of -1,082 (expert estimate: 2,337 mm; distribution data: 1,255 mm). It is possible that experts over-estimate maximum precipitation for species located near strong precipitation gradients. For most species, our results suggest that plant distribution data are likely to

produce a comparable or broader estimate of climatic habitat than currently available climatic tolerance estimates.

Although we find that herbarium records produce broader estimates of climatic tolerance, this does not necessarily suggest that distribution data are doing a good job of approximating the climate niche for most species. Instead, the differences between the two datasets may result from poor climatic estimates in both datasets. Currently, there are few repositories for climatic tolerance data and limited information available due to the difficulty of experimentally deriving tolerance across many species, particularly for some long-lived plants. Climate conditions experienced by species is also likely to be influenced by local topography and land cover (Latimer and Zuckerberg 2016), which cannot be effectively captured at coarser spatial resolutions such as the one used in this analysis. Moreover, climatic tolerances vary across species distributions as a result of local adaptation and provenance variations, making it all the more challenging to identify tolerance limits (Chown and Gaston 2016). Our findings suggest that the USDA PLANTS characteristics data underestimate climatic tolerance for the majority of species. Where these data are associated with the TRY database (Kattge et al. 2011), the same result is likely to be true. Alternatively, discrepancies between the data sets might be due to the biases inherent in their collection. Herbarium records tend to reflect species range edges, be skewed toward populations of rare species, and be biased toward populations that are convenient to sample (e.g., close to trails or roads) (Daru et al. 2017). Conversely, because the expert-based climatic tolerance estimates are used for conservation and restoration planning, they might be representative of the average climate conditions in areas where the plant has the highest likelihood of thriving. These

findings are important both for biogeographers interested in the niche as well as land managers involved in conservation and restoration projects, which rely on climatic tolerance data (see Brown et al. 2008 for examples). In order to produce more robust estimates of climatic tolerance, and to better infer how well distribution data approximate fundamental tolerance limits, more physiological data based on experimental manipulations are needed.

Species with larger range sizes had increasingly broader climatic tolerance estimates derived from distribution data (Figure 2-2). The linear regression models showed that for all climate variables, there was a positive relationship between range size and ΔCN values, although this relationship was not significant for maximum precipitation. This increasing disparity between the two datasets suggests that climatic tolerance inferred from species with small ranges is likely to underestimate the climatic niche more severely than widespread species. This result may be partially due to errors associated with modeling species with few occurrence points (Wisz et al. 2008). For species with a small number of occurrence records, SDMs tend to produce locally accurate models of suitable climate space but perform poorly at projecting outside the range of sampled conditions (Hernandez et al. 2006, Pearson et al. 2007). Several recent studies have also highlighted the importance of range size when considering how well distribution data approximate climatic tolerance. For example, species with larger ranges were less likely to show a climatic niche expansion when introduced outside their native ranges (Early and Sax 2014, Li et al. 2014, Bosci et al. 2016). Similarly, species with larger ranges were more likely to fill in available habitat at range margins (Sunday et al.

2015). Our results support these findings, suggesting that distribution data are more apt to produce robust estimates of climatic tolerance when species have large ranges.

Our comparison of ΔCN values between plant growth forms suggests that distribution data for different taxonomic groups have unequal climatic niche filling (Figure 2-3A-C). Previous studies suggest that niche filling might differ between groups. (Araújo and Pearson 2005) found a higher degree of niche filling among European vascular plants relative to reptile and amphibian species. In contrast, the mean range filling was found to be less than 40% for 55 native European tree species indicating that distributions were likely heavily influenced by non-climatic factors such as dispersal constraints (Svenning and Skov 2004). Our results suggest that distribution data for forbs and grasses generally encompass a broader climatic niche than distribution data for shrubs and trees.

However, a broader climatic niche for widespread forbs and grasses may not be generalizable across all plants. Shorter generation times might enable faster dispersal and greater niche filling amongst grasses and forbs relative to shrubs and trees. The species included in the USDA PLANTS database are planted throughout the USA for specific conservation or restoration needs (USDA NRCS 2018). For example, the database is used in support of the Natural Resources Conservation Service (NRCS) Plant Materials Program, which selects conservation plant species and implements planting protocols for ecoregions in the USA (USDA NRCS 2018). As a result, the broader climatic niches associated with forbs and grasses may be partially due to human introduction rather than to natural dispersal ability. Differences between the datasets could also occur if experts report an approximation of the average climate space (i.e., the climate space in which a

species will thrive in conservation/restoration projects), while herbarium records are more likely to include rare specimens which could lead to exaggerated climate niches relative to the core distribution.

For narrow range species in particular, combining distribution data with climatic tolerance information will likely improve model projections. However, we caution the biogeography community that climatic tolerance estimates available through USDA PLANTS or TRY (Kattge et al. 2011) should not necessarily be interpreted as `truth'. The expert-based estimates evaluated here appear overly conservative, but even experimentally derived tolerance is influenced by variation within populations (Valladares et al. 2014) and often differs across species ranges (Molina-Montenegro and Naya 2012, Chown and Gaston 2016). The combination of both distribution and climatic tolerance estimates is more likely than strictly correlative models to approximate a species' fundamental niche, thereby improving projections of suitable habitat under novel combinations of climatic conditions (Dormann et al. 2012). A combined approach also allows the modeler to identify areas of higher confidence within the projection (e.g., where the models overlap) and areas where the predictor variables failed to capture the factors limiting the species' distribution (e.g., where models differ (Kearney et al. 2010b, Ceia-Hasse et al. 2014). For example, species-specific temperature tolerance data were combined with distribution data to model macroalgae survival (Martínez et al. 2014) and the geographic responses of UK butterflies to climate change (Buckley et al. 2011). Similarly, variation in climatic factors generalized to a single widespread tree species were used to parameterize a hybrid model for six tree species in the Pacific Northwest USA (Coops et al. 2009).

Spatial models are powerful tools for understanding how species are likely to respond to global change, and independent climatic tolerance data are increasingly used to improve estimates derived from distribution data. Biogeographers recognize the need to develop more integrated, mechanistic models but the cost of developing mechanistic models precludes their use for large numbers of species. For the majority of the plants we evaluated, distribution data suggest a broader climatic tolerance than expert-based climate tolerance estimates. For widespread species in particular, distribution data produce a better approximation of climatic tolerance.

Acknowledgements

This research was supported by NASA's Biodiversity and Ecological Forecasting Program (NESSF: 15-EARTH15F-133) and by the National Institute of Food and Agriculture, U.S. Department of Agriculture, the Massachusetts Agricultural Experiment Station and the Department of Environmental Conservation under Project No. MAS00016. We thank Jesse Bellemare and Jack Finn for helpful advice.

Figures

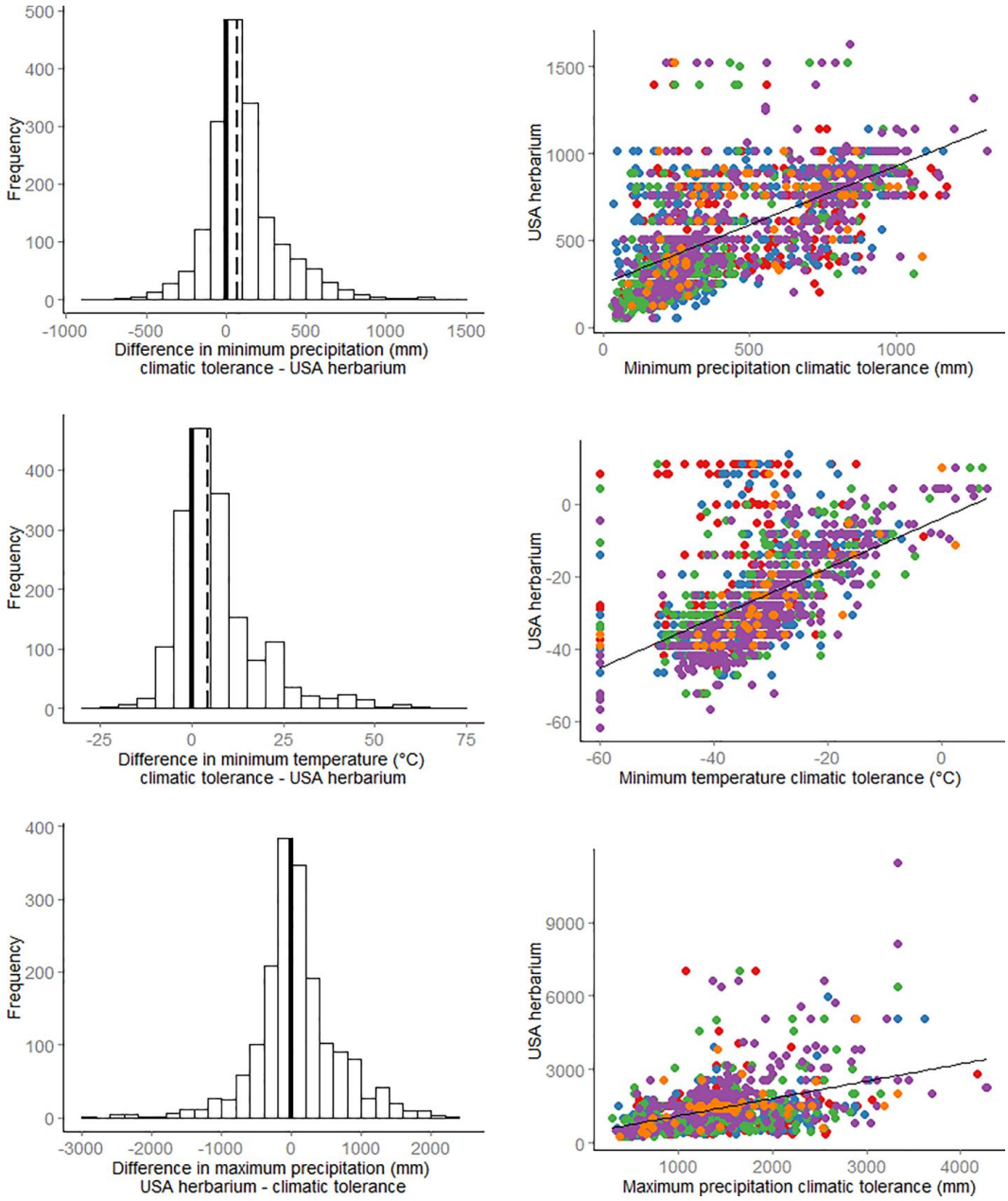

Figure 2-1. Frequency distributions of comparative niche values (ΔCN).

For all climate variables, herbarium records from GBIF tend to estimate broader climatic niches than climatic tolerance estimates. Histogram values to the right of zero (solid line) indicate species with broader climatic niches from herbarium records. The dashed line indicates the median ΔCN. Scatterplots show the raw values of climatic

tolerance derived from expert-estimates vs. herbarium records. Colored points differentiate species' primary growth forms (red = Forb, blue = Grass, green = Shrub, purple = Tree, orange = Vine). Points below the 1:1 line for minimum precipitation and minimum temperature and above the 1:1 line for maximum precipitation have broader niches described by herbarium records.

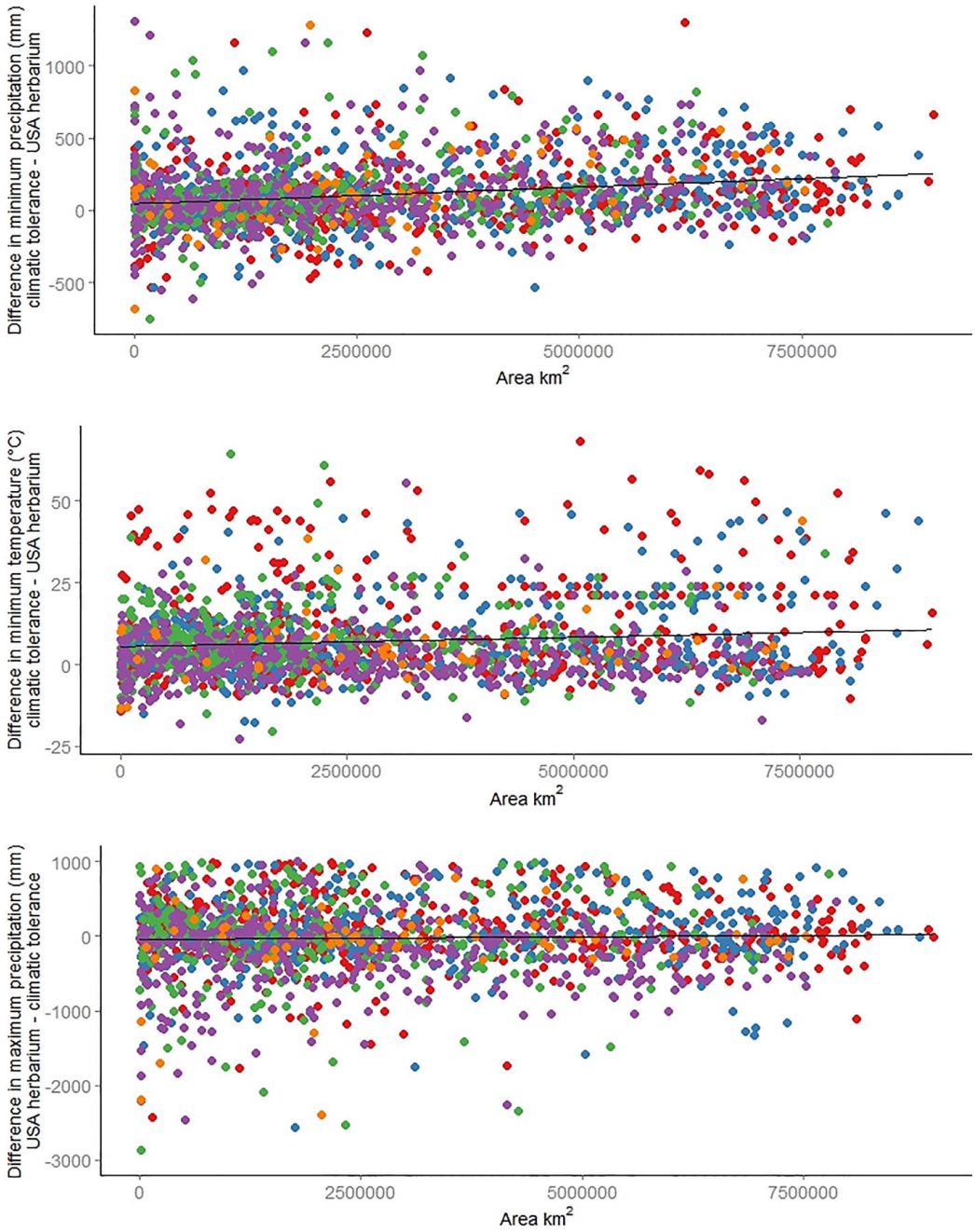

Figure 2-2. Change to ΔCN relative to species range size.

Herbarium records estimate an increasingly broader climatic tolerance relative to expert based climate tolerance (ΔCN) as range size increases. A significant positive relationship was found for minimum precipitation and minimum temperature. The trend was similar, although not significant, for maximum precipitation. ΔCN values for

maximum precipitation were truncated at -3,000 for ease of interpretation. Colored points differentiate species' primary growth forms (red = Forb, blue = Grass, green = Shrub, purple = Tree, orange = Vine).

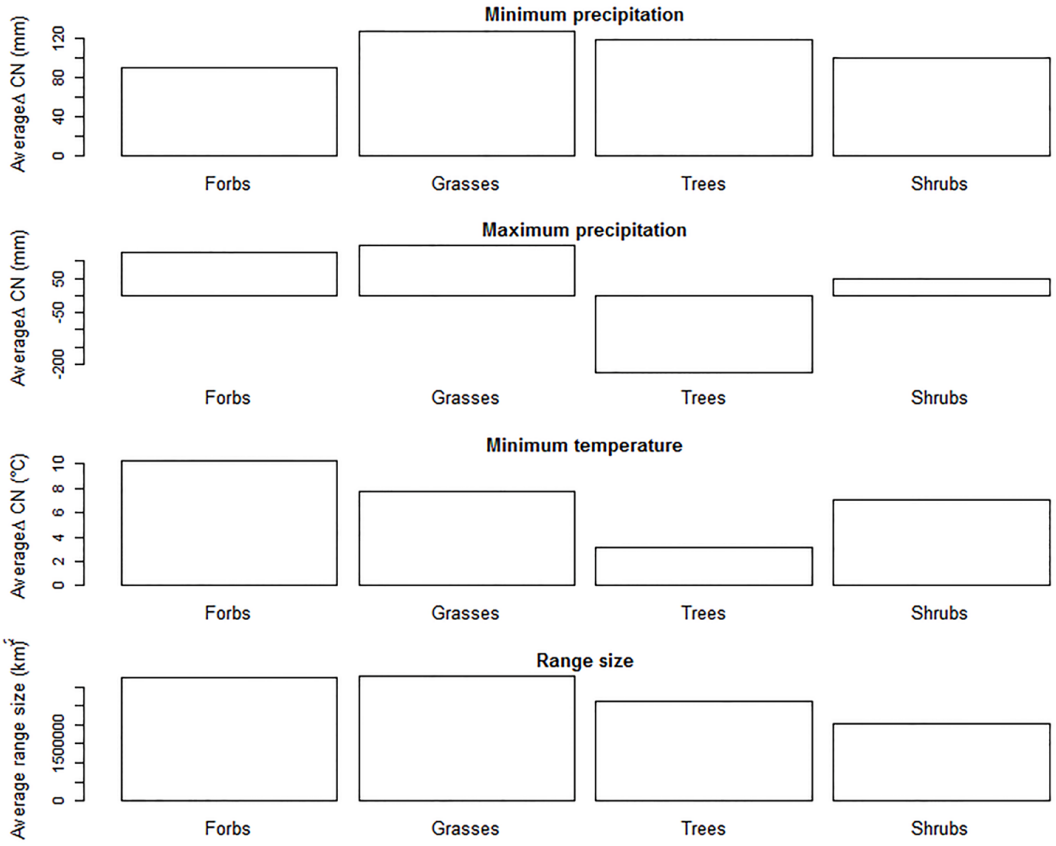

Figure 2-3. Difference between calculated climate niche (ΔCN) varies by growth form.

ΔCN was primarily positive (distribution data suggested a broader tolerance than expert-based climate tolerance), but differed by growth form for all climate variables, suggesting that the effectiveness of distribution data for identifying the climatic niche might vary with growth form. Plant growth forms had significantly different average ΔCN values for minimum precipitation, maximum precipitation and minimum temperature. Average range size also differed by growth form for all data.

CHAPTER 3

PROJECTING ABUNDANCE UNDER A CHANGING CLIMATE IMPROVES CONSERVATION PRIORITIZATION - A CASE STUDY WITH SAGEBRUSH

Authors

Caroline A. Curtis[1] and Bethany A. Bradley[2]

Abstract

Big sagebrush (*Artemisia tridentata)* characterizes shrublands of the intermountain western U.S. and provides habitat for many obligate species. However, sagebrush is threatened by several forms of global change, including invasive species, land cover change, and climate change. To characterize risks to sagebrush and sagebrush obligate species, several studies have projected the presence of sagebrush under current and future climate scenarios. However, populations of sagebrush and sagebrush obligate species are influenced more by the abundance of sagebrush than presence alone. Therefore, conservation prioritization would be better informed by spatial models that project change in sagebrush cover. Here, we leveraged unique spatial percent cover datasets to model potential sagebrush cover under current and future climate in the western U.S. We compiled 9,515 field surveys of vegetation percent cover collected between 1999-2016 across the floristic provinces of sagebrush and shrub-steppe. We used Random Forest regression to predict sagebrush cover based on bioclimatic predictor variables and topography under current and future conditions. We used potential

[1]Graduate Program in Organismic and Evolutionary Biology, University of Massachusetts Amherst, Amherst, Massachusetts 01003
[2]Department of Environmental Conservation, University of Massachusetts Amherst, Amherst, Massachusetts 01003

sagebrush cover to estimate habitat for five sagebrush-obligate species. The random forest model explained 36% of the variance in sagebrush percent cover. Consistent with previous research, projections with high model agreement show a decline in sagebrush cover over 53% of the study region and a strong decrease in climatic conditions suitable for high sagebrush cover. However, percent cover analysis suggests that the potential future distributions of sagebrush obligate species will vary markedly. The pygmy rabbit (*Brachylagus idahoensis*), which has the highest percent sagebrush requirements, is projected to lose up to 91% of currently suitable habitat. In contrast, the Brewer's sparrow (*Spizella breweri*), which has the lowest sagebrush percent cover requirements, is projected to gain up to 26% of additional sagebrush habitat. These results can guide conservation efforts by identifying regions and climate conditions most likely to support sagebrush and sagebrush obligate species in the context of climate change. Projections of abundance provide important inference about risks to species populations within their ranges.

Introduction

Species distribution models have been developed for many taxa to project how the ranges of species could respond to the unprecedented changes occurring as a result of climate change (Iverson and Prasad 1998, Perry et al. 2005, La Sorte and Thompson 2007, Moritz et al. 2008, Tingley et al. 2009). The goal of species distribution models (SDMs) is to quantify the relationship between a species and its environment in order to identify spatial changes in habitat as environmental conditions change. However, because the most readily available species distribution datasets measure presence only, corresponding SDMs typically focus on modeling the probability of species occurrence

(e.g., Elith et al. 2006, Elith and Leathwick 2007). While occurrence models identify climatic conditions suitable for an individual to establish, they do not provide insight into abundance, nor can they project population growth or decline within the range margins that remain stable. Quantifying abundance is critical for many ecological questions. Spatial variation in abundance provides insight into the physiological constraints of species and interspecies competition and can be used to monitor ecosystem health and identify suitable habitat (Brown et al. 1995).

Because of the importance of abundance for understanding landscape to regional populations, several studies have tested whether models based on widely-available occurrence data can serve as a proxy for projections of abundance. However, the results of these studies are equivocal. For example, Pearce and Ferrier (2001) developed models predicting environmental suitability based on presence and absence of 44 species of plants, but environmental suitability was significantly correlated to observed abundance in only 12 species. Similarly, Filz et al. (2013) found a significant correlation between modeled probability of species occurrence and observed abundance for only seven of the 61 butterfly species they tested. In contrast, VanDerWal et al. (2009) found a positive relationship between environmental suitability derived from occurrence data and abundance for 84% of the 69 vertebrates they tested. A recent meta-analysis of 30 studies found a significant, positive correlation between probability of occurrence and observed abundance (Weber et al. 2017). However, Weber et al. (2017) focused on studies that included absence information in observations of abundance. Pearce and Ferrier (2001) showed that, while relationships between probability of occurrence and abundance were significant when absences were included, the relationships were poor or

non-significant when absences were excluded. In other words, suitability models based on occurrence can effectively differentiate between presence and absence but cannot differentiate between levels of abundance if a species is present. Thus, we cannot assume that suitability models based on occurrence data alone are an effective proxy for species abundance.

Understanding abundance is an important aspect of sagebrush conservation as it allows us to make inferences regarding the likelihood of future stability or decline of sagebrush populations. The sagebrush ecosystem now covers only 50% (30-40 million hectares; (Knick 1999, Wisdom et al. 2005, Davies et al. 2011)) of its original extent in the arid and semi-arid land in western North America and Canada. Threats to the sagebrush ecosystem include shortened fire return interval (Whisenant 1990, Balch et al. 2013), invasive plants (Whisenant 1990, Nielsen et al. 2011, Bradley et al. 2017), oil and gas development (Holloran 2005, Thomson et al. 2005), and climate change (Chambers and Pellant 2008, Bradley 2010, Still and Richardson 2015). Changes to the sagebrush ecosystem alter vegetation community structure as well as populations of those species that rely on sagebrush for all or part of their lifecycle. Many of these sagebrush-obligate species are listed as "Species of Greatest Conservation Need" (Benson 2016) because of the imminent threat of sagebrush habitat loss.

Sagebrush obligate species have a range of habitat needs associated with sagebrush cover. For ground-dwelling and/or burrowing species, tall, dense shrub cover provides safety from predators and secluded burrow entrance points (Green and Flinders 1980, Mullican and Keller 1987). For example, pygmy rabbits have been shown to occupy sites with significantly greater sagebrush cover and height than in surrounding

patches (Green and Flinders 1980, Gabler et al. 2001). As a result, pygmy rabbits and sagebrush voles are thought to prefer relatively high percent cover of sagebrush (Mullican and Keller 1986, Keinath and Mcgee 2004, Reeder and Reeder 2005). Similarly, birds may select nesting habitat based on features that provide cover from predators, available supportive substrate for nest size, and the thermal environment within sagebrush foliage (Rich 1980, Petersen and Best 1985a, b). However, sagebrush-obligate birds such as the sage sparrow and sage thrasher are thought to occupy a wider range of sagebrush cover than ground-dwelling animals (Holmes and Altman 2012). Thus, sagebrush cover is an important consideration for conservation of sagebrush-obligate species.

Because of the importance of sagebrush ecosystems coupled with its rapid decline, a number of studies have investigated its distribution and abundance at landscape scales. At the landscape scale, studies have focused on modeling shrub cover through time, primarily using data derived from satellite imagery. For example, a study in Wyoming integrated presence data collected in situ and remote sensing data with resolutions of 2.4 m (Quickbird), 30 m (Landsat), and 56 m (AWiFS) to quantify shrub cover (Homer et al. 2012). Another multi-sensor study combined high resolution hyperspectral data with LiDAR data to characterize sagebrush stand distribution and structure (Mundt et al. 2006). While these studies provide important insight about the current distribution of sagebrush, they do not extend to the regional scale, nor do they consider potential changes in sagebrush cover associated with climate change.

At the regional scale, studies have focused on modeling presence-only or presence/absence data to predict areas with suitable climate habitat under current and

future conditions to inform conservation (Meinke et al. 2009, Still and Richardson 2015) and quantify risks from global change (Bradley 2010). Distribution models include empirical analyses (Meinke et al. 2009, Bradley 2010, Still and Richardson 2015) as well as more mechanistic models. For example, Schlaepfer et al. (2012) incorporated ecohydrological variables into distribution models to understand how hydrological changes could alter sagebrush distribution. Other studies have combined correlative models and mechanistic models to predict the impact of changing community structure on future sagebrush distribution (Nielson et al. 2005) and sagebrush climate sensitivity (Renwick et al. 2018). However, to date, no studies have used percent cover data to model sagebrush cover on a regional scale.

Here, we present a first regional model of sagebrush percent cover based on climate conditions and forecast change in sagebrush cover by 2100. We also present case studies showing how continuous cover data are essential for informing habitat projections of sagebrush-obligate species. Projections of future sagebrush cover can be used to identify areas with the potential to support sagebrush-obligate species long-term and, therefore, might be of high conservation priority.

Methods

Study System

Our study focused on the western US and encompassed approximately 1 million km^2, including the Great Basin, Wyoming Basin, and Columbia Plateau which account for 70% of the current sagebrush distribution (Wisdom et al. 2005). We restricted the analysis to the spatial extents of those regions in the intermountain west that have the

highest concentrations of sagebrush delineated by the *Floristic Provinces of Sagebrush and Associated Shrub-steppe Habitats in Western North America* (Meinke 2004).

Species Data

We compiled big sagebrush (*Artemisia tridentata*) percent cover data from the Bureau of Land Management (BLM), the Nevada Department of Wildlife (NDOW), and the Utah Division of Wildlife Resources (UDWR). Percent cover was recorded from 3 x 50 m line transects radiating from a central point (BLM, NDOW) or from 5 x 100 ft line transects (UDWR). These plot data were resampled to identify maximum percent cover within a 1 km cell size, which is comparable to the interpolated climate data used (30-arc seconds; (Thornton et al. 1997)). We chose to use maximum percent cover values to estimate the highest percent cover big sagebrush could achieve given the local climate conditions. However, we also tested the analysis using mean values and found comparable results (Appendix G).

Although there are many subspecies of sagebrush present in the western US, we modeled sagebrush cover at the species level. A species level analysis was necessary because only the UDWR dataset contained percent cover at the subspecies level. Furthermore, the natural history reports used to define obligate species' habitat preferences either did not specify preferred subspecies or reported that more than one subspecies of big sagebrush species was used. Therefore, we assume that each of the common subspecies of sagebrush in the Great Basin could provide equally good habitat.

Hundreds of species rely on the sagebrush ecosystem to some extent, but far fewer can be considered sagebrush obligates (depending entirely on the sagebrush ecosystem for all or part of their life-cycle). We chose to focus on the latter category as

they are the most likely to be affected by changes in sagebrush cover. We reviewed literature to compile a list of species that qualified as sagebrush obligates (Rowland et al. 2006, 2011). For those species, percent cover requirements were compiled by reviewing literature including field studies, natural history reports, and reports from surveys conducted by federal agencies.

Predictor Layers

To predict regional sagebrush cover, we created sets of 19 bioclimatic variables based on Daymet climate interpolations (Thornton et al. 1997) for current (1980-2014) and future (2070 -2099) time periods using the biovars function in the R dismo package (Hijmans et al. 2014). Rather than focusing on monthly or annual averaged climate, bioclimatic variables aim for greater biological relevance and include variables such as precipitation seasonality (coefficient of variation) and precipitation of warmest quarter. Future climate projections vary depending on the modeling group and emissions scenario. We used an ensemble of five Atmosphere-Ocean General Circulation Models (AOGCMs) and two Representative Concentration Pathways (emissions scenarios) to encompass likely future climate conditions. The models were selected based on their ability to capture the range of uncertainty in future climate projections in the western US (see Renwick et al. 2018 for details on model selection). Emissions scenario RCP4.5 assumes that peak emissions will occur before 2050 followed by a decline, resulting in a modeled mean increase of 1.8° C by 2100 (IPCC 2103). RCP8.5 assumes a continuous rise in emissions throughout the 21st century, resulting in a modeled mean temperature increase of 3.7° C (IPCC 2103). In the main text, we present the results for RCP4.5, with results from RCP8.5 in Appendix H. In addition to the bioclimate variables, we included

topographic data which were derived from the Shuttle Radar Topography Mission (SRTM) digital elevation model (DEM) and resampled to the same 1 km spatial resolution as the climate data.

Analysis

We modeled sagebrush percent cover using Random Forest regression (randomForest package in R; (Liaw and Wiener 2002)). Random Forest is an ensemble modeling approach which relies on a random bootstrap resampling of predictor data to create hundreds of regression trees. In this case, the response variable (sagebrush percent cover) was predicted based on values of the bioclimate variables and topographic data at the corresponding location. For each tree in the random forest (500 in our model), two-thirds of the data are randomly sampled and used for training with the remaining one-third retained for model testing. Three randomly selected predictor variables were drawn for use in each split of the tree. The best regression tree is then calculated for that unique set of randomly drawn percent cover data and predictor variables. The final prediction of percent cover is determined by a vote-counting process over all 500 trees. For each tree, the "Out-of-bag" (OOB) error estimates are calculated and can then be aggregated over all trees to determine both variable importance and model performance. Although the out-of-bag error estimates are robust, we also created an independent validation by withholding a random one-third of the response data to measure correlation between the observed and predicted values. Because the model randomly selects a set of predictor variables to use in each tree, Random Forest has low sensitivity to predictor variable auto-correlation. Nevertheless, we tested model performance to determine the optimal number and most important predictor variables. We selected the most important

predictor variables from the 20 available by using the Random Forest Cross-Validation for feature selection (rfcv) function in the randomForest package for R (Liaw and Wiener 2002). Random forest regression model predictions are the mean of the distribution of percent cover estimates from the 500 trees. Modeled percent cover values therefore tend to underestimate high values and overestimate low values. Therefore, we calculated a second regression model based on the training data and the predicted percent cover values. The gain and offset from this regression model was applied to the original output for all current and future models.

To calculate habitat suitability, we used the sagebrush cover models to create binary suitability maps based on the range of published cover values for each obligate species. For both current and future models, we excluded non-vegetated areas (salt flats and water bodies) based on the Landfire Version 1.13 classification (Rollins 2009, LANDFIRE 2014). We then created future ensemble maps by summing the binary maps for all five climate models under each emissions scenario. We used a threshold of four models to differentiate areas of high and low confidence in our model results. Pixels with four or five models predicting suitable habitat can be interpreted as suitable with high confidence. Pixels with one or more models predicting suitable habitat can be interpreted as suitable with lower confidence. Pixels with zero models predicting suitable habitat were interpreted as unsuitable. To calculate the influence of climate change on sagebrush cover across the study area, we averaged projected sagebrush cover from all five AOGCMs. We compared mean projected future cover to modeled current cover to estimate the magnitude and extents of change in sagebrush cover.

Results

After spatially aggregating the sagebrush data to a 1 km grid, the number of field observations was reduced from 13,196 to 9,515 points (Figure 3-1) which ranged from 0 to 73% cover (median = 2.7%). One-third of these points reflected sagebrush absence (i.e., 0% cover) and the majority of the data measured sagebrush cover of less than 50% (only 22 points were greater than 50%). We identified five species (three bird species and two mammal species) with sufficient information about sagebrush percent cover requirements to model regional habitat suitability (Table 3-1).

We retained 10 predictor variables with the highest importance for the random forest models based on the random forest cross-validation (Table 3-2). Most of the selected variables pertain to precipitation. This is consistent with previous studies of temperature and precipitation in the intermountain west, which suggest that plants in semiarid systems are vulnerable to changes in precipitation (Reynolds et al. 1999, Weltzin et al. 2003).

Based on the out-of-bag estimate, the random forest model explained 36% of the variance in sagebrush percent cover. An independent test withholding one-third of the dataset for testing showed a similar result, with an R^2 of 0.325 (Figure 3-2). Within the sagebrush floristic region (Figure 3-1), the Random Forest model projects that 69% of land area could currently support between 1-15% sagebrush cover, with 21% potentially supporting greater than 15% sagebrush cover (Figure 3-3) and the remaining 10% unsuitable for sagebrush. Although the model projections for future sagebrush extents highlight a loss (i.e. pixels projected to have at least 5% cover currently and declined to less than 5% percent cover under future climate) of only 51,601 km^2 (4.7% of the study

region) of sagebrush, the models suggest a marked decline in sagebrush percent cover throughout the range (Figure 3-4). Under future climate conditions, 94% of land area is projected to support between 1-15% cover, with the bulk of the increase in the 6-10% cover range. Only 6% of land area is projected to support greater than 15% sagebrush cover under future climate change (Figure 3-3). Among future projections, there were few areas where all five models projected zero percent cover. Therefore, after averaging the five future models, less than one percent of the study area is projected to be unsuitable (i.e., 0 % cover), but this modeling framework is designed to assess change in cover, not loss of suitability. Importantly, our models project a decrease of sagebrush abundance throughout 38% of the range (Figure 3-4).

Currently, there are over 500,000 km^2 with climate conditions suitable to support the sagebrush cover required by each of the three obligate birds. In contrast, less than 200,000 km^2 currently have suitable climate to support adequate sagebrush cover for the pygmy rabbit and the sagebrush vole (Table 3-3; Figure 3-5). Using a low confidence future scenario where a pixel is considered suitable by 2100 if percent cover modeled by any one or more AOGCM was suitable, climatic conditions for suitable sagebrush cover could increase for the bird species (*A. nevadensis* (37%), *O. mantanus* (36%), and *S. breweri* (25%)) but decrease for the mammal species (*B. idahoensis* (- 46%), and *L. curtatus* (-29%)). Using a high confidence future scenario where a pixel is considered suitable only if percent cover modeled by four or more AOGCMs was suitable, the projections are less optimistic. The high confidence future projections suggest an increase in climatic conditions that would support suitable sagebrush cover for one bird species (*S. breweri* (11%)), a slight decrease for two bird species (*A. nevadensis* (- 2%),

O. mantanus (- 3%)), and a larger decrease for the two mammal species (B. idahoensis (-91%), and L. curtatus (-70%)). Although both *B. idahoensis* and *L. curtatus* are projected to lose the majority of their suitable habitat space, there are areas that currently have climate conditions suitable for their sagebrush cover needs that are projected to remain so in the future (e.g., central Colorado; western Wyoming; Figure 3-5D). These areas might represent important refugia from the impacts of climate change.

Discussion

Regional projections of the effects of climate change on species distribution tend to focus solely on occurrence. The resulting models forecast shifts in species ranges but are not designed to assess changes in cover or abundance within species ranges. For sagebrush, which dominates vegetated cover in many areas and characterizes habitat for several obligate species, forecasting change in cover is critical for understanding risk. This study provides a first assessment of the effects of climate change on sagebrush cover.

Our models project a substantial loss of sagebrush cover throughout the study region. Southwest Wyoming and Nevada are expected to lose the highest percentage of sagebrush (up to 45%; Figure 3-3 and 3-4). Areas in Colorado, Idaho and Utah are projected to gain the largest percentage of sagebrush, although only up to 20% gain is predicted for any of the study region. Although low plant density is not necessarily linked to decreased population growth (Feldman and Morris 2011), low cover coupled with higher fire frequency could limit sagebrush recovery and increase the likelihood of a shift to an ecosystem dominated by other vegetation types (Young and Evans 1978,

Whisenant 1990, Baker 2006). In addition to mapping change, our models can be used to identify potential climate refugia. For example, the pygmy rabbit is projected to have persistent suitable sagebrush cover in western Colorado and Wyoming and southern Idaho (Figure 3-5). These areas could be considered high priority for conservation.

Although our models project a decrease of sagebrush abundance throughout 38% of the range, only 4.7% of the study region shifted from suitable (at least 5% cover) to unsuitable (less than 5% cover) with climate change. In comparison, Still & Richardson (2015) projected a loss of sagebrush presence across 39% of the Great Basin. This discrepancy might be due to the climate predictor variables selected for the two studies. The most important predictors for our percent cover model were largely precipitation driven (Table 3-2). In contrast, the most important predictors in Still & Richardson's (2015) occurrence model were related to temperature. It is plausible that different types of climate variables influence the presence (establishment) vs. the abundance (population growth) of a given species (Jiménez-Valverde et al. 2009). Despite the differences in goals, our model is consistent with previous studies in suggesting that substantial declines to sagebrush cover are likely with climate change.

Interestingly, despite projections of substantial declines in high sagebrush cover (Figure 3-4), the effects on sagebrush obligate species vary markedly. Species with low minimum sagebrush cover requirement could maintain or even gain habitat if sagebrush cover declines from areas where it was previously dense. Brewer's sparrow, Sage sparrow, and Sage thrasher all have low minimum requirements (5-10%) and a wide range of suitable habitat cover (Table 3-1). These minimum cover values fall within the most widely projected range of cover values under current and future climate conditions

(Figure 3-3). Because of the availability of these low sagebrush cover classes, the three bird species are all expected to gain climatically suitable area based on low confidence projections (Table 3-3). Brewer's sparrow is also expected to gain climatically suitable area based on the high confidence projections (Figure 3-5) while climatically suitable area for sage sparrow and sage thrasher decrease minimally (2% and 3% loss, respectively) (Table 3-3). In contrast, species that are dependent on dense sagebrush cover are projected to lose substantial habitat. The sagebrush vole and pygmy rabbit require at least 17% and 20% sagebrush cover, respectively (Keinath and Mcgee 2004; Reeder and Reeder 2005). Of the areas projected to have adequate sagebrush cover for these species, 70%-91% is projected to be lost under future climate conditions (Table 3-3). According to our models, both the sagebrush vole and the pygmy rabbit will lose climatically suitable area in the future based on either the low confidence models (-29% and -46%, respectively) or high confidence models (-70% and -91%, respectively) (Figure 3-5, Table 3-3). This type of analysis is not feasible with occurrence-based models. Focusing on abundance data and percent cover models allows us to better predict how climate change may impact species habitat.

This work highlights the need for more comprehensive data collection to support landscape or regional modeling of species abundance or cover. Few studies to date have focused on modeling abundance of native plants. Demographic-based models could provide the detail needed to model abundance. In one such case, abundance of a native *Pinu*s species relative to climate change was projected using a demographic model (García-Callejas et al. 2016). However, these models require intensive sampling of the species physiology and environmental requirements and, therefore, might be prohibitive

at large spatial scales. Instead, spatial models like the one presented here can be used to estimate relationships between abundance and environmental conditions and project change at regional scales, provided large-scale survey data are available. State and regional vegetation surveys, like the ones used in this study, are critical for advancing spatial analyses of species abundance.

Although our analysis focused on percent cover requirements of sagebrush obligate species derived from natural history reports (Table 3-1), many factors affect species habitat, including landscape characteristics (e.g., sagebrush connectivity), other environmental conditions (e.g., soil, topography, and climate), and anthropogenic land use (e.g., Leu et al. 2008). As a result, habitat projections for these species based on sagebrush cover (Table 3-3) are likely to be further constrained.

Our model explained 36% of the variation in regional sagebrush cover. This finding is consistent with other models of regional abundance. For example, Kulhanek et al. (2011) had success modeling carp abundance based on occurrence for lakes within the same state in which data were collected with 73% of the variation abundance explained. However, their ability to explain variation in abundance dropped to 32% when the models were extrapolated to a neighboring state. Regional models of invasive cheatgrass (*Bromus tectorum*) cover explained 24% and 34% of variation in cheatgrass cover (Peterson 2006, Bradley et al. 2017). Our model's explanatory power is consistent with these models of regional abundance. However, the modest correlation values add uncertainty to projections of cover under current and future climates. It is likely that some of this uncertainty stems from extrapolation of plot surveys as representative of cover within a 1 km^2 pixel. It is also likely that landscape-scale characteristics and

anthropogenic land use, which were not included in our model, also influence observed sagebrush cover.

Although sagebrush growth is strongly influenced by climate (Epstein et al. 2002, Lauenroth and Bradford 2006, Schlaepfer et al. 2012), climate alone does not determine percent cover. At landscape to local scales, disturbances such as oil and gas development (Walston et al. 2009), roads and housing development (Gaines et al. 2003, Leu et al. 2008), and livestock management (Knapp 1996) can decrease sagebrush cover. Sagebrush cover is also strongly influenced by invasive cheatgrass cover, which increases fire return intervals and reduces sagebrush cover (Whisenant 1990, Brooks and Pyke 2001, Balch et al. 2013, Bradley et al. 2017). Adding predictor variables at multiple scales (e.g., Bradley 2010) may improve future models of sagebrush cover and habitat for sagebrush obligate species.

In this study, we used an ensemble of five climate projections. Taken separately, variation between the five AOGCMs caused the upper threshold of mean sagebrush percent cover projections to range from 28% to 39%. By averaging across five climate models, we reduced the effect of variability associated with any one AOGCM. Similarly, a multi-model approach in which more than one model is used to predict current and future distributions can be used to create projections with higher confidence. Renwick et al. (2018) used a multi-model approach to evaluate the climate sensitivity of big sagebrush and found that biogeographic models can overestimate risk of range expansion or contraction because they generally do not include fine-scale variables which contribute to a species' local distribution. However, Renwick et al. (2018) also suggest that sagebrush is likely to decline at warmer sites, but increase at cooler sites. Our spatial

projections are consistent with this finding, suggesting an increase in sagebrush cover only at higher elevation margins of its current range (Figure 3-4). Nonetheless, Renwick et al. (2018) recommend the use of both multiple climate projections as well as multiple modeling approaches for forecasting change spatially. Our results therefore provide an important first step for regional analyses of sagebrush abundance.

Conclusions

Sagebrush ecosystems and sagebrush obligate species are under threat from a variety of forms of anthropogenic global change. Previous studies based on occurrence data have projected marked contractions of the sagebrush range. This study suggests that even areas likely to maintain the presence of sagebrush will likely experience declines in sagebrush cover due to climate change. These declines in cover could have very different implications for sagebrush obligate species, with obligates dependent on higher sagebrush cover the most vulnerable.

Acknowledgements

We thank Meghan Holton (BLM), Maria Jesus & Lee Turner (NDOW), and Jason Cox (UTRT) for collecting and sharing vegetation surveys. CAC was supported by NASA's Biodiversity and Ecological Forecasting Program (NESSF: 15-EARTH15F-133). BAB acknowledges support from the Joint Fire Sciences Program 15-2-03-6.

Tables

Table 3-1. List of sagebrush-obligate species and reported sagebrush cover requirements.

Species	Required % cover	Source
Brewer's Sparrow (*Spizella breweri*)	5-35	(Holmes and Altman 2012)
Sage Sparrow (*Artemisiospiza nevadensis*)	10-35	(Holmes and Altman 2012)
Sage Thrasher (*Oreoscoptes montanus*)	10-40	(Holmes and Altman 2012)
Sagebrush Vole (*Lemmiscus curtatus*)	17-29	(Reeder and Reeder 2005)
Pygmy Rabbit (*Brachylagus idahoensis*)	20-46	(Keinath and Mcgee 2004)

Table 3-2. Selected predictor variables used in the random forest models (1 is highest importance based on the Random Forest model).

Importance	Predictor Variable
1	Precipitation Seasonality
2	Elevation (DEM)
3	Precipitation of Warmest Quarter
4	Precipitation of Coldest Quarter
5	Mean Temperature of Wettest Quarter
6	Min Temperature of Coldest Month
7	Precipitation of Driest Quarter
8	Precipitation of Wettest Month
9	Precipitation of Driest Month
10	Precipitation of Wettest Quarter

Table 3-3. With climate change, habitat for sagebrush obligate species varies from a gain or little change for the three birds, to a large decline for the two mammals.

Projections are based on RCP 4.5 and maximum sagebrush cover per pixel. 'Low confidence' includes all pixels with climate projected to support suitable sagebrush cover from any one or more of the five AOGCMs. 'High confidence' includes just those pixels where four or five AOGCMs projected that climate was suitable for the required sagebrush cover. Future models include less than 1 km^2 of area predicted to have greater than 35% sagebrush. Therefore, *A. nevadensis* and *O. montanus*, which have the similar sagebrush requirements (10-35% and 10-40%, respectively), are predicted to have the same amount of future suitable area. Slight differences in percent change are due to different predicted current suitable area.

	Area (km^2)		
Species	Current	Low Confidence Future (% change)	High Confidence Future (% change)
S. breweri	766,542	955,182 (+25%)	851,515 (+11%)
A. nevadensis	521,904	712,793 (+37%)	508,974 (-2%)
O. montanus	522,790	712,794 (+36%)	508,974 (-3%)
L. curtatus	181,486	129,744 (-29%)	54,499 (-70%)
B. idahoensis	102,721	55,083 (-46%)	9,329 (-91%)

Figures

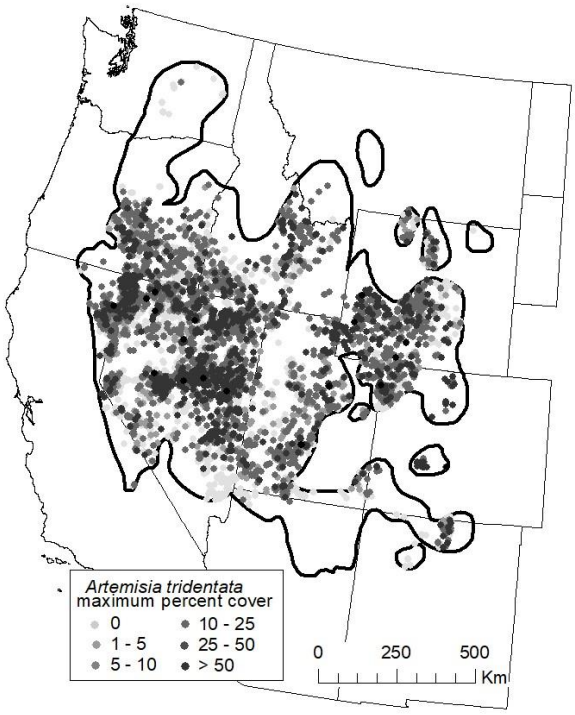

Figure 3-1. Distribution of sagebrush percent cover data within the Floristic Provinces of Sagebrush and Associated Shrub-steppe Habitats in Western North America (black line; (Meinke 2004). Darker points have higher maximum sagebrush cover.

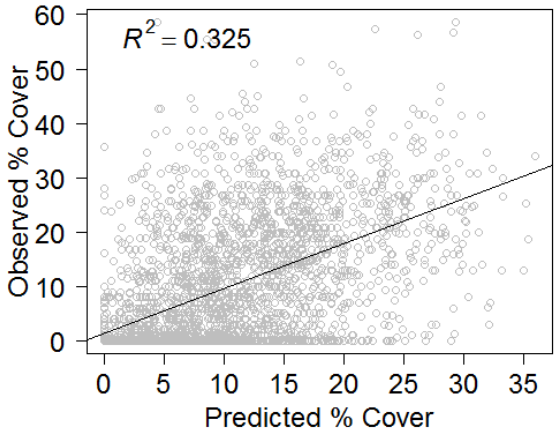

Figure 3-2. An independent validation of the Random Forest model shows a significant relationship between predicted and observed cover ($R^2 = 0.325$; $\rho << 0.001$). The model was trained with two-thirds of the data and the remaining one-third were used to test the projected sagebrush percent cover.

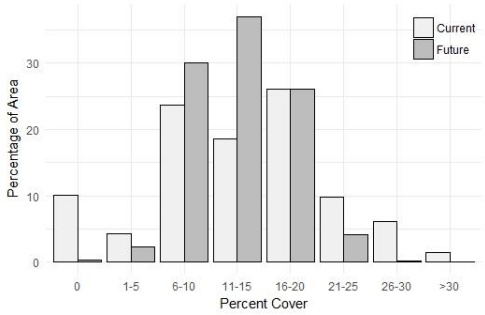

Figure 3-3. A histogram of current and projected future percent cover of sagebrush suggests a marked decline in higher percent cover classes.

Percent cover changes were calculated by comparing current predicted cover to future predicted cover based on the average model output from all five AOGCMs. Averaging the five model projections substantially reduces zeroes and high percent cover values, nonetheless there is a clear shift towards lower sagebrush percent cover.

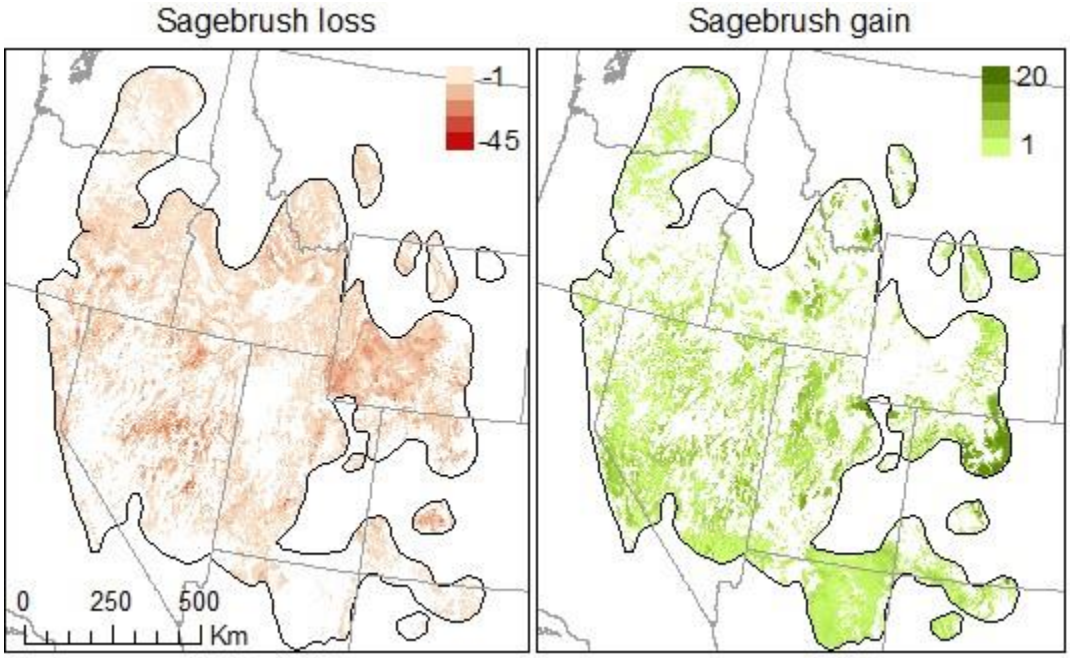

Figure 3-4. Projected changes in percent cover per pixel of sagebrush throughout the sagebrush floristic region.

Sagebrush is projected to decline over 38% of the study area and portions of central Nevada and southwest Wyoming could lose up to 45 percent cover . Sagebrush

cover is projected to increase over 53% of the study area. Cover gains are smaller than losses, but some portions of Colorado and Utah could gain up to 20 percent cover .

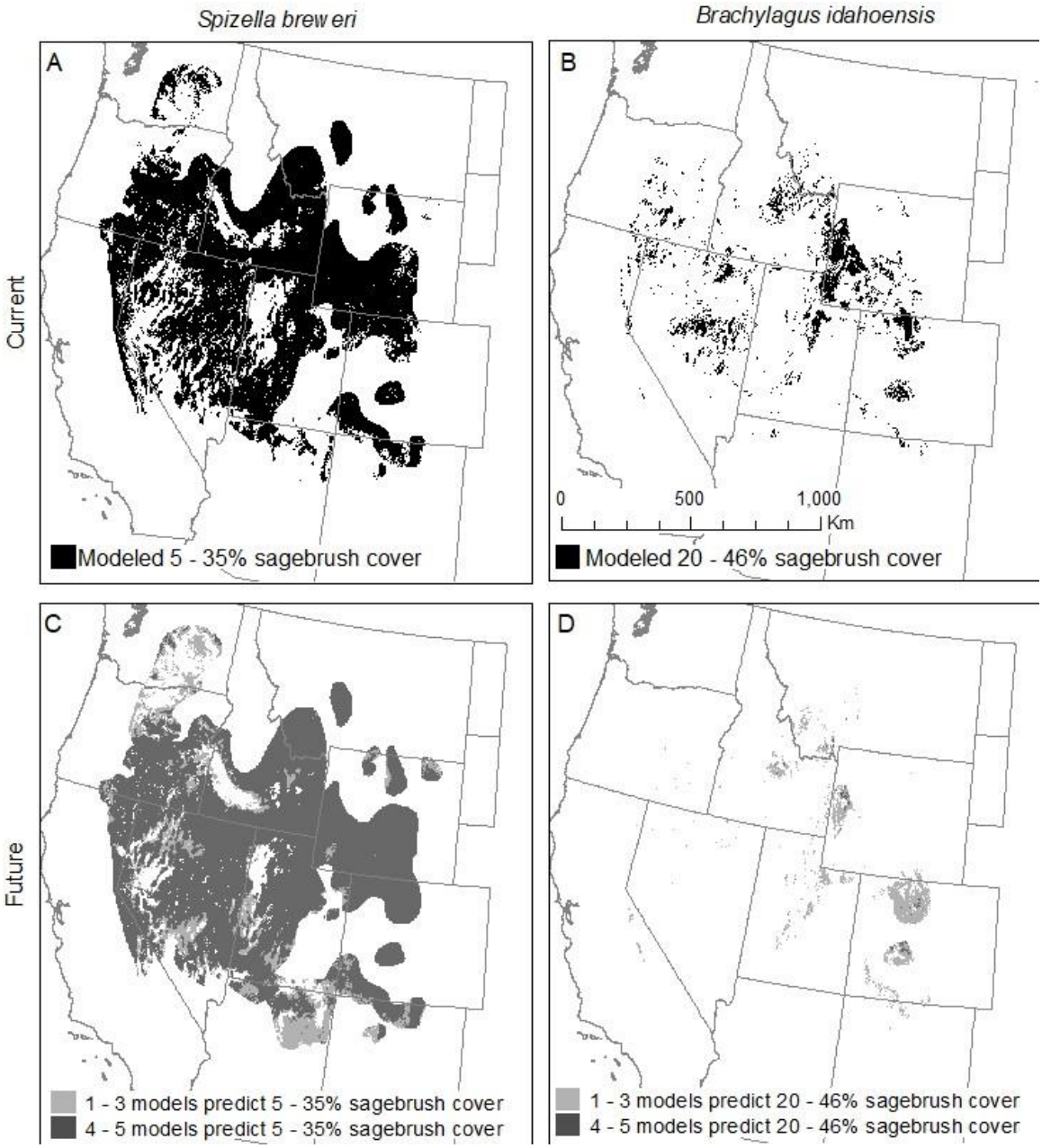

Figure 3-5. Current (A, B) and future (C, D) projected suitable climate for adequate sagebrush cover for the species with the largest (Brewer's sparrow (*Spizella breweri*)) and smallest (Pygmy rabbit (*Brachylagus idahoensis*)) modeled current habitat.

CHAPTER 4

LANDSCAPE CHARACTERISTICS OF NON-NATIVE PINE PLANTATIONS AND INVASIONS IN SOUTHERN CHILE

Authors

Caroline A. Curtis[1], Valerie J. Pasquarella[2,3], and Bethany A. Bradley[2]

Abstract

The spread of non-native conifers into areas naturally dominated by other vegetation types is a growing problem in South America. This process results in a landscape transformation as the conifers suppress native vegetation and leads to altered water and nutrient availability and reduced biodiversity. Previous research highlights the broad spatial extents of this land cover change in parts of Chile. However, in Southern Chile, the extent of plantations and the landscape characteristics associated with plantations and ongoing pine invasions are poorly understood. Here, we characterized pine land cover within two overlapping Landsat scenes (World Reference System 2 Path 231/Row 092 and Path 232/Row 092; ~58,000 km^2) in Southern Chile. We created training data based on historical high-resolution imagery, derived land cover predictors from a time series model, and used a Random Forest classification to map current land cover. The overall classification accuracy was 88%, and the accuracy of the non-native pine class exceeded 90%. Although 71% of pine patches are within 500 m of other pine patches, isolated pine patches were found to occur up to 55 km from the nearest neighbor.

[1]Graduate Program in Organismic and Evolutionary Biology, University of Massachusetts Amherst, Amherst, Massachusetts 01003
[2]Department of Environmental Conservation, University of Massachusetts Amherst, Amherst, Massachusetts 01003
[3]DOI Northeast Climate Adaptation Science Center, Amherst, MA, USA

These distant plantations could exacerbate problems of future invasion by creating propagule sources for novel invasion fronts. In relation to landscape characteristics, non-native pines were found to be more likely to occur in low slope and mid elevation areas. Because most of the study area is native forest, most pine patches border native forest. However, pine patches were almost three times more likely than random patches to border grass/agriculture. This suggests that grasslands and disturbed sites, which have low resistance to pine invasion, are disproportionately exposed to pine propagules. Our results indicate that pine plantations are extensive across Southern Chile, and well poised to cause future invasion.

Introduction

The introduction of non-native tree species has the potential to drastically change the structure and function of recipient ecosystems (e.g., Simberloff et al. 2010, Richardson et al. 2013). This process can lead to an abrupt conversion of land cover and a decrease in native biodiversity as the non-native species replace native forest, grass- or shrubland. In South America, the introduction of northern temperate pine species (e.g., *Pinus radiata* and *Pinus contorta*) and their subsequent invasion is a relatively recent phenomenon and little is known about the total extent of pine plantations or the landscape characteristics of areas where non-native pines occur.

There is a long history of pine species being introduced outside of their native ranges for ornamental or ecological purposes (e.g., erosion control) and for use in commercial timber plantations (see review in Simberloff et al. 2009). Most pine species are native to the northern hemisphere (Procheş et al. 2012) but their ability to adapt to local conditions (Richardson and Bond 1991) and their economic importance (Salas et al.

2016) have driven their spread throughout the southern hemisphere. In many parts of the southern hemisphere, non-native pine plantations were established by the early to mid-1800s. Several pine species were recognized as invasive by the mid to late 1800s in South Africa and New Zealand and by the 1950s in Australia (Simberloff et al. 2009). However, widespread planting of non-native pines in the South American country of Chile did not begin until the mid-1900s (Lara and Veblen 1993). Given the success of pine invasions elsewhere in the southern hemisphere, Richardson et al. (2008) suggested that Chile might be on the verge of a large-scale invasion.

The negative impacts of non-native pines on the ecological function of host landscapes are well documented. Pine invasions are associated with increased fire frequency and intensity, and the post-fire ecosystem is prone to soil erosion and susceptible to pine invasion (Agee 1998, Veblen et al. 2003, Nuñez and Estela 2007, van Wilgen and Richardson 2012, Cóbar-Carranza et al. 2014, Paritsis et al. 2018). Pines require substantially more water than vegetation that undergoes seasonal dormancy and thus can reduce water availability (Le Maitre et al. 2000, van Wilgen and Richardson 2012). In South Africa, for example, streamflow was reduced by 55-100% following the introduction of *Pinus* and *Eucalypt* species (Van Lill et al. 1980, Van Wyk 1987). Pine species have also been shown to alter nutrient availability and increase soil acidity (Scholes and Nowicki 1998). Soil alteration is especially prominent in areas where trees replace native grasslands. For example, an experimental plot in New Zealand showed a decrease of topsoil carbon, nitrogen, and phosphorus by 16%, 17% and 13%, respectively, after five years of commercial forestry growth (Chirino et al. 2010).

The spread of non-native pines also negatively affects native biodiversity. In South Africa, pine plantations have significantly lower grassland bird diversity (Allan et al. 1997) and invertebrate richness than native vegetation types (Pryke and Samways 2009). In Australia, pine invasion reduced the density of native trees and understory species by decreasing light availability (Gill and Williams 1996). In South America, non-native pine plantations were associated with an increase in other non-native and invasive species, a decrease in habitat structural complexity, and a decrease in diversity of native understory plants, invertebrates, and birds (Paritsis and Aizen 2008, Braun et al. 2017). Given the array of negative impacts on biodiversity and ecosystem function, understanding the establishment and spread of non-native pines is a prominent research question.

Several studies have measured patterns of pine establishment and dispersal at the local scale. In Australia, (Williams and Wardle 2005) surveyed two areas of native Eucalypt forest to quantify pine invasion from adjacent pine plantations. Several other field studies have reported that native forests inhibit pine growth and dispersal (Richardson and Bond 1991, Despain 2001, Bustamante et al. 2003, Bustamante and Simonetti 2005, Peña et al. 2008). In Chile, Pena et al. (2008) and Langdon et al. (2010) surveyed three and five plantation sites, respectively and found that propagule pressure was related to proximity to plantations, but long distance dispersal could spread pines up to 3 km from plantation edges. Field studies such as these provide important insight into spatial patterns of pine dispersal. However, non-native pines occur across broad spatial extents. For example, *Pinus radiata* is the most widely planted non-native conifer globally with plantations occupying over 4 million hectares, 1.5 million of which are in

Chile (Mead 2013). As a result, local field studies might not be representative of landscape or regional patterns of invasion.

Given the increasing urgency to understand conifer invasions at landscape scales (Simberloff et al. 2009), recent studies have used remote sensing imagery to characterize pine establishment and invasion over various spatial and temporal extents. The large spatial extent and high detectability of non-native pines make them well-suited for remote sensing analysis of land cover change. In Chile, increasing pine land cover is typically coincident with decreasing native forest (Echeverria et al. 2006, Schulz et al. 2010, Zamorano-Elgueta et al. 2015, Heilmayr et al. 2016). For example, in central Chile, (Nahuelhual et al. 2012) mapped land cover change over ~5,300 km^2 using Landsat images from 1975, 1990, and 2007 and found that, within their study region, non-native conifers increased from 5.5% of the landscape in 1975 to 42.4% in 2007. Similarly, Locher-Krause et al. (2017) measured a seven-fold increase in the area of non-native forest plantation in Southern Chile going from 0.7% of a 16,000 km^2 study region in 1985 to 6% by 2006 (Locher-Krause et al. 2017). Although pine plantations have been documented throughout the country (e.g., Langdon et al. 2010), remote sensing analyses to date have focused primarily on areas of central Chile. Expanding mapping of pine plantations into Southern Chile is an important next step for characterizing current and future pine invasions at a national scale.

In addition to the spatial distribution of pine plantations, which act as propagule sources, the size and proximity of plantations also influences non-native plant invasion (Moody & Mack, 1988; Vila & Ibanez, 2011). For example, Vila and Ibanez (2011) found evidence of higher invasion rates in small, isolated patches of native land cover

and greater invasion in edge habitat than core habitat. Among non-native pine plantations, Zamorano-Elgueta et al. (2015) found that four landscape metrics (plantation patch density, largest patch size, edge length, and nearest-neighbor distance) increased at a constant rate over 26 years indicating the expansion of existing plantations and the addition of isolated plantations. Additionally, non-native pine invasion risk can vary by native ecosystem type (Langdon et al. 2010, Taylor et al. 2015). Mead (2013) noted that pines expand exceptionally well in cultivated areas where native vegetation does not prevent seedling establishment and Langdon et. al. (2010) found shrub steppe to be more easily invaded than grasslands due to lower competition from vegetation. In contrast, several native forest types appear resistant to pine invasion (Richardson et al. 1994, Bustamante and Simonetti 2005, Peña et al. 2008, Langdon et al. 2010, Taylor et al. 2015), although forest edges and disturbed sites may be more susceptible (Bustamante and Simonetti 2005). Focusing on landscape characteristics and surrounding land cover in addition to the distribution of non-native pines will lead to a more thorough understanding of invasion risk (Ledgard 2001).

In 2010, Langdon et al. sampled five sites with mature plantation and in Coyhaique province in Southern Chile and found evidence of invasion (i.e. regenerating pines outside of the cultivated plantation) and long-distance dispersal (up to 368 m from the seed source). However, there has not been a landscape-scale assessment of pine plantations and invasion in this area. Here, we address this gap by mapping the distribution of non-native pines in southern Coyhaique and Aisén provinces. Additionally, we quantify landscape characteristics associated with pine populations, which can be used to inform landscape-scale risk assessment. Specifically, we

hypothesize that (1) pine patches will occur in relatively low, flat areas for easier planting and cutting; (2) pine patches are more likely to occur adjacent to grasslands for easier cultivation; and (3) pine patches will be spatially clumped to take advantage of the most suitable areas.

Methods

Study Area

Our study area is located in the Coyhaique and Aisén provinces of Chile and is comprised of two overlapping Landsat scenes (World Reference System 2 (WRS2) Path 231/Row 92 and Path 232/Row 92). These scenes included areas identified by Langdon et al. (2010) as having pine plantations and associated pine invasion (Figure 4-1) and cover approximately 58,000 km^2.

Landsat Imagery

We downloaded all available level-one terrain corrected (L1T) images from Landsats 4, 5, 7, and 8 with less than 80% cloud cover. Images were downloaded through the USGS EROS Science Processing Architecture (ESPA). L1T data have been masked to exclude clouds, cloud shadows, and snow/ice, georeferenced relative to ground control points, radiometrically calibrated to adjust for time-dependent sensor performance, and terrain corrected using digital elevation models (Loveland and Dwyer 2012, Markham and Helder 2012). This pre-processing makes data from different sensors comparable through time and spatially accurate at the pixel level (Markham and Helder 2012). We used time series of images acquired from 1997-2016 to identify the spectral-temporal patterns (see below) associated with non-native pines, native forest cover, and other land cover types. Though several images acquired before 1997 are

available in the USGS archive, we excluded these images from our analysis due to their sparse temporal coverage, focusing instead on the period of greatest observation density.

Masking Topographic Shadows

Southern Chile is a region with high topographic relief due to two major mountain ranges, the Andes Mountains and the Cordillera de la Costa. This topography coupled with the high latitude of the study region creates pronounced shadowing, which was not sufficiently addressed with L1T terrain correction. Existing methods for topographic correction tend to be computationally intensive and some require defining a unique correction for every band and land cover type (see review in Hantson and Chuvieco 2011). In an effort to simplify pre-processing, we developed a simplified approach for masking topographic shadows. We first used the solar angle and elevation associated with each Landsat image to create a hillshade for each image (GDAL/OGR Contributors 2018). We then tested a series of thresholds to identify a hillshade value that eliminated the majority of shadowed pixels while retaining high quality data from as much of the image as possible (Appendix I). Using this approach, we applied a threshold value of 100 (hillshades range in value from 0 = full shadow to 255 = full illumination) to each image such that all pixels with hillshade values below 100 were masked and excluded from the spectral-temporal analysis.

We applied the Tasseled Cap transformation to convert the six Landsat reflectance bands into three vegetation indices using the surface reflectance coefficients presented by Crist (1985). This transformation creates spectral features more directly associated with the physical characteristics of land cover types while retaining comparability across scenes (Kauth and Thomas 1976, Crist and Kauth 1986). The result

is three orthogonal indices each of which describe different land cover attributes: Tasseled Cap Brightness (TCB) characterizes the overall reflectance of the image, Tasseled Cap Greenness (TCG) describes variation in photosynthetically-active vegetation, and Tasseled Cap Wetness (TCW) is generally considered a measure of surface moisture and/or structure (Cohen and Goward 2004).

Spectral-Temporal Analysis

We used the Continuous Change Detection and Classification (CCDC) algorithm (Zhu and Woodcock 2014) to model spectral-temporal patterns for different land cover types. CCDC uses a harmonic regression approach to fit models to time series of spectral reflectance or vegetation index values resulting in a series of segments and breaks. By making use of all available imagery and including a longer time series, the CCDC approach is more robust to noise and periods of missing data than more conventional approaches that utilize fewer images (Zhu and Woodcock 2014). We created time series plots for single pixels within each land cover type to identify spectral-temporal characteristics that can be used to differentiate land cover types (See example in Appendix J). We ultimately extracted spectral-temporal features from the CCDC segment intersecting the year 2014, which was the most recent year for which there were both adequate Landsat images to create time series models, and high-resolution images to validate the resulting maps. Our final set of twelve spectral-temporal features included model intercept, slope, annual amplitude, and Root Mean Squared Error (RMSE) for Tasseled Cap Brightness, Greenness, and Wetness.

Training Data

In order to classify land cover across our two Landsat scenes, we developed a training dataset with six land cover classes (Table 4-1). These training data were created by digitizing polygons of each land cover type from high-resolution imagery acquired between 2004-2016 and available in Google Earth. Pine plantation training data were based on sites identified by Langdon et al. (2010) and visual inspection of the broader landscape for additional sites. Pine plantations are readily identifiable based on the texture of their evenly spaced rows and linear boundaries, and immature pine invasions were identifiable as trees expanding outwards from the edge of plantations over the time period. Multiple years of high resolution imagery were inspected to ensure training polygons were assigned to the correct class through time.

To create the final training dataset, hand-digitized land cover polygons were converted to points within 30 x 30 m pixels (the spatial resolution of the Landsat images). A total of 637,925 training points within 572 polygons were created and used in the analysis, ranging from 887 points for immature non-native pines to 498,069 points for native forest. To aid in testing the generalizability of our approach and classifier, all the training data were derived from a single scene (Landsat Path 231/Row 92), then later mapped and validated for the second scene.

Land Cover Classification

We used Random Forest (randomForest package in R; (Liaw and Wiener 2002) to generate our 2014 land cover maps. Random Forest is an ensemble modeling approach which relies on a random bootstrap resampling of the data to create regression trees. We used the twelve spectral-temporal predictor layers previously described, as well as three

topographic features (slope, aspect, and elevation) derived from an Advanced Spaceborne Thermal Emission and Reflection Radiometer (ASTER) Digital Elevation Model (DEM) to predict the land cover label for each pixel. We generated a total of 500 regression trees, and final land cover labels were assigned by majority vote. Though the model was trained on data from Landsat Path 231/Row 32, we also applied the trained RF to Path 232/Row 92 to produce a 2014 land cover map for each scene.

Because we were interested primarily in patch-level characteristics, the Random Forest land cover maps were post-processed to remove salt-and-pepper noise in the classification results. We ran a sieving process using QGIS (QGIS 2018) to find isolated pixels that were likely misclassified and reassign them to the surrounding land cover type. We chose a threshold of 4 pixels within an 8-pixel window to delineate land cover patches from noise.

In order to assess the quality of our final land cover maps, we used both Random Forest "out-of-bag" error, which is estimate by withholding 1/3 of the training data for measuring model performance, as well as an independent estimate of error based on post hoc land cover identification of stratified validation points. To characterize the transferability of the classification to other parts of the region, validation data was collected for Path 232/Row 92, i.e. the scene not used to collect training data.

We found that the RF model did not reliably separate pine plantations from new pine growth occurring outside plantations from, but it did consistently identify both as non-native pine. Therefore, we merged these two classes prior to selecting our validation sample. We created 100 random points within areas classified as non-native pine, grass/agriculture, water, and bare ground, and 200 random points in native forest (the

class with the largest extent) to improve our accuracy estimate for this largest land cover class. In order to test how identifiable non-native pines are at plantation or invasion edges, we also created and validated two separate edge classes associated with non-native pine. The first, 'pine edge' samples from a 30 m buffer inside patches classified as pine. The second, 'non-pine edge' samples from a 30 m buffer outside patches classified as pine. We validated the classified image at each point using high resolution Google Earth images acquired between 2012-2016. We used contingency tables to evaluate the over accuracy of the classification, as well as the accuracies of each land cover class.

Landscape Analysis

To better understand where pine plantations and invasions occur in relation to the surrounding landscape, we quantified landscape characteristics. For these analyses, we focused on the scene (Path 232/Row 92) that corresponded with the majority of non-native pine patches. This area overlapped the vegetated part of the adjacent Landsat scene (Path 231/Row 92) so we did not run the analysis across both scenes. To test the hypothesis that non-native pine plantations tend to be found in flat, low-elevation areas, we extracted the elevation and slope for each pixel classified as pine and compared it to available topography within the Landsat image based on 50,000 random pixels. We tested for significant topographic biases in the pines using a Mann Whitney U test. To determine if non-native pine plantations tend to be established adjacent to particular land cover classes, we counted the number and types of land cover classes bordering each pine patch and compared this to land cover bordering randomly placed patches equal to the median pine patch size. Many patches (pine and random) shared boundaries with more than one land cover type resulting in total surrounding land cover of >100%. Finally, we

assessed spatial patterns of dispersion across the landscape. Many plantations included 1-2 pixel patches adjacent to the core plantation, and we aimed to assess dispersion of individual plantations and invaded sites across the landscape. As such, we included only core non-native pine (i.e. not within a 30 m buffer of an edge) in our dispersion analysis. To measure patterns of distribution, we assessed spatial autocorrelation of core non-native pine areas by using a Global Morans I test. This measures the degree to which similar or dissimilar patches are dispersed across the landscape, with clustering suggesting that factors other than random chance affect patch distribution (Dubin 1998, Mitchell 2005, Getis and Ord 2010). We also calculated the shortest linear distance between any two core non-native pine patches which we used to infer patch isolation.

Results

We downloaded 396 and 293 Landsat images for WRS2 Path 231/Row 92 and Path 232/Row 92, respectively (Figure 4-1). After applying the hillshade mask (Figure 4-2), the available images per pixel in Path 231/Row 92 and Path 232/Row 92 averaged 121 +/- 72 (SD) and 60 +/- 38 (SD), respectively. Some areas had zero available images, but these were typically at high elevation and covered with ice, snow, or shadow throughout the year and were excluded from the analysis.

The spectral-temporal signature of non-native pine was fairly distinct from native land cover classes. Native forest and grass/agriculture have high intra-annual variation and a greater range of Tasseled Cap Greenness values (consistent with the growth pattern of grasses and deciduous trees) relative to non-native pines (Figure 4-3). Native forests and grass/agriculture also tend to have more intra-annual variation in Tasseled Cap Brightness and Tasseled Cap Wetness values than non-native pines, respectively

(Appendix J). For non-native pines, Tasseled Cap Brightness values tend to decrease through time while Tasseled Cap Wetness values increase (Appendix J). The decreasing brightness likely occurs as the pines mature and create more shade and dark vegetated material. Increasing wetness likely reflects the increased structural complexity that occurs as pines mature. These trends can also be used to differentiate non-native pine from native forest and grass/ag which remain stable through time for both Tasseled Cap indices (Figure J).

The majority of the large non-native pine plantations were located along the eastern edge and in the northeast corner of Path 232/Row 92, although non-native pine was found in smaller patches throughout the Landsat scene (Figure 4-4). Based on the validation dataset, the overall accuracy of the classification was 88% ($\kappa = 0.85$; (Cohen 1960)). Overall accuracy for classification of non-native pine was even higher, with an omission error (likelihood of missing pine) of 8% and a commission error (likelihood of falsely identifying pine) of only 1% (Table 4-2). Although the classification did not specifically target edge as its own land cover class, the model captured 81% of pine edges (i.e. pixels within 30 m of the inside of the pine patch edge) (Table 4-3). The model was less effective for classifying non-pine edges (i.e. pixels within 30 m of the outside of the pine patch edge) with an overall accuracy of 69% (Table 4-4).

Of the 55,990 pixels classified as pine, 84% were found on slopes less than 20°, whereas 64% of the landscape contained similar shallow slopes based on a set of 50,000 random points. Pines were located in a distinct elevation band; 60% of pine pixels were found at elevations between 600-900 m, whereas 21% of the landscape was in this

elevation range. Pine pixels were significantly more likely to be found on shallow slopes and at higher elevation (Figure 4-5; Mann Whitney U: $\rho << 0.001$).

There were 3,842 patches classified as pine with an average size of 13,115 m^2 (+/- 93,599 m^2 SD; median 2,700 m^2). Pine and random patches were similarly likely to share a border with native forest (89% and 84%, respectively), which was the most extensive land cover class. Less than 4% of pine patches shared borders with water or bare ground, which was proportional to the available land cover. However, pine patches were more likely to share a border with the grass/agriculture class than the random patches (50% and 17%, respectively) (Figure 4-6).

Pine patches were more spatially dispersed than would be expected by random chance (Morans I: $\rho << 0.01$; z -8.9). The average distance between pine patches was 1,450 m (+/- 5271 m StDev). However, 66 pine patches (22%) were at least 1 km away from any other patch, and one patch was remotely located at 55 km distant (Figure 4-7).

Discussion

The geographic isolation created by Chile's unique biogeography has led to a remarkably high rate of endemism among Chilean species (e.g., 90% of seed plants (Villagran and Hinojosa 1997) and 45% of all vertebrates (Armesto et al. 1996)). These ecosystems are threatened by the establishment of non-native pine plantations and subsequent pine invasion, which has negative impacts on native ecosystems, including altering fire severity, soil properties, water availability, and reducing native diversity (Robson et al. 2009, Chirino et al. 2010, van Wilgen and Richardson 2012, Paritsis et al. 2018). While the establishment and spread of non-native pines is well documented and mapped in some parts of Chile (Echeverria et al. 2006, Peña et al. 2008, Schulz et al.

2010, Nahuelhual et al. 2012, Zamorano-Elgueta et al. 2015, Heilmayr et al. 2016, Locher-Krause et al. 2017), the extents of pines in parts of Southern Chile and risk to the surrounding landscape are poorly understood. Our analysis suggests that Chile's southern Coyhaique and Aisén provinces contain approximately 295 distinct patches of non-native pine that contain core and interior pine (i.e. patches of at least 9 30x30m pixels), that many of these patches are in isolated locations far from other plantations, and that pines are disproportionately located next to grassland systems, which may be susceptible to invasion (Richardson et al. 1994). Consistent with previous research, these results suggest that Southern Chile is in the early stages of a large-scale pine invasion (Richardson et al. 2008, Langdon et al. 2010).

Propagule pressure is a critical component of invasion risk (Colautti et al. 2006). Although occasional long-distance dispersal events have the potential to move pine seeds hundreds of meters to a few kilometers (e.g., Benkman 1995, Ledgard 2001, Williams and Wardle 2005, Peña et al. 2008, Langdon et al. 2010), the majority of propagules fall within 60 m of plantation edges (Langdon et al. 2010). Without a nearby seed source, pine invasion is unlikely. The widespread establishment of plantations thus facilitates invasion. We found that plantations are widely dispersed across the landscape, with many pine patches located tens of kilometers from their nearest neighbor (Figure 4-7). These patches create new source points for invasion, which increases the likelihood of a rapid and difficult to control invasion front (Moody et al. 1988, Richardson et al. 1994). Seedling establishment outside plantations in Argentina was influenced more by seed density than by biotic or abiotic factors (Pauchard et al. 2016). Thus, it is likely that where plantations can establish, pines can also invade.

Although non-native pines are able to grow across a range of abiotic conditions (Tomiolo et al. 1960, Pauchard et al. 2016), some native ecosystems are particularly vulnerable to pine invasion. We found that half of pine patches were sited adjacent to grassland and agricultural land (Figure 4-6). Disturbed areas and grasslands are particularly vulnerable to pine invasion because of lower biotic resistance (Richardson and Bond 1991, Richardson et al. 1994, Bustamante et al. 2003, Bustamante and Simonetti 2005). In contrast, native forest may be more resistant to invasion because pine seedlings are shade intolerant and unlikely to survive under forest canopies or when in direct competition with other trees for resources (Richardson and Bond 1991, Bustamante and Simonetti 2005).

Our results indicated that non-native pines are most likely to occur in relatively flat areas (slope less than 20°) and at mid-elevations (600-900 m; Figure 4-5). These ranges are consistent with previous research, which reported pine plantations between 765 – 950 m (Paritsis et al. 2018). The high topographic relief in Chile creates strong temperature and moisture gradients which likely limit plant growth at high elevation (Veblen et al. 1977). However, pines were present on steeper than 20° slopes and at lower elevations. Given that pines are known to have broad climatic tolerance (Tomiolo et al. 1960, Despain 2001), it is likely that the elevation and slope ranges found here are indicative of conditions favored for plantations rather than areas most susceptible to invasion. While future invasions will begin at plantations within these elevation and slope conditions, they are unlikely to be constrained by them.

Our models performed well at classifying native and non-native land cover in Chile, with User's and Producer's accuracies for the non-native pine class of 99% and

92%, respectively and for the native forest class of 96% and 89%, respectively (Table 4-2). These values are comparable to previous studies, which have reported classification accuracies of 79–92% for non-native pine and 85-96% for native forest (Echeverria et al. 2008, Nahuelhual et al. 2012, Zamorano-Elgueta et al. 2015, Heilmayr et al. 2016). Additionally, because our training data were derived from one scene, but testing data were collected from a neighboring Landsat scene, it is likely that this approach could be expanded to classify non-native pines across the country. Our use of the Continuous Change Detection and Classification (CCDC) approach algorithm (Zhu and Woodcock 2014) facilitated this consistency between Landsat scenes. Because our predictor variables were derived from model-estimated values based on many observations in a time series, the predictor values and resulting classification are relatively robust to clouds or errors associated with any single image. Thus, this approach is better able to support classification across a broader study region than single-date classifications (Zhu et al. 2012).

The robust classification accuracy reported here also suggests that a relatively straightforward hillshade correction is effective for masking topographic shadows in areas of high topographic relief. Hantson and Chuvieco (2011) review topographic correction methods, which include, for example, calculating the statistical fit between each band's reflectance and the values of the illumination angle and using the average illumination angle to correct pixels on a rough landscape. These approaches seek to correct effects and retain spectral observations. However, when using dense time series, reliance on individual values decreases and masking/removing topographic shadowing is a suitable alternative. Our use of a threshold value associated with the day of year of each

image reduced noise and led to an effective classification. This approach could simplify future time series analysis in similar areas of high relief and latitude.

Non-native pines are established in Southern Chile, and invasion away from these plantations has already been observed (Langdon et al. 2010). Our analysis shows that pine patches are widespread across this landscape, creating well-dispersed sources of propagules for future invasion. Moreover, plantations are disproportionately sited next to vulnerable grassland and agricultural areas where pine invasions can rapidly alter ecosystem function and biodiversity. Our work highlights the need for continued focus on reducing invasion risk from non-native pine plantations in the Southern Hemisphere.

Acknowledgements

CAC was supported by NASA's Biodiversity and Ecological Forecasting Program (NESSF: 15-EARTH15F-133).

Tables

Table 4-1. Land cover characteristics used for defining training data and the number of training points collected.

Land cover type	Defining characteristics	Number of training points
Mature non-native pine	Evenly spaced, linear rows; Linear boundaries; Evidence of logging	7,596
Immature non-native pine	Radial spread of dark, woody vegetation away from plantation edge; Increasing density (i.e., darkness) through time	887
Native forest	Dark green; Irregularly spaced; Taller than surrounding vegetation	498,069
Grass/agriculture	Photosynthetic cover; Lack of woody vegetation	34,666
Water	Lack of vegetation or impermeable surfaces	9,759
Bare ground	Lack of vegetation and water	86,948

Table 4-2. Confusion matrix with land cover class validation. Overall accuracy: 88%.

		Observation						
		Bare ground	Water	Grass/ag	Native forest	**Non-native pine**	Total	User's Accuracy
Classification	Bare ground	91	16	14	7	0	128	71%
	Water	0	84	0	1	0	85	99%
	Grass/ag	9	0	86	14	0	109	79%
	Native forest	0	0	0	177	8	185	96%
	Non-native pine	0	0	0	1	92	93	99%
	Total	100	100	100	200	100	600	
	Producer's Accuracy	91%	84%	86%	89%	92%		88%

Table 4-3. To assess how accurate classifications of the pine class were, we separately validated a 30 m buffer inside pixels and patches classified as pine. 81% of the validation pixels within the pine edge class were correctly classified.

		Observation
Classification		Pine edge
	Bare ground	4
	Water	0
	Grass/ag	2
	Native forest	13
	Non-native pine	81
	Total	100
	Producer's Accuracy	81%

Table 4-4. To assess how accurate classifications of the non-native pine class were, we separately validated a 30 m buffer outside pixels and patches classified as pine and found an overall accuracy of 69%.

		Observation						
Classification		Bare ground	Water	Grass/ ag	Native forest	Non-native pine	Total	User's Accuracy
	Bare ground	0	0	0	0	0	0	0%
	Water	0	0	0	0	0	0	0%
	Grass/ag	1	0	21	0	4	26	81%
	Native forest	2	0	10	48	14	74	65%
	Non-native pine	0	0	0	0	0	0	0
	Total	3	0	31	48	18	100	
	Producer's Accuracy	0%	0%	68%	100%	0%		69%

Figures

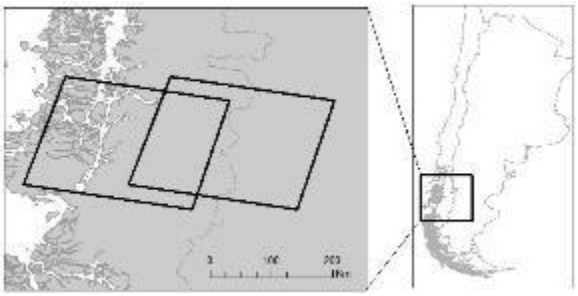

Figure 4-1. Study site in Southern Chile. Inset: black boxes show the outlines of Landsat scenes WRS2 Path 232/Row 92 (left) and Path 231/Row 92 (right).

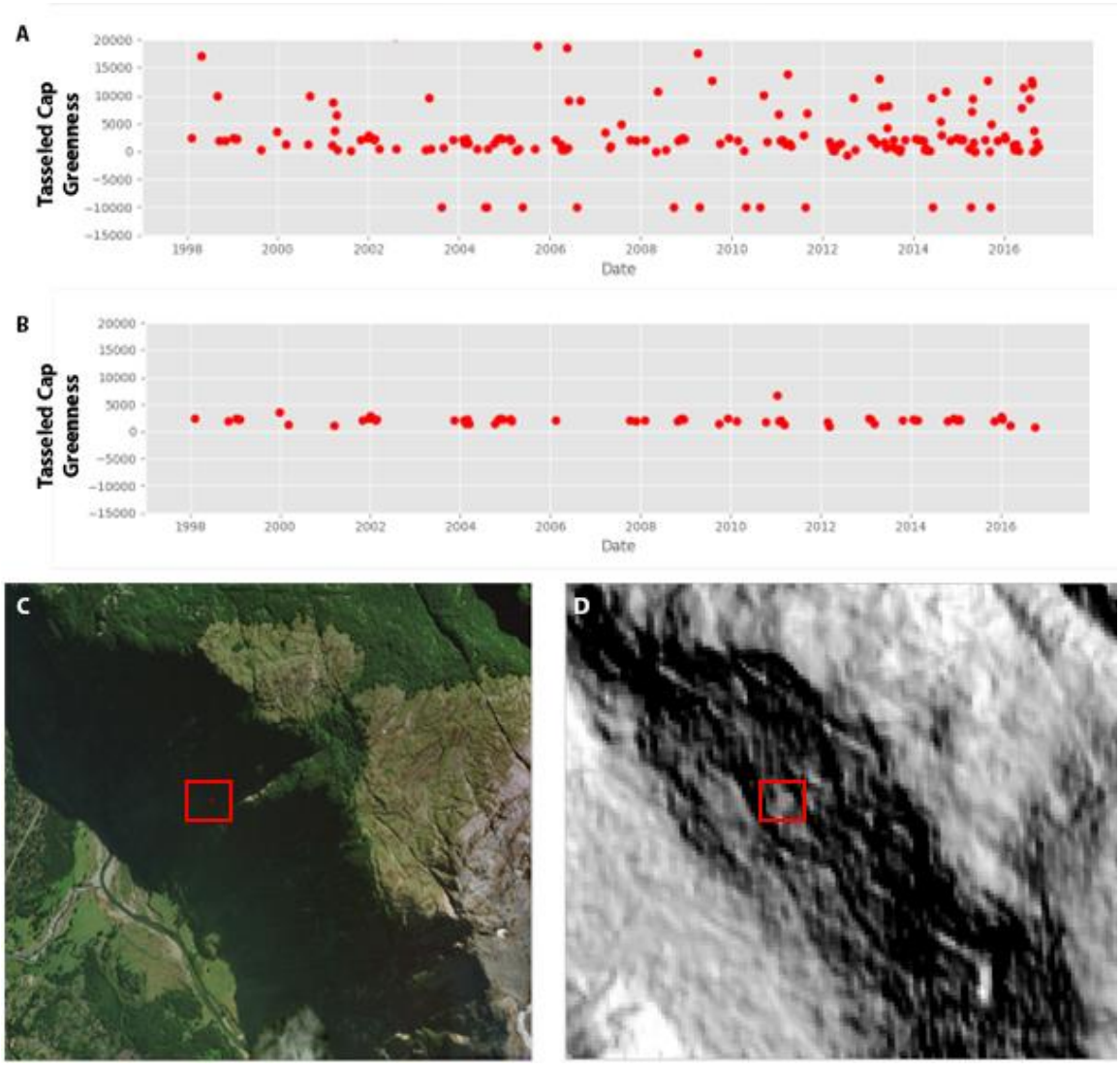

Figure 4-2. Time series plots of Tasseled Cap Greenness values derived from a single pixel with each point representing a single Landsat image shown before (A) and after (B) the hillshade mask was applied.

The removal of shaded pixels results in a more stable spectral-temporal signal from this patch of native forest. The area from which the time series plots were created is shown in a high resolution aerial image (C) and the image-specific hillshade (D). The red squares show the example pixel.

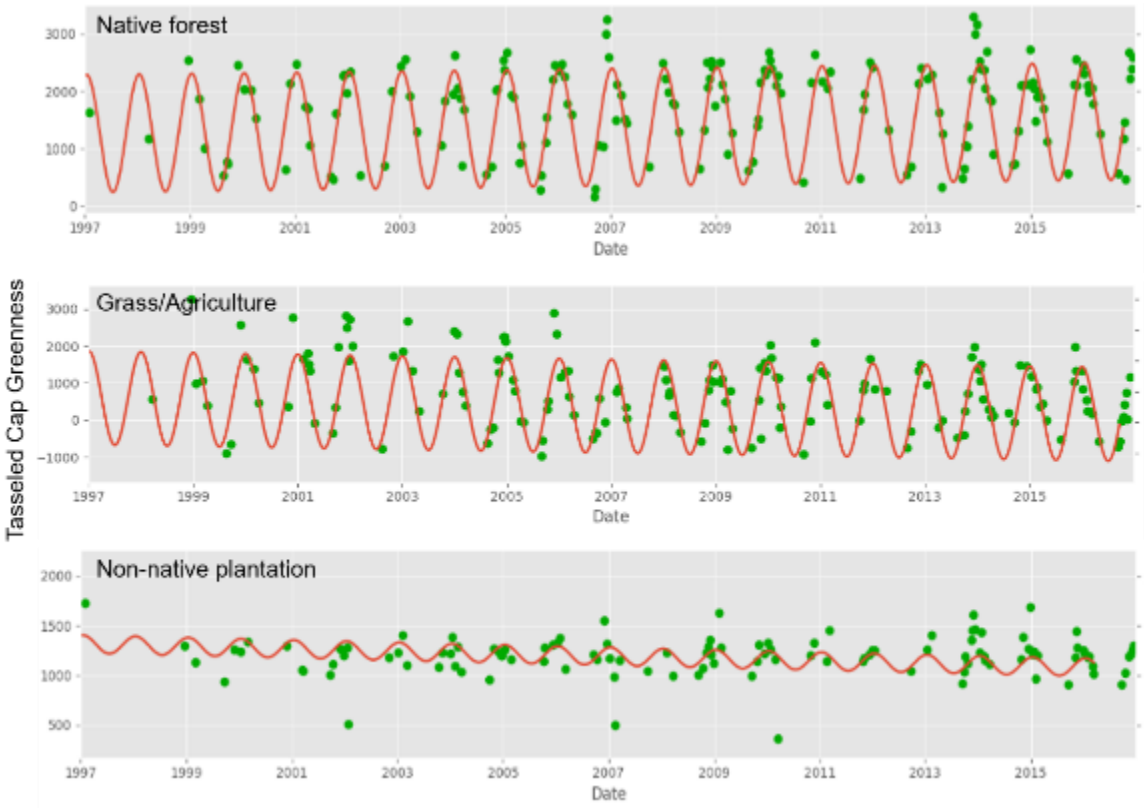

Figure 4-3. Spectral-temporal features for non-native pine are distinct from native land cover classes.

Green points represent pixels from each available image in the time series. Native forest and Grass/Agriculture have higher intra-annual variability and a greater range of Tasseled Cap Greenness values than non-native plantations.

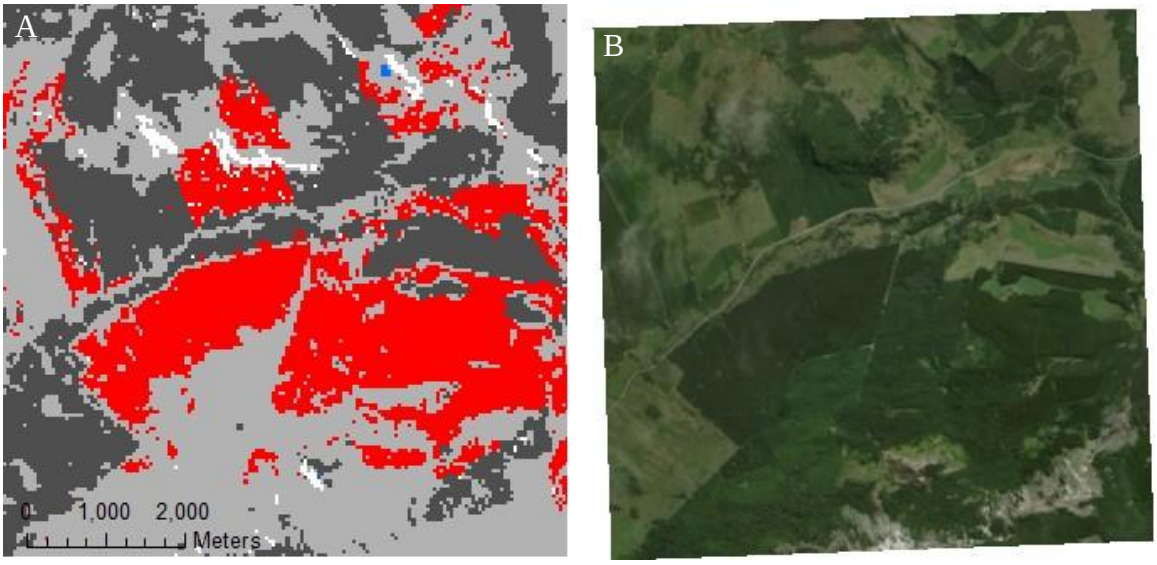

Figure 4-4. Land cover was classified using Random Forest. Similar land cover patterns can be seen between the classified image (A) and a high-resolution image from the same location (B).

In the classified image, dark grey, light grey and red correspond to grass/agriculture, native forest, and non-native pine, respectively. Water and bare ground were also classified but are not visible in this example. White areas were masked due to shadow or missing data

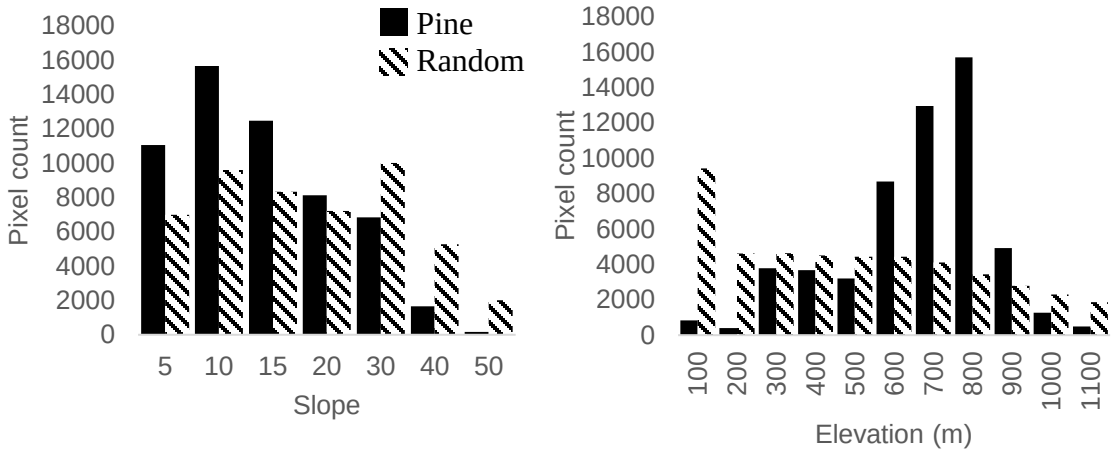

Figure 4-5. Most pine pixels occur on slopes less than 20° and at an elevation between 600m and 900m. Pine pixels occur at slopes and elevations that differ significantly from an equal number of random background points (Mann Whitney U: $\rho << 0.001$).

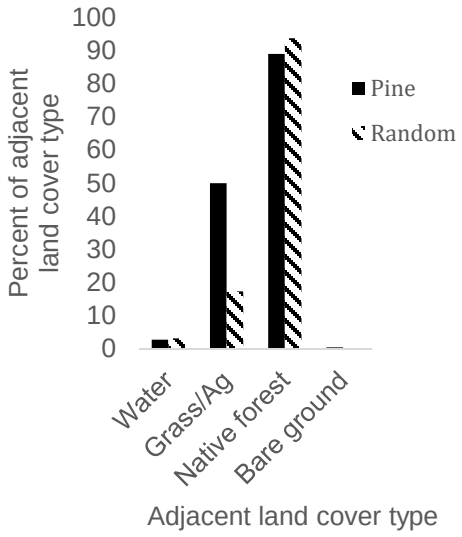

Figure 4-6. Non-native pine was disproportionately likely to share a border with grassland or agriculture. Most non-native pine also shared a border with native forest. Less than four percent of the 3,842 pine patches share a border with bare ground or water

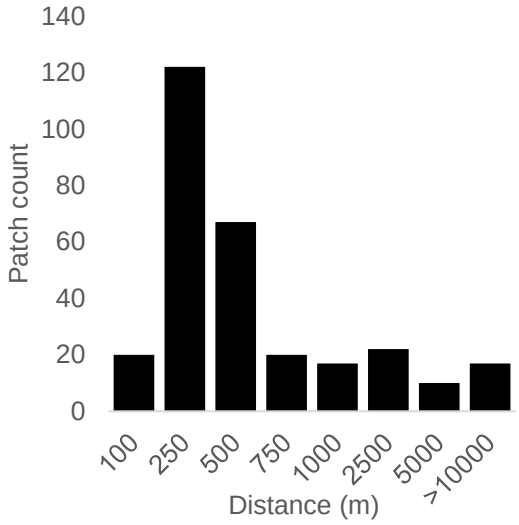

Figure 4-7. The majority of pine patches were located within 500m of other pine patches. However, many isolated patches occurred >1 km away from other patches. Note that this figure includes the 295 larger patches containing interior (non-edge) pine.

APPENDIX A

DISTRIBUTION AND ABUNDANCE DATA

Distribution and abundance data for this analysis were compiled from a variety of sources detailed in Table A1.

Table A1. List of data sources compiled to create the final datasets of presence and high abundance for *Bromus rubens* and *Brassica tournefortii*.

The number in each cell indicates how many data points were available for each category. In cases where percent cover data were available but identified as less than 10% for the target species, the data were retained as presence points. This table reflects all compiled data, before duplicate entries per 2.5 arcminute climate grid cell were removed.

		B. rubens		*B. tournefortii*	
Source	Description	P[1]	HA[2]	P	HA
Regional botanists (1)	Percent cover	318	0	15	0
Southwest Regional GAP Training Sites Databases (2)	Percent cover	38	8	28	1
NPS botanists (3)	Percent cover	1169	49	67	2
NPS botanists (Lake Mead NRA) (3)	Distribution categories: Under shrub Scattered Isolated patch Isolated individual Gradient Continuous cover Clumped	0	0	5041	469
NPS botanists (Joshua Tree NP) (3)	Percent cover	0	0	443	63
NPS botanists (Death Valley NP) (3)	Examples of qualitative descriptions: very dense, creating ground cover in most areas dense in places, creating	42	0	15	6

	ground cover, thinning quickly southward up canyon remnants 1+ years locally dense beneath shrubs and on banks; mostly new growth, few remnants abundant plant population; Field survey; plants outside property and surrounding areas as well				
Roadside surveys in CA, NV, AZ (4)	Abundance rank (0-3) 0: None detected 1: Present at low abundance 2: Present at high abundance along road corridors 3: Present at high abundance extending away from road corridors	234	55	79	13
Herbarium records (5)	N/A	864	0	0	0
CalIPC (6)	Abundance rank (0-3) 0: None detected 1: Present at low abundance 2: Present at moderate abundance 3: Present at high abundance	0	0	9475	269
CAlFlora (7)	Percent cover	6342	156	0	0
Vegbank (8)	Percent cover	71	8	0	0
SWEMP (9)	N/A	772	0	0	0
USGS (10)	N/A	733	0	0	0
BLM (11)	N/A	6	0	0	0

[1]Points of recorded presence

[2]Points of recorded high abundance

(1) Regional botanists. S. Abella, University of Nevada Las Vegas, and Cindy Salo, Sage Ecosystem Science

(2) Southwest Regional Gap Training Sites Databases. (http://earth.gis.usu.edu/swgap/trainingsites.html).

(3) National Park Service Botanists. Data were provided by the National Park Service Mojave Desert Network Inventory & Monitoring Program, the NPS National Vegetation Mapping Program, and regional botanists J. Cipra (Death Valley National Park), K. Kain (Joshua Tree National Park), and C. Norman (Lake Mead National Recreation Area).

(4) Roadside surveys in CA, NV, AZ. Field surveys were conducted in 2011 and 2012 by L. Pelech and B.Bradley (University of Massachusetts Amherst) and focused on roadsides only in southern Nevada, southern California, and Arizona.

(5) Herbarium records. Data were compiled from regional herbaria including the following: University of Arizona Herbarium, Northern Arizona University Deaver Herbarium, Arizona State University Plant Herbarium, Northern Great Plains Herbarium, University of California Riverside Herbarium, University of New Mexico Herbarium, Herbarium of the University of Sonora, Mexico, Utah State University Intermountain Herbarium, Grand Canyon National Park Herbarium, Desert Botanical Garden Herbarium Collection.
(6) CalIPC. California Invasive Plant Council (http://www.cal-ipc.org/).
(7) CAlFlora. (http://www.calflora.org/).
(8) Vegbank. (http://vegbank.org/vegbank/index.jsp)
(9) Southwest Exotic Plant Information Clearinghouse: Southwest Exotic Mapping Program (http://sbsc.wr.usgs.gov/research/projects/swepic/swemp/swempa.asp).
(10) United States Geological Survey (http://www.usgs.gov/)
(11) Bureau of Land Management, Arizona (http://www.blm.gov/az/st/en.html)

APPENDIX B

PROJECTED ABUNDANCE AND DISTRIBUTION (RCP8.5)

This analysis identified future projected shifts of presence and high abundance based on RCP8.5.

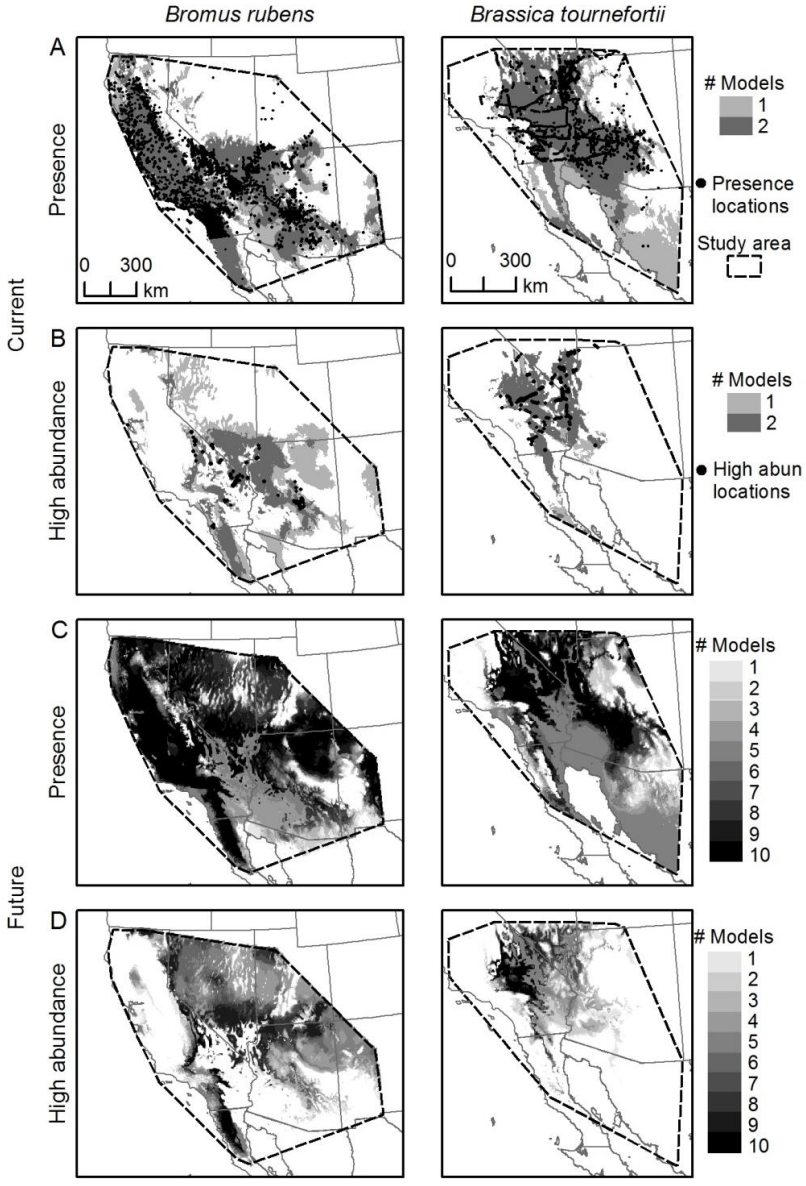

Figure B1. Species distribution models for *B. rubens* and *B. tournefortii*.

Point locations indicate where presence (A) and high abundance (B) data were collected. The predicted current presence (A) and high abundance (B) distributions

include the MaxEnt and Bioclim projections and encompass 95% of the original distribution data. Future ensemble models are based on RCP8.5. The future ensemble models for presence (C) and high abundance (D) were created by combining the projections of 10 models: two bioclimate envelope models and five Atmosphere-Ocean General Circulation models. Values indicate how many of the 10 models projected that the location would support presence or high abundance.

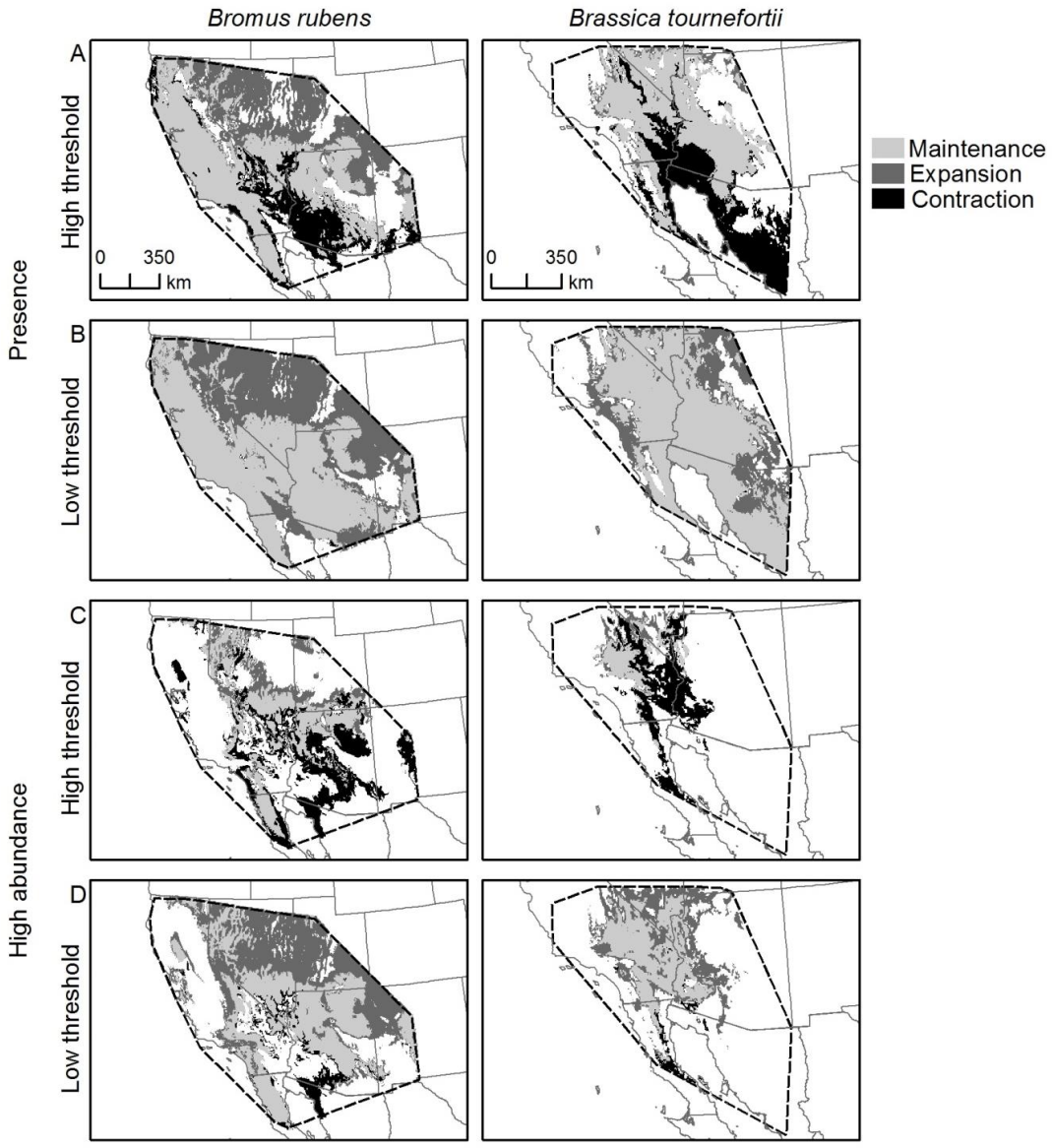

Figure B2. Distribution models showing the areas of maintenance, expansion, and contraction under future climate conditions for RCP8.5.

Each model shows the difference between the current and future predicted distributions. Maintenance indicates that a species was predicted to occur in an area both under current and future climate conditions. Expansion indicates the spread of suitable climate conditions and represents the areas into which the species will be able to expand under future climate conditions. Contraction appears in areas where the future climate conditions are no longer suitable for a species. The high threshold models (A and C) are

based on a cautious view of future invasion establishment or impact risk, and all areas where six or more models indicated suitable habitat are included as future potential habitat. Low threshold models (B and D) include all areas where at least one future model indicates suitable habitat.

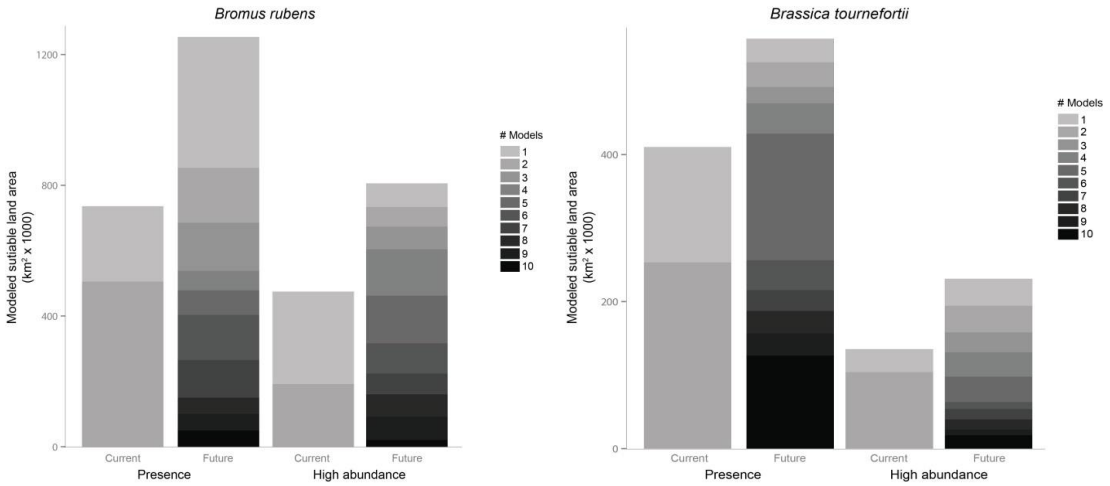

Figure B3. Predicted suitable land area for the target species currently and by 2050 under RCP8.5.

Table B1. Projected increases in distribution size within the study areas based on the low and high thresholds under future climate conditions for RCP8.5

			Low Threshold		High Threshold	
			Area	% Change	Area	% Change
B. rubens	Presence	Current	736		736	
		Future	1253.8	70	403.6	-45
	High abundance	Current	475		475	
		Future	805.8	70	316.5	-33
B. tournefortii	Presence	Current	410		410	
		Future	557.4	36	256.3	-38
	High abundance	Current	135		135	
		Future	231.1	71	63.5	-53

APPENDIX C

MESS ANALYSES

Models of future climatic suitability require extrapolation to climate layers representative of times (and potentially climate conditions) not sampled in the training data. Models trained to current climate conditions will be unable to define suitability of future, novel climate conditions (i.e., those not present in the training data). To assess similarity of the climate conditions in the current and future climate data, and the ability of the models to predict future suitability, the multivariate environmental similarity surface (MESS) was calculated between the current data and each set of future climate data used. MESS calculations were implemented through MaxEnt to determine similarity between the current and future climate data (Elith et al. 2010). This method was applied to the study areas for *Bromus rubens* and *Brassica tournefortii* and for the RCP4.5 and RCP8.5 future data in each area. As part of the MESS analysis, MaxEnt also provides a map of the novel limiting features which can be used to infer which environmental variable contributes most to the MESS value in each grid cell.

The current and future climate layers used in this study are highly similar. Areas of divergence appear in the Death Valley region of California, and Sonora, Mexico (for both species), and in California west of the San Gabriel Mountains and on the Baja peninsula (*B. rubens*). July maximum and January minimum temperature and spring precipitation are the most important variables for determining the MESS values in areas of divergence. Summer and spring precipitation are important drivers of the MESS values in few pixels. The areas where current and future climates diverge are relatively small and, therefore, do not limit our ability to make predictions of future climatic

suitability. However, caution should be used when inferring risk of invasion from *B. rubens* and *B. tournefortii* in these areas.

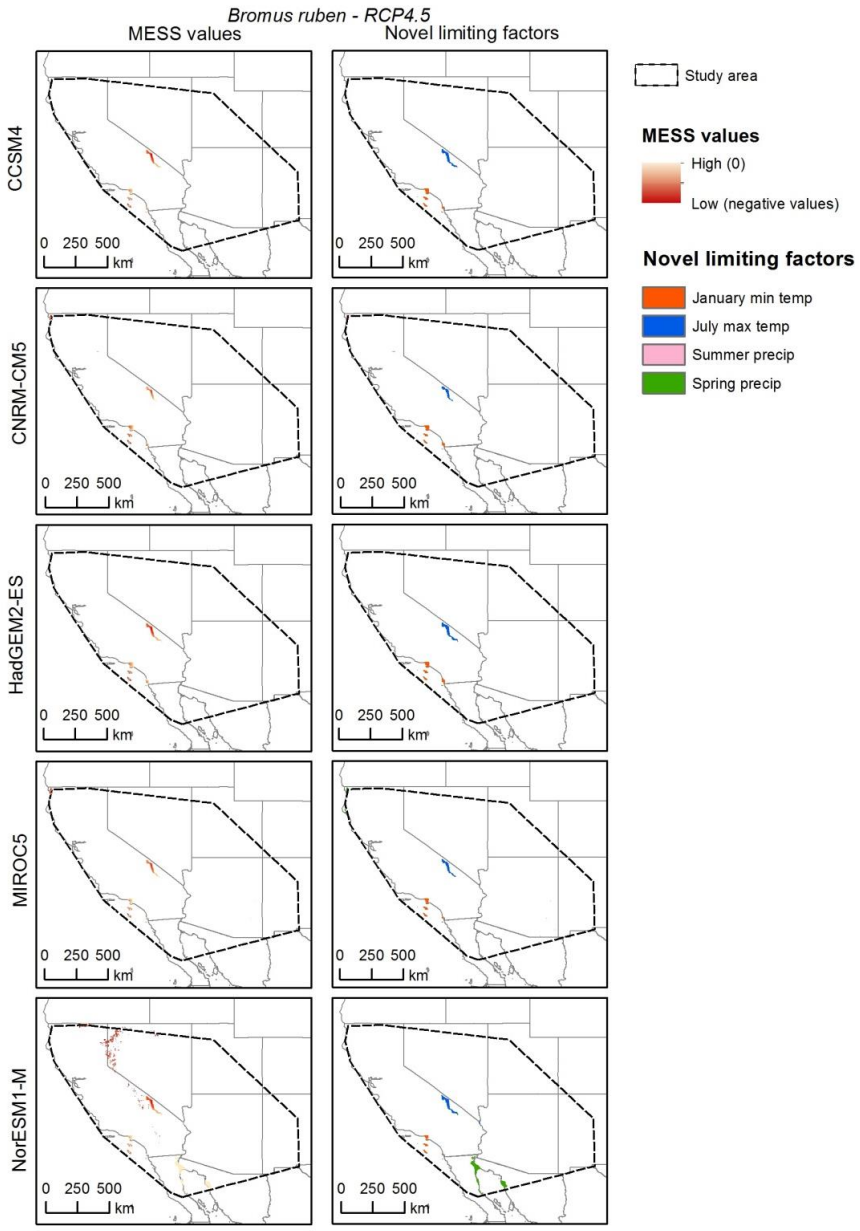

Figure C1. MESS maps for model projections to the RCP4.5 future climate within the *B. rubens* study area.

Only areas with negative MESS values are displayed and the intensity of the color indicates similarity (areas with darker color are more dissimilar). Maps of novel limiting

factors indicate which environmental variable contributes most strongly to the MESS value.

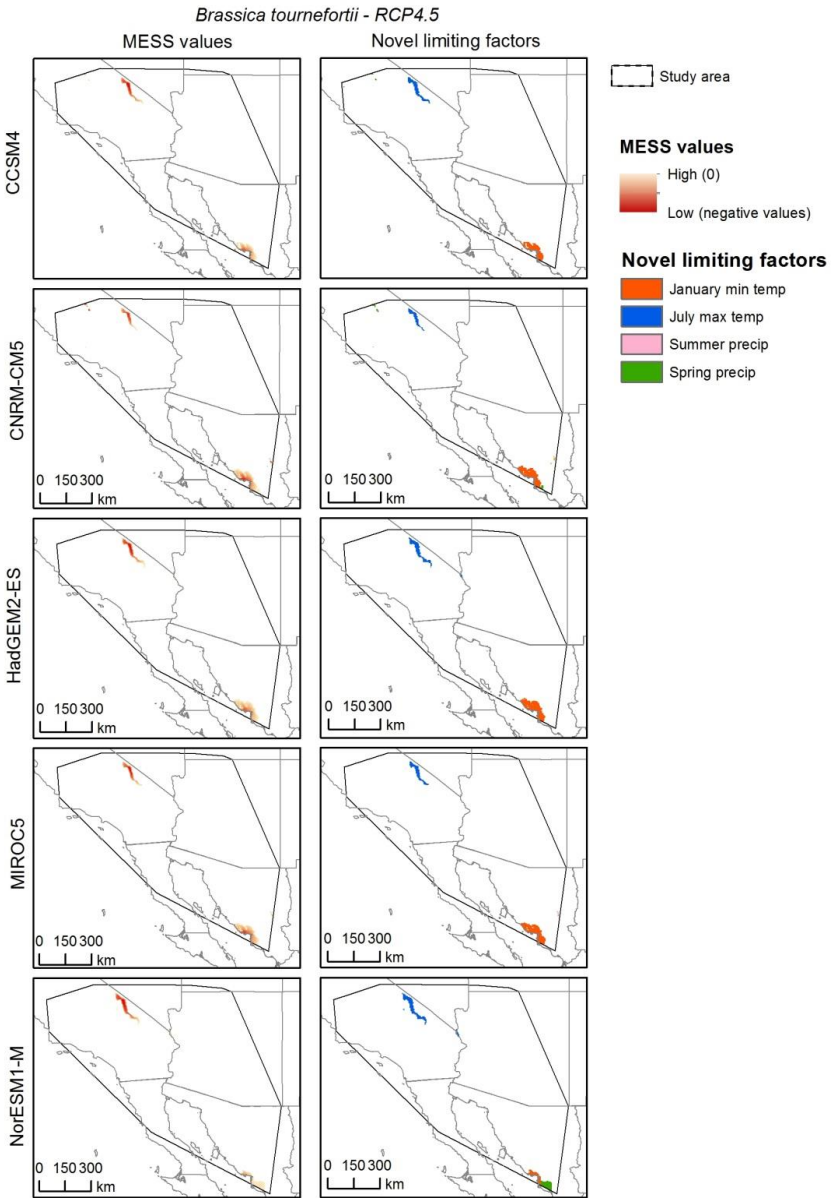

Figure C2. MESS maps for model projections to the RCP4.5 future climate within the *B. tournefortii* study area.

Only areas with negative MESS values are displayed and the intensity of the color indicates similarity (areas with darker color are more dissimilar). Maps of novel limiting

factors indicate which environmental variable contributes most strongly to the MESS value.

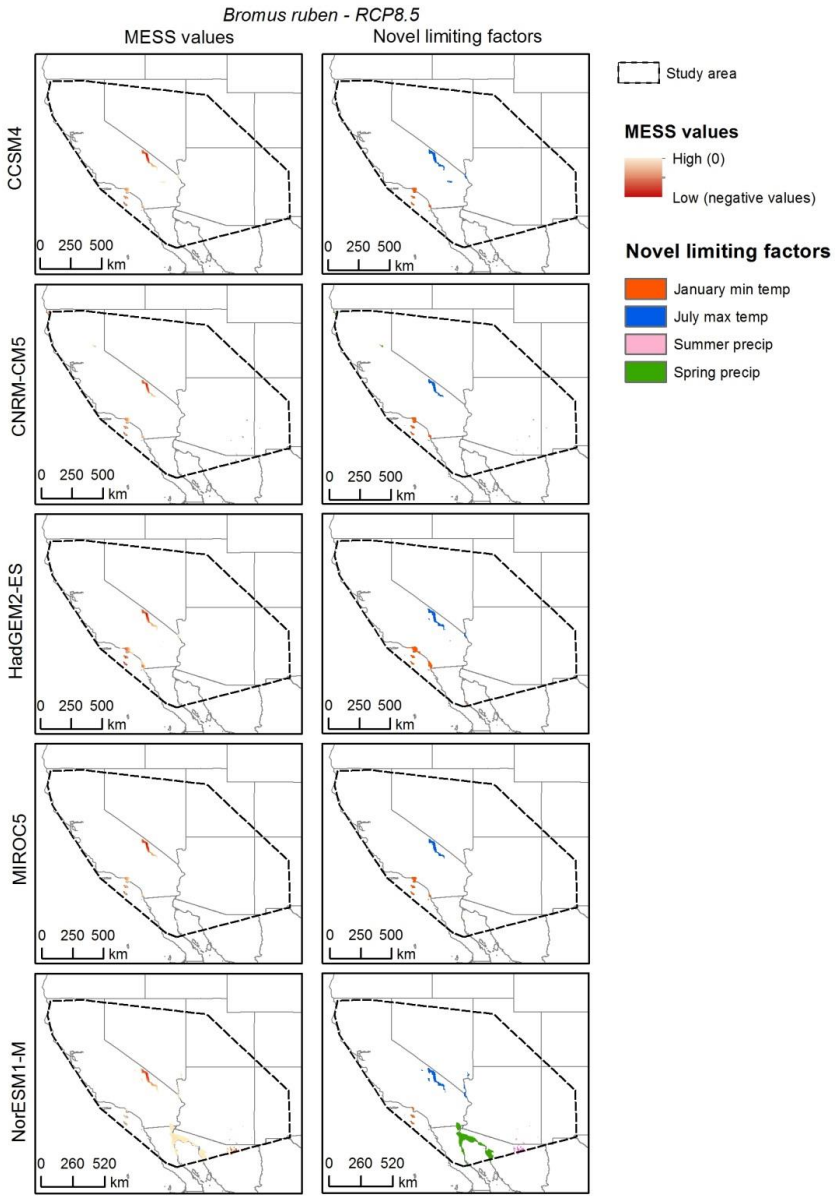

Figure C3. MESS maps for model projections to the RCP8.5 future climate within the *B. rubens* study area.

Only areas with negative MESS values are displayed and the intensity of the color indicates similarity (areas with darker color are more dissimilar). Maps of novel limiting

factors indicate which environmental variable contributes most strongly to the MESS value.

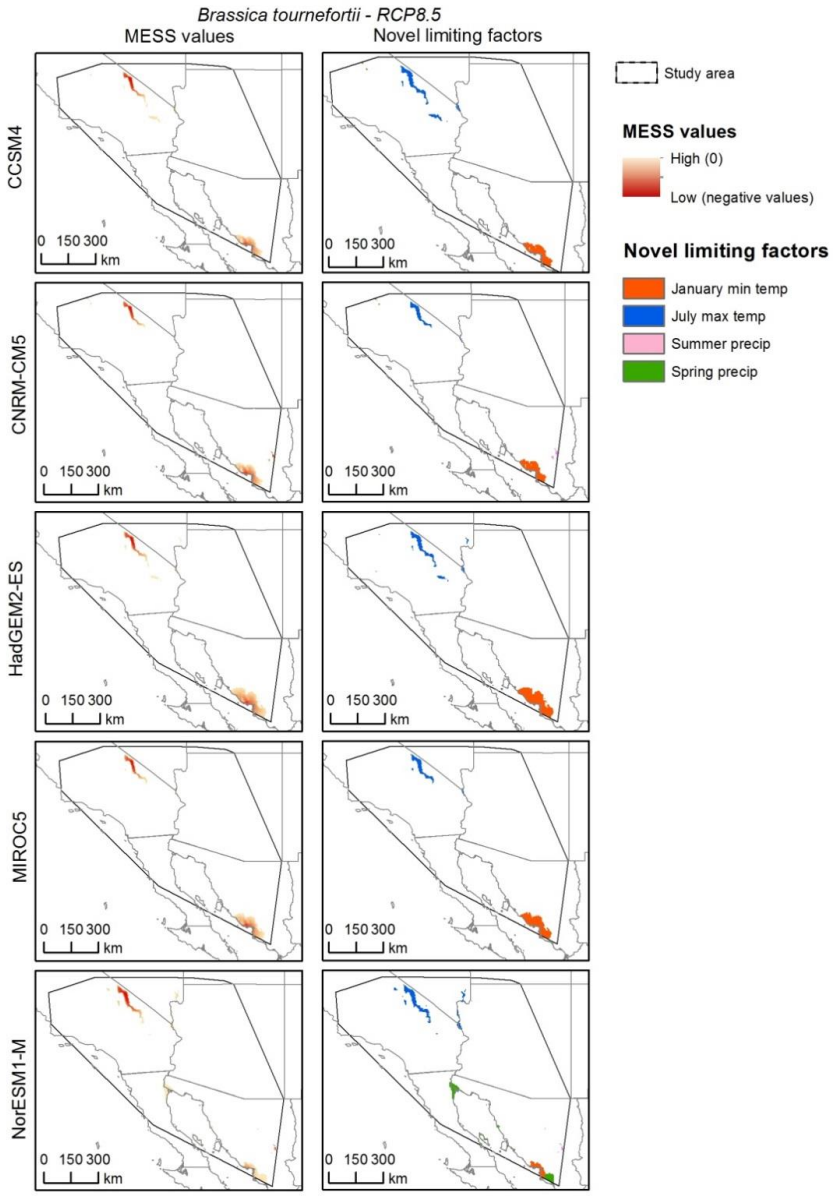

Figure C4. MESS maps for model projections to the RCP8.5 future climate within the *B. tournefortii* study area.

Only areas with negative MESS values are displayed and the intensity of the color indicates similarity (areas with darker color are more dissimilar). Maps of novel limiting factors indicate which environmental variable contributes most strongly to the MESS value.

APPENDIX D

ENSEMBLE MODEL PROJECTIONS

The use of different species distribution modeling (SDM) methods can lead to variation in projections of suitable habitat (Araújo and New 2007). The primary difference between the two models used here in terms of future projections is their interpretation of climatic suitability at the hot end of both species potential establishment. Maxent predicts continued climatic suitability for temperatures slightly above those recorded at current occurrences, while Bioclim predicts a threshold effect which limits climatic suitability to the highest current occurrence temperatures. For future projections, which uniformly project a rise in temperature, this difference leads to the broader suitability forecast by Maxent for both *B. rubens* and *B. tournefortii* in the hot desert region between Arizona and California. The extent and spatial configuration of disagreement between the 2 types of SDM used can be seen in the maps below.

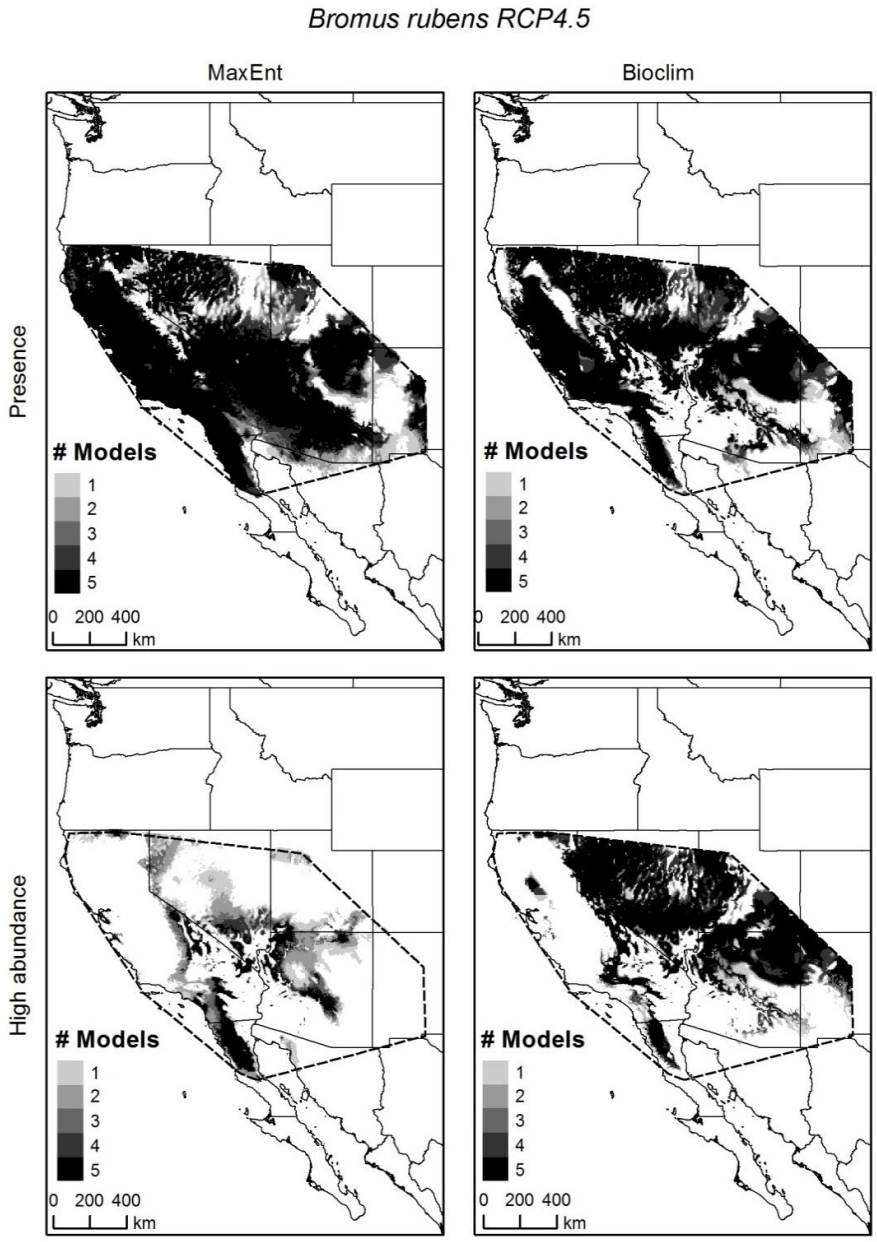

Figure D1. Ensemble models for *B. rubens* under future climate projections for RCP4.5.

Projections were made by using MaxEnt and Bioclim to model future suitable habitat for each of the five Atmosphere Ocean General Circulation Models. Ensemble models were created by adding the five models created by each species distribution modeling method together. Darker areas indicate higher model agreement.

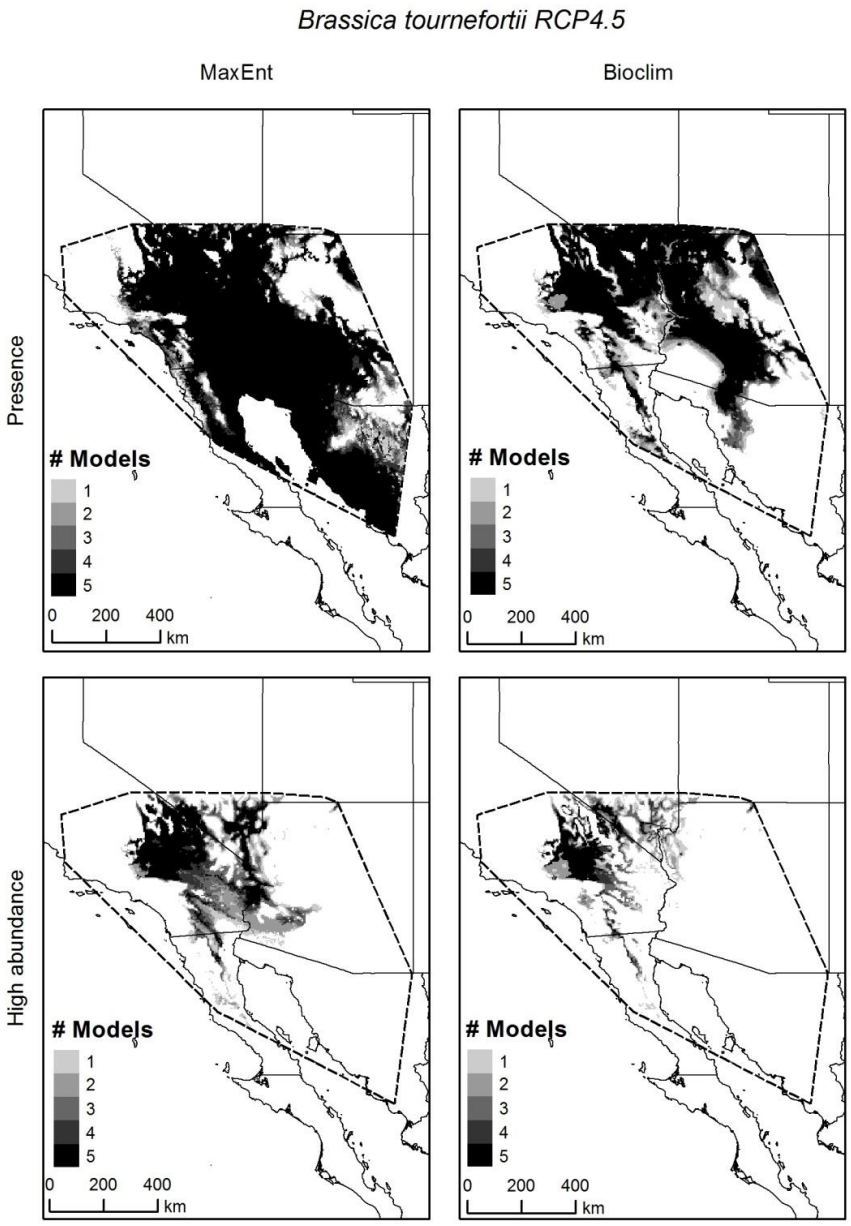

Figure D2. Ensemble models for *B. tournefortii* under future climate projections for RCP4.5.

Projections were made by using MaxEnt and Bioclim to model future suitable habitat for each of the five Atmosphere Ocean General Circulation Models. Ensemble models were created by adding the five models created by each species distribution modeling method together. Darker areas indicate higher model agreement.

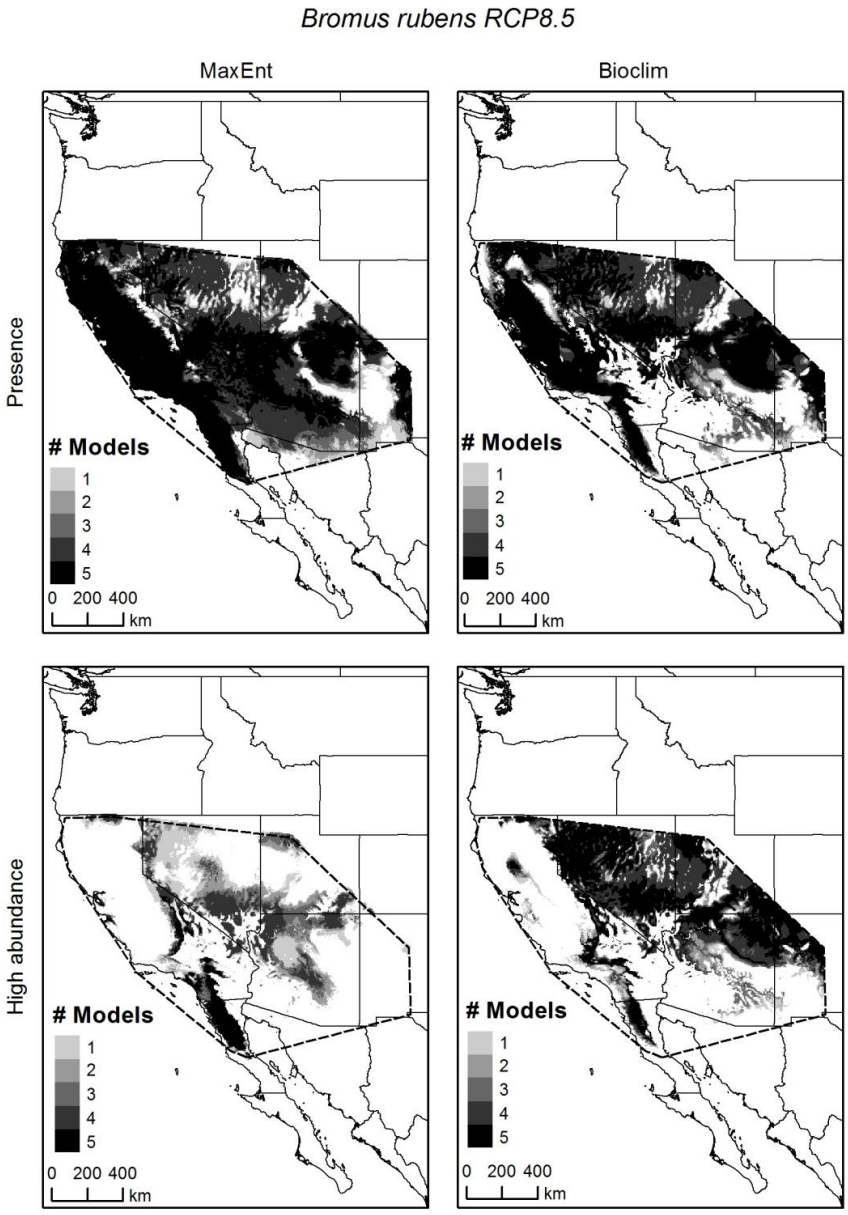

Figure D3. Ensemble models for *B. rubens* under future climate projections for RCP8.5.

Projections were made by using MaxEnt and Bioclim to model future suitable habitat for each of the five Atmosphere Ocean General Circulation Models. Ensemble models were created by adding the five models created by each species distribution modeling method together. Darker areas indicate higher model agreement.

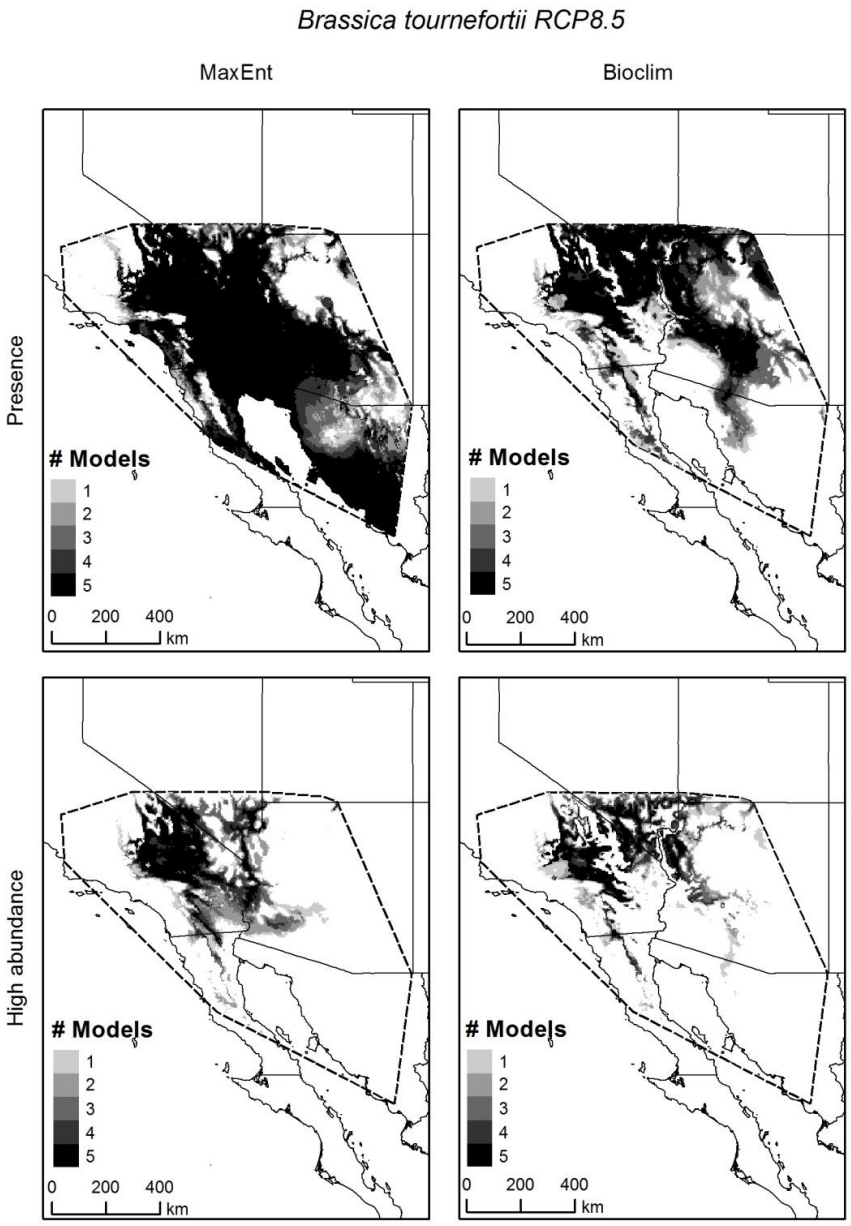

Figure D4. Ensemble models for *B. tournefortii* under future climate projections for RCP8.5.

Projections were made by using MaxEnt and Bioclim to model future suitable habitat for each of the five Atmosphere Ocean General Circulation Models. Ensemble models were created by adding the five models created by each species distribution modeling method together. Darker areas indicate higher model agreement.

APPENDIX E

COMPARATIVE NICHE VALUE BASED ON ALL DATA

In addition to the conservative calculations based on the 95th percentile, we created a more robust set of calculations based on the entire dataset. We calculated a comparative niche value (hereafter ΔCN) for each species and each of the three climate variables (maximum precipitation, corrected minimum precipitation, and corrected minimum temperature). For consistent visual comparison, ΔCN was calculated for all climate variables such that positive values indicate broader a climatic niche measured from the herbarium data. We used Mann-Whitney-Wilcoxon tests to compare the climate niches derived from the physiological tolerance estimates and the herbarium records.

Results based on the entire dataset (rather than a more conservative 95% of data) indicate broader climatic tolerance from herbarium records for all three of the climate variables tested. The average plant can withstand an extreme minimum temperature of 15° C lower than estimated by experts. Herbarium records also suggest greater tolerance of drought (250 mm lower than expert-based estimate) and wet conditions (566 mm higher than expert-based estimates).

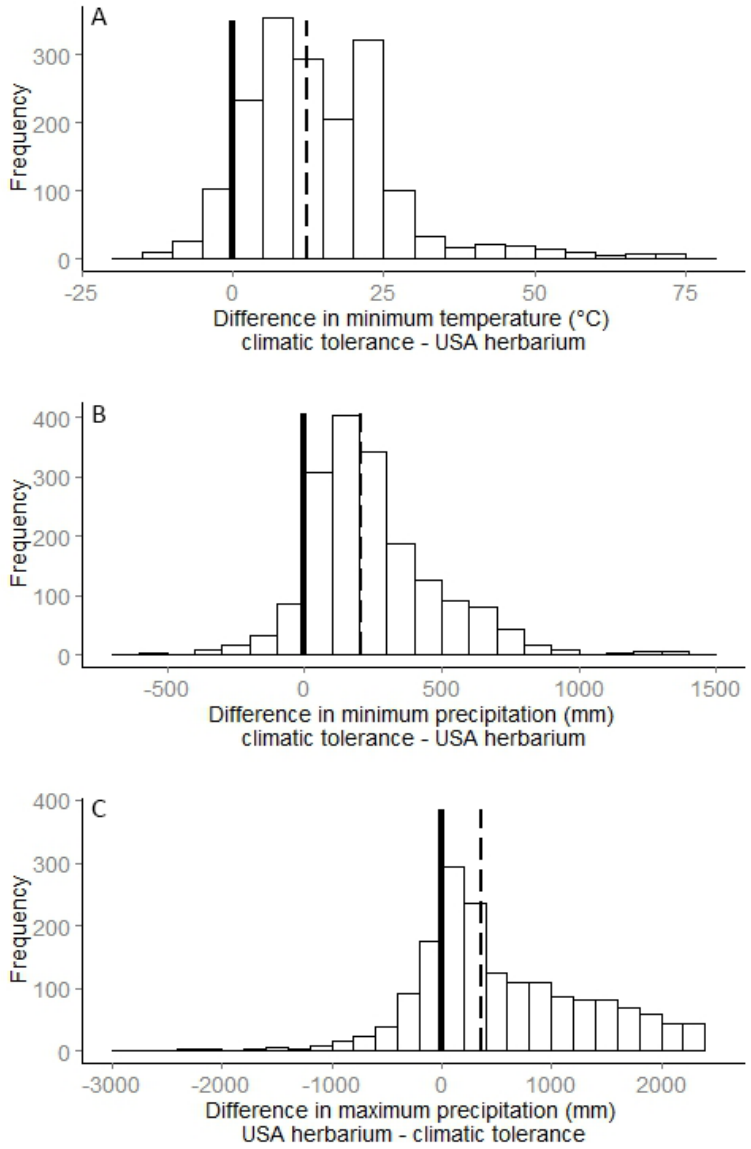

Figure E1. ΔCN calculated for entire dataset (rather than the conservative 95% threshold) reveal broader climatic tolerance estimated from herbarium records for all climate variables.

Frequency distributions of the comparative niche values (ΔCN) calculated for the entire dataset (rather than the 95th percentile) show that herbarium records tend to estimate broader climatic niches than physiological tolerance estimate. Positive differences indicate broader climatic niches measured from the herbarium records. The solid line indicates zero and the dashed lines indicate the median ΔCN. Herbarium

records predicted a lower minimum temperature tolerance (A) for 92% of species (median ΔCN = 12.5°C). Lower minimum (B) and maximum precipitation (C) was found for 91% and 78% of species, respectively (median ΔCN = 209 mm and 357 mm, respectively).

APPENDIX F

WEATHER STATION LOCATIONS

The USDA PLANTS database provides physiological tolerance estimates based on extreme values of minimum and maximum precipitation and minimum temperature. Meanwhile, climate data from the WorldClim dataset is based on temporal averages from 1950-2000 which results in a loss of extreme values. To make the datasets comparable, we calculated the extreme and average minimum temperature for each location from a time series (1950-2000) of daily January minimum temperature from over 80 weather stations throughout the USA (FigureF1, Table F1). We then calculated a linear gain and offset based on the average and extreme values and applied the linear correction to the climate values derived from Worldclim.

Figure F1. Locations of weather stations used to calculate the linear gain and offset between the Worldclim and PRISM datasets.

Weather stations were selected from each state in the USA, with additional stations selected as needed to fill gaps in the covered climate space. Daily January minimum temperature data were downloaded for each of the weather stations (black points).

Table F1. Weather station name and locality data.

Station Name	State	LATITUDE	LONGITUDE
Albany Airport	NY	42.75	-73.8
Albuquerque International Airport	NM	35.05	-106.617
Allentown Lehigh Valley International Airport	PA	40.65	-75.4333
Amarillo International Airport	TX	35.23333	-101.7
Anacortes	WA	48.51667	-122.617
Annette Weather Service Office Airport	AK	55.03333	-131.567
Atlanta Hartsfield International Airport	GA	33.65	-84.4167
Atlantic City International Airport	NJ	39.45	-74.5833
Baltimore Washington International Airport	MD	39.18333	-76.6667
Billings International Airport	MT	45.8	-108.533
Birmingham Airport	AL	33.45	-86.85
Bismarck Municipal Airport	ND	46.7825	-100.757
Blythe Airport	CA	33.61667	-114.6
Boise Air Terminal	ID	43.56667	-116.241
Boston Logan International Airport	MA	42.36667	-71.0167
Bozeman Montana SU	MT	45.67056	-111.05
Burlington International Airport	VT	44.46667	-73.15
Butte Bert Mooney Airport	MT	45.95	-112.5
Casper Natrona CO International Airport	WY	42.8975	-106.464
Centralia	WA	46.71667	-122.95
Charleston International Airport	SC	32.9	-80.0333
Charleston Yeager Airport	WV	38.36667	-81.6
Chewelah	WA	48.25	-117.717
Cleveland Hopkins International Airport	OH	41.4	-81.85
Concord Municipal Airport	NH	43.2	-71.5
Corpus Christi NAS	TX	27.7	-97.2667
Davenport	WA	47.65	-118.15
Daytona Beach International Airport	FL	29.18333	-81.05
Denver Stapleton	CO	39.75	-104.867
Des Moines International Airport	IA	41.53333	-93.65
Desert National WL Range	NV	36.43778	-115.36

Desert Resorts Regional Airport	CA	33.63333	-116.167
Dodge City Regional Airport	KS	37.76667	-99.9667
Duluth International Airport	MN	46.83694	-92.21
Encinal	TX	28.05	-99.35
Fairbanks International Airport	AK	64.83333	-147.717
Flint Bishop International Airport	MI	42.96667	-83.75
Follett	TX	36.43333	-100.133
Fort Wayne International Airport	IN	41	-85.2
Grand Island Central NE Regional Airport	NE	40.96667	-98.3167
Grayland	WA	46.8	-124.083
Green Bay Austin Straubel International Airport	WI	44.487	-88.138
Greensboro Piedmont Triad International Airport	NC	36.08333	-79.95
Hartford Bradley International Airprot	CT	41.93806	-72.6825
Hawaii Volcano National Park HQ 54	HI	19.43306	-155.26
Helena Regional Airport	MT	46.6	-112
Honolulu International Airport	HI	21.33333	-157.917
Imlay	NV	40.66667	-118.15
Indianapolis International Airport	IN	39.73333	-86.2667
Kentfield	CA	37.95	-122.55
Lower Klamath	CA	41.52167	-124.032
Lahontan Dam	NV	39.46667	-119.067
Las Vegas McCarran International Airport	NV	36.08333	-115.167
Little Roack Airport Adams Field	AR	34.73333	-92.2333
Los Angeles International Airport	CA	33.93333	-118.383
Louisville International Airport	KY	38.18333	-85.7333
Lovelock Derby Field	NV	40.06667	-118.55
Lynchburg Regional Airport	VA	37.33333	-79.2
Makaweli 965	HI	21.91667	-159.633
Medford Gogue Valley International Airport	OR	42.36667	-122.867
Memphis International Airport	TN	35.05	-89.9833
Meridian Key Field	MS	32.33333	-88.75
Miles City 1.2 ENE	MT	46.43333	-105.867
Mina	NV	38.38333	-118.1
Monroe	WA	47.85	-121.983
Montello	NV	41.26667	-114.2
Nevada City	CA	39.24806	-121.002
New Orleans International Airport	LA	29.98333	-90.25
Oklahoma City Will Rogers World Airport	OK	35.38861	-97.6003
Port Angeles Fairchild International Airport	WA	48.12028	-123.498
Port Arthur SE Texas Regional Airport	TX	29.95	-94.0167
Portland International Jetport	ME	43.64222	-70.3044

Providence TF Green State Airport	RI	41.73333	-71.4333
Punchbowl Crater 709	HI	21.31667	-157.85
Salt Lake City International Airport	UT	40.76667	-111.967
Smoky Valley Carvers	NV	38.78333	-117.167
St. Louis Lambert International Airport	MO	38.7525	-90.3736
St. Paul Island Airport	AK	57.15	-170.217
Tanana Calhoun Memorial Airport	AK	65.16667	-152.1
Texas Post Office	TX	-28.8544	151.1681
Tuscon International Airport	AZ	32.13333	-110.95
Twin Bridges	MT	45.55	-112.317
Valdez Weather Service Office	AK	61.11667	-146.267
Washington Reagan National Airport	VA	38.85	-77.0333
Wilmington New Castle CO Airport	DE	39.66667	-75.6
Winnemucca Municipal Airport	NV	40.9	-117.8
Wrangell Airport	AK	56.46667	-132.383

APPENDIX G

MEAN SAGEBRUSH COVER PROJECTIONS

In addition to models of maximum sagebrush percent cover, we modeled mean sagebrush percent cover. We compiled sagebrush percent cover from the Bureau of Land Management (BLM), the Nevada Department of Wildlife (NDOW), and the Utah Division of Wildlife Resources (UDWR). We spatially aggregated 13,196 points, taking the mean percent cover value for pixels with more than one record, resulting in 9,515 points. We calculated variable importance using the cover using the Random Forest Cross-Validation for feature selection (rfcv) function in the randomForest package in R (Liaw and Wiener 2002) and retained the top 10 predictor variables (Table G1). We then used random forest to model mean percent cover for current and future climate conditions. Pixels with four or five models predicting suitable habitat can be interpreted as suitable with high confidence. Pixels with one or more models predicting suitable habitat can be interpreted as suitable with lower confidence. Pixels with zero models predicting suitable habitat were interpreted as unsuitable.

Results for projected mean sagebrush cover are similar to those for projected maximum sagebrush cover. For all species, the area projected to have suitable climate based on mean sagebrush cover under current conditions is lower than the projected area based on sagebrush cover. This is also true for high confidence future projections. Low confidence future projections based on mean sagebrush cover are lower than those based on maximum sagebrush cover for species except the pygmy rabbit. Consistent with projections based on maximum sagebrush cover, Brewer's sparrow (*Spizella breweri*) is projected to have the largest area with suitable climate based on mean sagebrush cover.

Brewer's sparrow is also projected to gain slightly more area with suitable climate in the future according to models based on mean sagebrush models than models based on maximum sagebrush (Table G2) (Figure G1). Both sage sparrow (*Artemisiospiza nevadensis*) and sage thrasher (*Oreoscoptes montanus*) are projected to gain area with suitable climate in the future based on low confidence projections. However, based on the high threshold, these species are projected to have less climatically suitable area in the future according to the model based on mean sagebrush cover (14% loss) relative to the models based on maximum sagebrush cover (2% and 3% loss). Low confidence projections show that the sagebrush vole (*Lemmiscus curtatus*) and pygmy rabbit (*Brachylagus idahoensis*) are both projected to lose less area in the future according to models based on mean sagebrush cover (18% and 36% loss) than models based on maximum percent cover (29% and 46% loss). High confidence projections for these species show similar results with the sagebrush vole projected to lose less area with suitable climate (68% loss based on mean, 70% loss based on maximum) and the pygmy rabbit projected to lose 91% of area with suitable climate regardless of model type (Table G2).

Overall, the results for our models based on mean sagebrush cover were similar to those based on maximum sagebrush cover. All losses and gains are projected to occur in a consistent direction between models, although the magnitude of change varies. We chose to present results from models based on maximum percent cover in the main text because we felt it was better to err on the conservative side and identify the full extent of climatically suitable area. Projections from models based on mean sagebrush cover might represent a more ecologically realistic scenario in which sagebrush is not present in

all climatically suitable area. Given how similar our model results were, either approach would yield useful results.

Table G1. Selected predictor variables used in the random forest models were nearly identical to those used to predict maximum cover.

Importance	**Predictor Variable**
1	Precipitation Seasonality
2	Elevation (DEM)
3	Precipitation of Warmest Quarter
4	Precipitation of Coldest Quarter
5	Mean Temperature of Wettest Quarter
6	Annual Precipitation
7	Precipitation of Driest Quarter
8	Precipitation of Wettest Month
9	Precipitation of Driest Month
10	Precipitation of Wettest Quarter

Table G2. Suitable area for each species based on potential sagebrush cover under current and future projections (RCP 4.5; mean sagebrush value per pixel).

Low confidence future area includes all pixels with modeled climate to support suitable sagebrush cover from any one or more of the five AOGCMs while the high confidence future includes just those pixels where four or five AOGCMs indicated suitable climate for required sagebrush cover. *A. nevadensis* and *O. montanus* have the same minimum sagebrush cover threshold and similar current projected suitable area. Therefore, they have the same projection of future suitable area.

	Area (km^2)		
Species	**Current**	**Low Confidence Future (% change)**	**High Confidence Future (% change)**
S. breweri	748,913	952,603 (+27%)	848,750 (+13%)
A. nevadensis	484,323	665,048 (+37%)	416,905 (-14%)
O. montanus	485,007	665,058 (+37%)	416,914 (-14%)
L. curtatus	155,041	127407 (-18%)	50,305 (-68%)
B. idahoensis	85,726	55,291 (-36%)	7,851 (-91%)

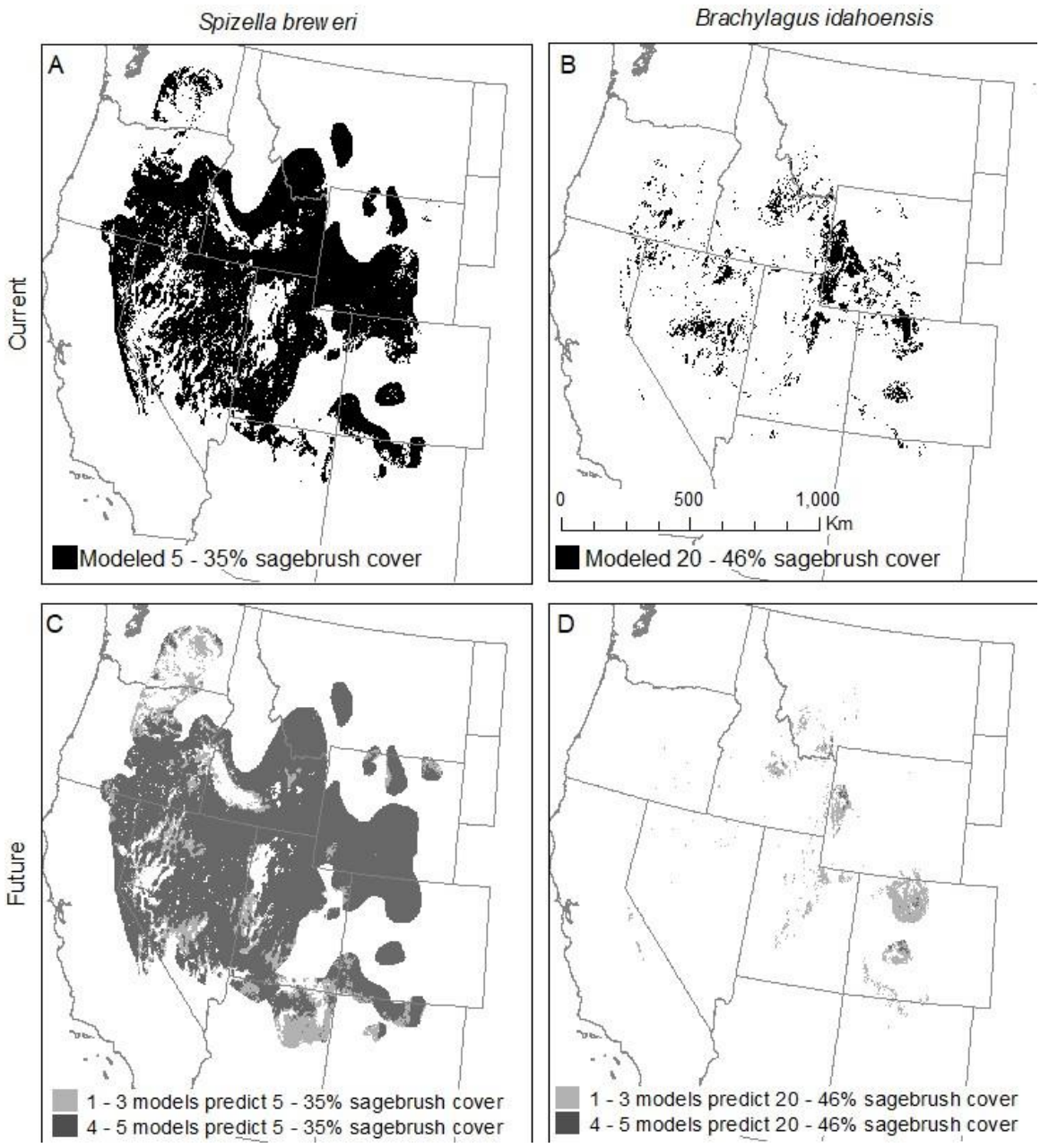

Figure G1. Current (A, B) and future (C, D) projected suitable climate for adequate sagebrush cover for the species with the largest (Brewer's sparrow (*Spizella breweri*)) and smallest (Pygmy rabbit (*Brachylagus idahoensis*)) modeled current habitat.

APPENDIX H

MAXIMUM SAGEBRUSH COVER PROJECTIONS (RCP8.5)

In addition to the future models for RCP4.5 presented in the main text, we projected suitable area for RCP8.5 based on maximum sagebrush cover. Because future climate projections vary depending on the modeling group and emissions scenario we created future projections for RCP8.5 in addition to those for RCP 4.5 presented in the main text. These were based on the same model used in the main text; therefore, projection of area with currently suitable climate is the same. Pixels with four or five models predicting suitable habitat can be interpreted as suitable with high confidence. Pixels with one or more models predicting suitable habitat can be interpreted as suitable with lower confidence. Pixels with zero models predicting suitable habitat were interpreted as unsuitable.

Results from the RCP8.5 projections were consistent in the direction of change with results from the RCP4.5 projection with the exception of the high confidence future projections for sage sparrow (*Artemisiospiza nevadensis*) and sage thrasher (*Oreoscoptes montanus*). For RCP4.5, these species are projected to lose 2% and 3% of area with suitable climate while, for RCP8.5, they are projected to gain less than 1%%. The magnitude of change is greater for RCP8.5, with all species projected to gain or lose more area with suitable climate than was found for RCP4.5 (Table H1). Brewer's sparrow (*Spizella breweri*), sage sparrow, and sage thrasher are projected to gain area with suitable climate according to both low and high confidence projections. Sagebrush vole (*Lemmiscus curtatus*) and pygmy rabbit (*Brachylagus idahoensis*) are both projected to lose area with suitable climate according to both low and high confidence projections.

Although the magnitude of change differs from the results of the RCP4.5 projections, they are similar in direction and spatial configuration. Therefore, the RCP8.5 projections could be treated as a 'worst-case-scenario' of distribution changes in response to a more extreme climate change scenario.

Table H1. Suitable area for each species based on potential sagebrush cover under current and future projections (RCP 8.5; maximum sagebrush value per pixel).

Low confidence future area includes all pixels with modeled climate to support suitable sagebrush cover from any one or more of the five AOGCMs while the high confidence future includes just those pixels where four or five AOGCMs indicated suitable climate for required sagebrush cover. *A. nevadensis* and *O. montanus* have the same minimum sagebrush cover threshold and similar current projected suitable area. Therefore, they are projected to have change within 0.1% of each other.

	Area (km^2)		
Species	**Current**	**Low Confidence Future (% change)**	**High Confidence Future (% change)**
S. breweri	766,525	971,779 (+7%)	883,828 (+15%)
A. nevadensis	521,904	749,547 (+44%)	525,160 (+0.6%)
O. montanus	522,790	749547 (+43%)	525,160 (+0.5%)
L. curtatus	181,486	118,706 (-35%)	47,810 (-74%)
B. idahoensis	102,721	42,739 (-58%)	4,189 (-96%)

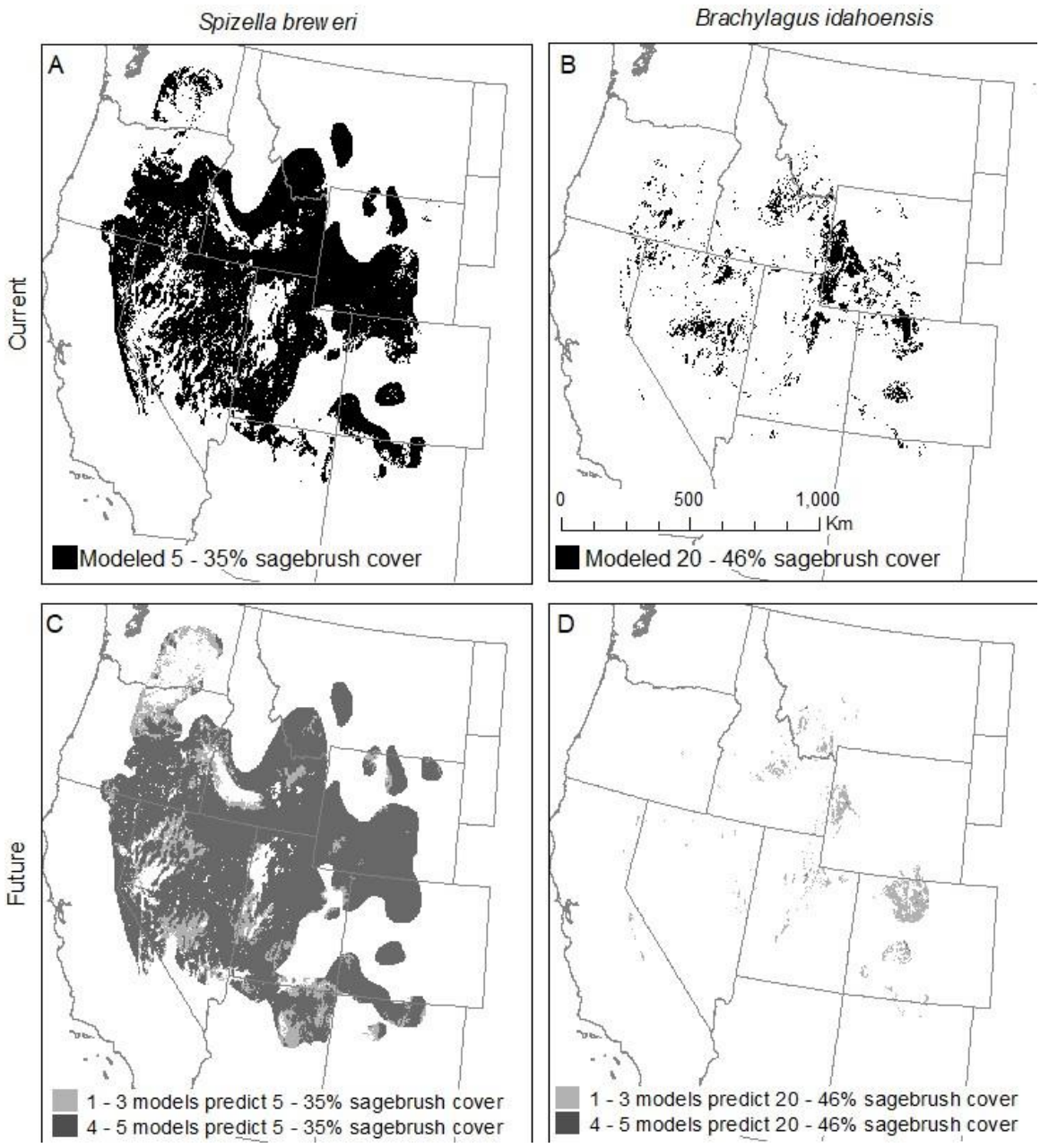

Figure H1. Current (A, B) and future (C, D) projected suitable climate for adequate sagebrush cover for the species with the largest (Brewer's sparrow (*Spizella breweri*)) and smallest (Pygmy rabbit (*Brachylagus idahoensis*)) modeled current habitat.

APPENDIX I

HILLSHADE MASK

The unique topography of Chile required us to apply a secondary mask to filter areas in shadow. We applied a series of hillshade thresholds to the same Landsat image from February 8, 2001 (summer) to determine what level would allow us to keep pertinent information while masking out artificially dark pixels. A threshold hillshade value of 100 (Figure I1 panels B, E) effectively excluded the darkest shadows while retaining the bulk of the image. Pixels with hillshade values less than or equal to the threshold value were masked out (black areas in Figure I1).

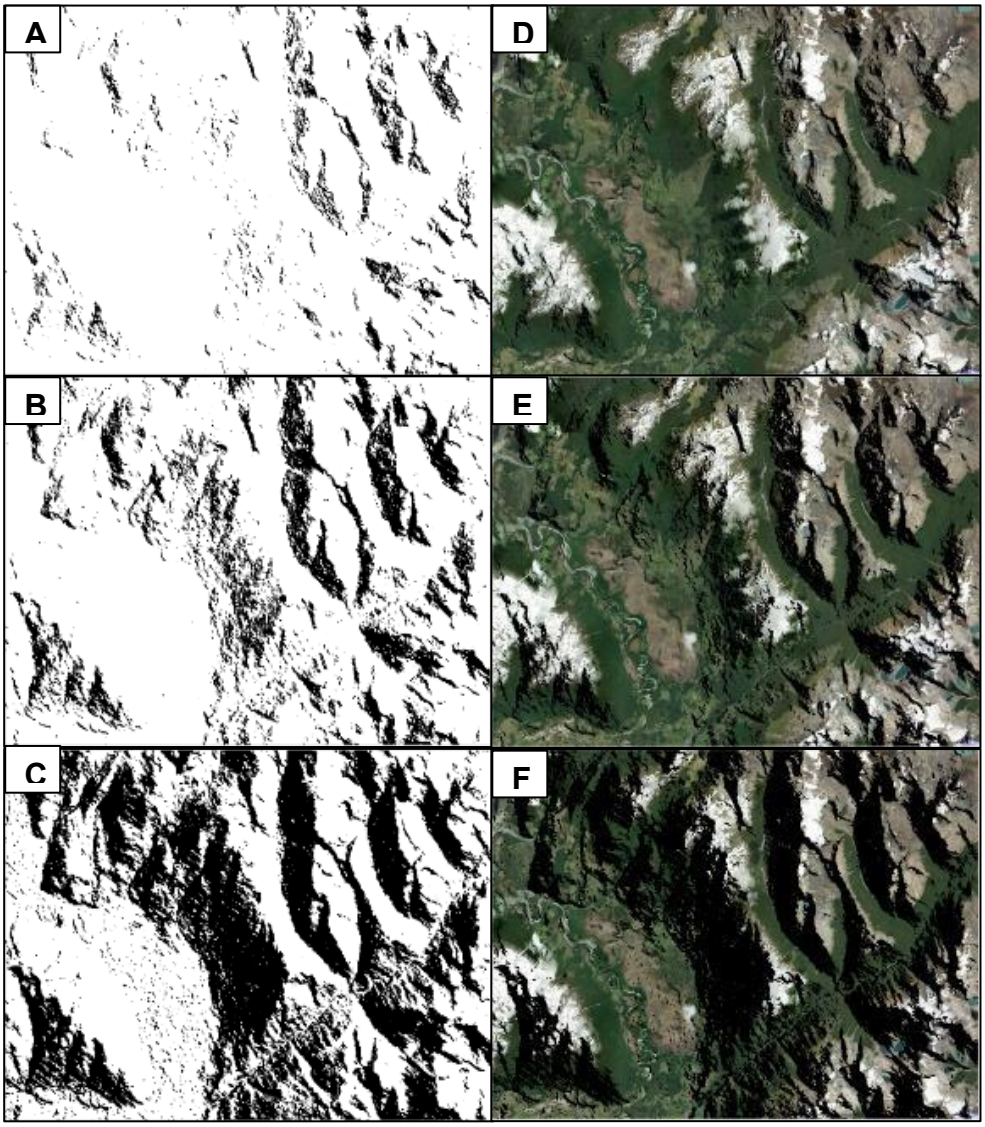

Figure I1. We applied various masks to a single hillshade to determine the best threshold. Black areas indicate masked land based on masking areas with hillshade less than 50, 100, and 150 (A-C). The same hillshade masks are overlaid on a high resolution image (D-F).

APPENDIX J

EXAMPLE SPECTRAL-TEMPORAL PLOTS

The spectral-temporal signature of non-native pine was fairly distinct from native land cover classes. By surveying spectral-temporal features for Tasseled Cap Brightness, Greenness, and Wetness across the different land cover classes (Figure J1, J2), we were able to infer patterns about that can be used to characterize land cover.

Native forest tends to have more intra-annual variation in Tasseled Cap Brightness values than non-native pine (Figure J1). Native forest and grass/agriculture also have a relatively stable signal (i.e., no change in average value through time) whereas non-native pine Tasseled Cap Brightness tends to decrease through time (Figure J1). Pines are more structurally complex, with reflectance comprising needles, bark, and shadow, than the grasses or cleared land they may be replacing, creating a long-term decline in Brightness.

Grass/agriculture tends to have more intra-annual variation in Tasseled Cap Wetness values than non-native pine and native forest (Figure J2). Tasseled Cap Wetness values for non-native pine tends to increase through time likely because pine stands become more structurally complex as they mature. In contrast, native forest and grass/agriculture Tasseled Cap Wetness values tend to remain stable through time (Figure J2).

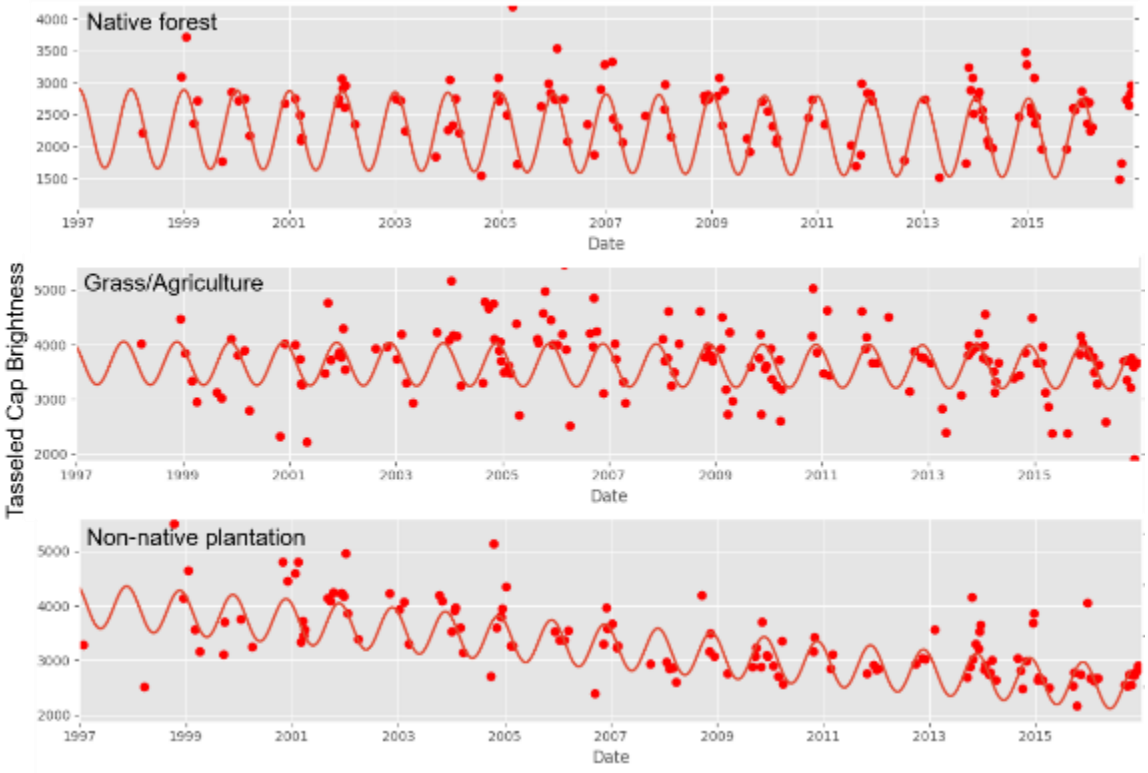

Figure J1. Spectral-temporal plots of a single pixel for Tasseled Cap Brightness values of three land cover types.

Red points represent available images. Non-native pines are characterized by less intra-annual variation and decreasing Tasseled Cap Brightness values through time.

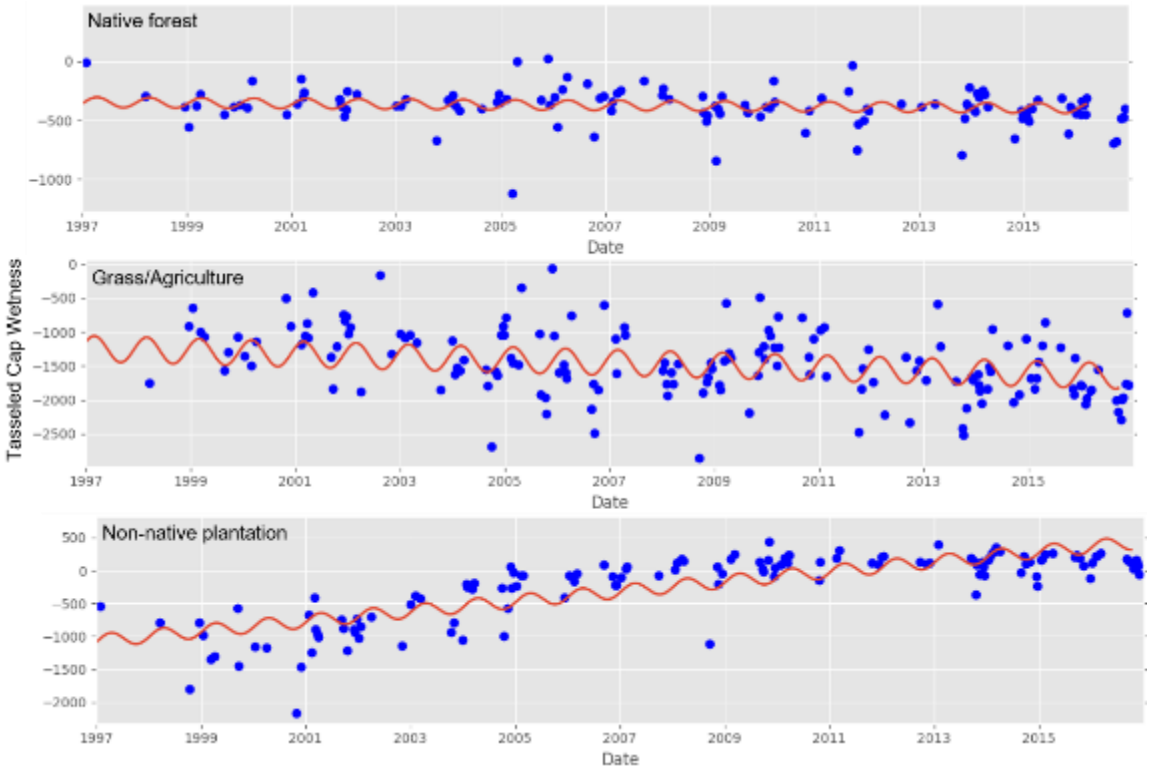

Figure J2. Spectral-temporal plots of a single pixel for Tasseled Cap Wetness values of three land cover types.

Blue points represent available images. Non-native pine is characterized by less intra-annual variation than grass/agriculture and an increasing Tasseled Cap Wetness value.

BIBLIOGRAPHY

Agee, J. K. 1998. Fire and pine ecosystems. In: Richardson, D.M. (ed), Ecology and Biogeography of *Pinus*. Cambridge University Press, pp. 193–213.

Allan, D.G., J.A. Harrison, R.A. Navarro, B.W. Van Wilgen, and M.W. Thompson. 1997. The impact of commercial afforestation on bird populations in Mpumalanga Province, South Africa - Insights from bird-atlas data. *Biol. Conserv.* **79**: 173–185.

Araújo, M.B. and R.G. Pearson. 2005. Equilibrium of species' distributions with climate. *Ecography*. **28**: 693–695.

Araújo, M.B. and M. New. 2007. Ensemble forecasting of species distributions. *Trends Ecol. Evol*. **22**: 42–47.

Araújo, M.B., M. Cabeza, W. Thuiller, L. Hannah, and P.H. Williams. 2004. Would climate change drive species out of reserves? An assessment of existing reserve-selection methods. *Glob. Chang. Biol.* **10**: 1618–1626.

Araújo, M.B., D. Alagador, M. Cabeza, D. Nogués-Bravo, and W. Thuiller. 2011. Climate change threatens European conservation areas. *Ecol. Lett.* **14**: 484–492.

Armesto, J.J., J.C. Aravena, C. Villagrán, C. Pérez, G.G. Parker. 1996. Bosques templados de la cordillera de la costa. In: Armesto, J., C. Villagrán, and M. Kalin Arroyo (eds), Ecología de los Bosques Nativos de Chile. Editorial Universitaria Santiago, p. 199-214.

Baker, W.L. 2006. Fire and restoration of sagebrush ecosystems. Wildl. Soc. Bull. 34: 177–185.

Balch, J.K., B.A. Bradley, C.M. D'Antonio, and J. Gómez-Dans. 2013. Introduced annual grass increases regional fire activity across the arid western USA (1980-2009). G*lob. Chang. Biol*. **19**: 173–183.

Barrows, C.W., E.B. Allen, M.L. Brooks, and M.F. Allen. 2009. Effects of an invasive plant on a desert sand dune landscape. *Biol. Invasions*. **11**: 673–686.

Beatley, J.C. 1974. Phenological events and their environmental triggers in Mojave Desert ecosystems. *Ecology* **55**: 856–863.

Benkman, C.W. 1995. Wind dispersal capacity of pine seeds and the evolution of different seed dispersal modes in pines. *Oikos*. **73**: 221-224.

Benson, A. 2016. A national look at Species of Greatest Conservation Need as reported in State Wildlife Action Plans. *U.S. Geological Survey Core Science Analytics Synthesis, and Library.* Available: www.usgs.gov/ core_science_systems/csas/swap/sgcn.

Booth, T.H. 2014. Using biodiversity databases to verify and improve descriptions of tree species climatic requirements. *For. Ecol. Manage*. **315**: 95–102.

Booth, T.H., L.M. Broadhurst, E. Pinkard, S.M. Prober, S.K. Dillon, D. Bush, K. Pinyopusarerk, J.C. Doran, M. Ivkovich, and A.G. Young. 2015. Native forests and climate change: Lessons from eucalypts. *For. Ecol. Manage.* **347**: 18–29.

Bosci, T., J. Allen, J. Bellemare, J. Kartesz, M. Nishino, and B.A. Bradley. 2016. Species distributions do not reflect climatic tolerance. Divers. Distrib. 22: 615-624.

Bradley, B.A. 2010. Assessing ecosystem threats from global and regional change: hierarchical modeling of risk to sagebrush ecosystems from climate change, land use and invasive species in Nevada, USA. *Ecography*. **33**: 198–208.

Bradley, B. A. 2013. Distribution models of invasive plants over-estimate potential impact. *Biol. Invasions*, **15**: 1417–1429.

Bradley, B.A., R. Early, and C.J.B. Sorte. 2015. Space to invade? Comparative range infilling and potential range of invasive and native plants. *Glob. Ecol. Biogeogr.* **24**: 348–359.

Bradley, B.A., C.A. Curtis, E.J. Fusco, J.T. Abatzoglou, J.K. Balch, S. Dadashi, and M.N. Tuanmu. 2017. Cheatgrass (*Bromus tectorum*) distribution in the intermountain Western United States and its relationship to fire frequency, seasonality, and ignitions. *Biol. Invasions*, **20**: 1493-1506.

Braun, A.C., D. Troeger, R. Garcia, M. Aguayo, R. Barra, and J. Vogt. 2017. Assessing the impact of plantation forestry on plant biodiversity: A comparison of sites in Central Chile and Chilean Patagonia. *Glob. Ecol. Conserv.* **10**: 159–172.

Broennimann, O., Treier, U.A., H. Müller-Schärer, W. Thuiller, A.T. Peterson, A. Guisan. 2007. Evidence of climatic nich shift during biological invasion. *Ecol. Lett.* **10**: 701–709.

Brooks, M.L. and D.A. Pyke. 2001. Invasive plants and fire in the deserts of North America. In: The First National Congress on Fire Ecology, Prevention, and Management, San Diego, CA, Tall Timbers Research Station.

Brown, J.H., D.W. Mehlman, and G.C. Stevens. 1995. Spatial Variation in Abundance. *Ecology*, **76**: 2028–2043.

Buckley, L.B., M.C. Urban, M.J. Angilletta, L.G. Crozier, L.J. Rissler, M.W. Sears et al. 2010. Can mechanism inform species' distribution models? *Ecol. Lett.* **13**: 1041–54.

Buckley, L.B., S.A. Waaser, H.J. MacLean, R. Fox. 2011. Does including physiology improve species distribution model predictions of responses to recent climate change? *Ecology* **92**: 2214–2221.

Bustamante, R.O. and J.A. Simonetti. 2005. Is *Pinus radiata* invading the native vegetation in Central Chile? Demographic responses in a fragmented forest. *Biol. Invasions* **7**: 243–249.

Bustamante, R.O., I.A. Serey, S.T.A. Pickett et al. 2003. Forest fragmentation, plant regeneration and invasion process in Central Chile. - In: Bradshaw, G.A. and P.A. Marquet. (eds), How Landscapes Change: Human Disturbance and Ecosystem Fragmentation in the Americas, vol 162. Springer, Berlin, Heidelberg, pp. 145–160.

Bykova, O. and R.F. Sage. 2012. Winter cold tolerance and the geographic range separation of *Bromus tectorum* and *Bromus rubens*, two severe invasive species in North America. *Glob. Chang. Biol.* **18**: 3654–3663.

Ceia-Hasse, A., B. Sinervo, L. Vicente, H.M. Pereira. 2014. Integrating ecophysiological models into species distribution projections of European reptile range shifts in response to climate change. *Ecography*. **37**: 679–688.

Chamberlain, S., K. Ram, V. Barve, D. Mcglinn. 2014. rgbif: Interface to the Global Biodiversity Information Facility API. - R Package version 0.7

Chambers, J.C. and M. Pellant. 2008. Climate change impacts on northwestern and intermountain United States rangelands. *Rangelands.* **30**: 29–33.

Chirino, I., L. Condron, R. McLenaghen, and M. Davis. 2010. Effects of plantation forest species on soil properties. *19th World Congress of Soil Science, Soil Solutions for a Changing World*. p. 49-51.

Chown, S.L. and K.J. Gaston. 2016. Macrophysiology - progress and prospects. *Funct. Ecol.* **30**: 330–344.

Cóbar-Carranza, A.J., R.A. García, A. Pauchard, and E. Peña. 2014. Effect of *Pinus contorta* invasion on forest fuel properties and its potential implications on the fire regime of *Araucaria araucana* and *Nothofagus antarctica* forests. *Biol. Invasions*. **16**: 2273-2291.

Cohen, J. 1960. A coefficient of agreement for nominal scales. *Educ. Psychol. Meas.* **20**: 37–46.

Cohen, W.B. and S.N. Goward. 2004. Landsat's role in ecological applications of remote sensing. *Bioscience* **54**: 535–545.

Colautti, R.I., I.A. Grigorovich, H.J. MacIsaac. 2006. Propagule pressure: a null model for biological invasions. *Biol Invasions*. **8**: 1023-1037.

Colwell, R.K. and E.R. Fuentes. 1975. Experimental studies of the niche. *Annu. Rev. Ecol. Syst.* **6**: 281–310.

Coops, N.C., R.H. Waring, and T.A. Schroeder. 2009. Combining a generic process-based productivity model and a statistical classification method to predict the presence and absence of tree species in the Pacific Northwest, U.S.A. *Ecol. Modell.* **220**: 1787–1796.

Crist, E.P. 1985. A TM Tasseled Cap equivalent transformation for reflectance factor data. *Remote Sens. Environ*. **17**: 301–306.

Crist, E.P. and R.J. Kauth. 1986. The Tasseled Cap de-mystified. *Photogramm. Eng. Remote Sens.* **52**: 81–86.

Cuddington, K.. M.J. Fortin, L.R. Gerber, A. Hastings, A. Liebhold, M. O'Connor, and C. Ray. 2013. Process-based models are required to manage ecological systems in a changing world. *Ecosphere* **4**: 1–12.

Daly, C., W.P. Gibson, G.H. Taylor, G.L. Johnson, and P. Pasteris. 2002. A knowledge-based approach to the statistical mapping of climate. *Clim. Res.* **22**: 99–113.

Daru, B.H., D.S. Park, R.B. Primack, C.G. Willis, D.S. Barrington, T.J.S. Whitfeld, T.G. Seidler, P.W. Sweeney, D.R. Foster, A.M. Ellison, C.C. Davis. 2017. Widespread sampling biases in herbaria revealed from large-scale digitization. *New Phyto*. **217**: 939-955.

Davies, K.W., C.S. Boyd, J.L. Beck, J.D. Bates, T.J. Svejcar, and M.A. Gregg. 2011. Saving the sagebrush sea: An ecosystem conservation plan for big sagebrush plant communities. *Biol. Conserv.* **144**: 2573–2584.

Davis, A.J., L.S. Jenkinson, J.H. Lawton, B. Shorrocks, and S. Wood. 1998. Making mistakes when predicting shifts in species range in response to global warming. *Nature*. **391**: 783–786.

Despain, D.G. 2001. Dispersal ecology of lodgepole pine (*Pinus contorta* Dougl.) in its native environment as related to Swedish forestry. *For. Ecol. Manage*. **141**: 59–68.

Diamond, S.E., L.M. Nichols, N. McCoy, C. Hirsch, S.L. Pelini, N.J. Sanders, A.M. Ellison, N.J. Gotelli, and R.R. Dunn. 2012. A physiological trait-based approach to predicting the responses of species to experimental climate warming. *Ecology* **93**: 2305–2312.

Dormann, C.F., S.J. Schymanski, J. Cabral, I. Chuine, C. Graham, F. Hartig, M. Kearney, X. Morin, C. Römermann, B. Schröder, and A. Singer. 2012. Correlation and process in species distribution models: bridging a dichotomy. *J. Biogeogr.* **39**: 2119–2131.

Dubin, R.A. 1998. Spatial autocorrelation: A primer. *J. Hous. Econ.* **7**: 304–327.

Early, R. and D.F. Sax. 2014. Climatic niche shifts between species' native and naturalized ranges raise concern for ecological forecasts during invasions and climate change. *Glob. Ecol. Biogeogr.* **23**: 1356–1365.

Echeverria, C., D.A. Coomes, J. Salas, J.M. Rey-Benayas, A. Lara, and A. Newton. 2006. Rapid deforestation and fragmentation of Chilean Temperate Forests. *Biol. Conserv.* **130**: 481–494.

Echeverria, C., D.A. Coomes, M. Hall, A.C. Newton. 2008. Spatially explicit models to analyze forest loss and fragmentation between 1976 and 2020 in southern Chile. *Ecol. Modell.* **212**: 439-449.

Elith, J. and J. Leathwick. 2007. Predicting species distributions from museum and herbarium records using multiresponse models fitted with multivariate adaptive regression splines. *Divers. Distrib.* **13**: 265–275.

Elith, J., C.H. Graham, R.P. Anderson, M. Dudík, S. Ferrier, A. Guisan, R.J. Hijmans, F. Huettmann, J.R. Leathwick, A. Lehmann, and J. Li. 2006. Novel methods improve prediction of species' distributions from occurrence data. Ecography. 29: 129–151.

Elith, J., M. Kearney, and S. Phillips. 2010. The art of modelling range-shifting species. *Methods Ecol. Evol.* **1**: 330–342.

Epstein, H.E., R.A. Gill, J.M. Paruelo, W.K. Lauenroth, G.J. Jia, and I.C. Burke. 2002. The relative abundance of three plant functional types in temperate grasslands and shrublands of North and South America: effects of projected climate change. *J. Biogeogr.* **29**: 875–888.

Evans, T.G., S.E. Diamond, and M.W. Kelly. 2015. Mechanistic species distribution modelling as a link between physiology and conservation. *Conserv. Physiol.* **3**: 1–16.

Feldman, T.S. and W.F. Morris. 2011. Higher survival at low density counteracts lower fecundity to obviate Allee effects in a perennial plant. *J. Ecol.* **99**: 1162–1170.

Filz, K.J., T. Schmitt, and J.O. Engler. 2013. How fine is fine-scale? Questioning the use of fine-scale bioclimatic data in species distribution models used for forecasting abundance patterns in butterflies. *Eur. J. Entomol.* **110**: 311–317.

Gabler, K.I., L.T. Heady, and J.W. Laundré. 2001. A habitat suitability model for Pygmy Rabbits (*Brachylagus Idahoensis*) in southeastern Idaho. *West. North Am. Nat.* **61**: 480–489.

Gaines, W.L., P.H. Singleton, R.C. Ross. 2003. Assessing the cumulative effects of linear recreation routes on wildlife habitats on the Okanogan and Wenatchee National Forests. General Technical Report. PNW-GTR-586. Portland, OR U.S. Department of Agriculture, Forest Service, Pacific Northwest Research Station. 79 p.

Gallagher, R.V., L.J. Beaumont, L. Hughes, and M.R. Leishman. 2010. Evidence for climatic niche and biome shifts between native and novel ranges in plant species introduced to Australia. *J. Ecol.* **98**: 790–799.

García-Callejas, D., R. Molowny-Horas, and J. Retana. 2016. Projecting the distribution and abundance of Mediterranean tree species under climate change: a demographic approach. *J. Plant Ecol.* **10**: 731-743.

GDAL/OGR Contributors 2018. GDAL/OGR Geospatial Data Abstraction software Library. *Open Source Geospatial Foundation.* Available: http://gdal.org.

Getis, A. and J.K. Ord. 2010. The analysis of spatial association by use of distance statistics. *Geogr. Anal.* **24**: 189–206.

Gill, A.M. and J.E. Williams. 1996. Fire regimes and biodiversity: the effects of fragmentation of southeastern Australian eucalypt forests by urbanisation, agriculture and pine plantations. *For. Ecol. Manage.* **85**: 261–278.

Green, J.S. and J.T. Flinders. 1980. Habitat and dietary relationships of the pygmy rabbit. *J. Rangel. Mangement* **33**: 136–142.

Grinnell, J. 1914. Barriers to Distribution as Regards Birds and Mammals. *Am. Nat.* **48**: 248–254.

Hantson, S. and E. Chuvieco. 2011. Evaluation of different topographic correction methods for Landsat imagery. *Int. J. Appl. Earth Obs. Geoinf.* **13**: 691–700.

Heilmayr, R., C. Echeverria, R. Fuentes, and E.F. Lambin. 2016. A plantation-dominated forest transition in Chile. *Appl. Geogr.* **75**: 71–82.

Helmuth, B. 2009. From cells to coastlines: how can we use physiology to forecast the impacts of climate change? *J. Exp. Biol.* **212**: 753–60.

Helmuth, B., J.G. Kingsolver, and E. Carrington. 2005. Biophysics, physiological ecology, and climate change: does mechanism matter? *Annu. Rev. Physiol.* **67**: 177–201.

Hernandez, P.A., C.H. Graham, L.L. Master, and D.L. Albert. 2006. The effect of sample size and species characteristics on performance of different species distribution modeling methods. *Ecography*. **29**: 773–785.

Hijmans, R.J., S.E. Cameron, J.L. Parra, P.G. Jones, and A. Jarvis. 2005. Very high resolution interpolated climate surfaces for global land areas. *Int. J. Climatol.* **25**: 1965–1978.

Hijmans, R.J., S. Phillips, J. Leathwick, and J. Elith. 2014. dismo: Species distribution modeling. R package version 1.0-15.

Holloran, M.J. 2005. Greater Sage-grouse (*Centrocercus urophasianus*) population response to natural gas field development in western Wyoming. *Doctoral Dissertation, University of Wyoming*.

Holmes, A. and B. Altman. 2012. Bird habitat guide: sagebrush communities in the intermountain west. *Western Working Group of Partners in Flight.* US Department of the Interior, Bureau of Land Management.

Homer, C.G., C.L. Aldridge, D.K. Meyer, and S.J. Schell. 2012. Multi-scale remote sensing sagebrush characterization with regression trees over Wyoming, USA: Laying a foundation for monitoring. *Int. J. Appl. Earth Obs. Geoinf.* **14**: 233–244.

Hutchinson, G.E. 1957. Concluding Remarks. - *Cold Spring Harb. Symp. Quant. Biol.* **22**: 415–427.

Iverson, L.R. and A.M. Prasad. 1998. Predicting abundance of 80 tree species following climate change in the eastern United States. *Ecol. Monogr.* **68**: 465–485.

Jiménez-Valverde, A., F. Diniz, E.B. de Azevedo, and P.A. Borges. 2009. Species distribution models do not account for abundance: The case of arthropods on Terceira Island. *Ann. Zool. Fennici* **46**: 451–464.

Kattge, J., S. Diaz, S. Lavorel, I.C. Prentice, P. Leadley, G. Bönisch, E. Garnier, M. Westoby, P.B. Reich, I.J. Wright, and J.H.C. Cornelissen. 2011. TRY - a global database of plant traits. *Glob. Chang. Biol.* **17**: 2905–2935.

Kauth, R.J. and G.S. Thomas. 1976. The Tasselled Cap --A graphic description of the spectral-temporal development of agricultural crops as seen by LANDSAT. *LARS Symposia* (p. 159).

Kearney, M. and W. Porter. 2009. Mechanistic niche modelling: Combining physiological and spatial data to predict species' ranges. *Ecol. Lett.* **12**: 334–350.

Kearney, M., B.L. Phillips, C.R. Tracy, K.A. Christian, G. Betts, and W.P. Porter. 2008. Modelling species distributions without using species distributions: the cane toad in Australia under current and future climates. *Ecography*. **31**: 423–434.

Kearney, M., S. J. Simpson, D. Raubenheimer, and B. Helmuth. 2010a. Modelling the ecological niche from functional traits. *Philos. Trans. R. Soc. Lond. B. Biol. Sci.* **365**: 3469–83.

Kearney, M.R., B.A. Wintle, and W.P. Porter. 2010b. Correlative and mechanistic models of species distribution provide congruent forecasts under climate change. *Conserv. Lett.* **3**: 203–213.

Keinath, D.A. and M. Mcgee. 2004. Species assessment for Pygmy Rabbit (*Brachylagus idahoensis*) in Wyoming. - In: Wyoming natural diversity database report to U.S. Department of the Interior Bureau of Land Management.

Knapp, P.A. 1996. Cheatgrass (*Bromus tectorum* L) dominance in the Great Basin Desert: History, persistence, and influences to human activities. *Glob. Environ. Chang.* **6**: 37–52.

Knick, S.T. 1999. Requiem for a Sagebrush Ecosystem? *Northwest Sci.* **73**: 53–57.

La Sorte, F.A. and F.R. Thompson. 2007. Poleward shifts in winter ranges of North American birds. *Ecology* **88**: 1803–1812.

LANDFIRE 2014. Existing vegetation type layer, LANDFIRE 1.4.0, U.S. Department of the Interior, Geological Survey. Accessed 9 January 2018. Available: https://www.landfire.gov/version_comparison.php?mosaic=Y.

Langdon, B., A. Pauchard, and M. Aguayo. 2010. *Pinus contorta* invasion in the Chilean Patagonia: Local patterns in a global context. *Biol. Invasions* **12**: 3961–3971.

Lara, A. and T.T. Veblen. 1993. Forest plantations in Chile: a successful model? - In: Mather, A. (ed), *Afforestation: Policies, Planning and Progress.* Belhaven Press, pp. 118–139.

Latimer, C.E. and B. Zuckerberg. 2016. Forest fragmentation alters winter microclimates and microrefugia in human-modified landscapes. *Ecography*. **40**: 158-170.

Lauenroth, W.K. and J.B. Bradford. 2006. Ecohydrology and the partitioning AET between transpiration and evaporation in a semiarid steppe. *Ecosystems* **9**: 756–767.

Le Maitre, D.C., D.B. Versfeld, and R.A. Chapman. 2000. Impact of invading alien plants on surface water resources in South Africa: a preliminary assessment. *Water Research Commission*. **26**: 397-408.

Ledgard, N. 2001. The spread of lodgepole pine (*Pinus contorta*, Dougl.) in New Zealand. *For. Ecol. Manage.* **141**: 43–57.

Leu, M., S.E. Hanser, and S.T. Knick. 2008. The human footprint in the west: A large-scale analysis of anthropogenic impacts. *Ecol. Appl.* **18**: 1119–1139.

Li, Y., X. Liu, X. Li, B. Petitpierre, and A. Guisan. 2014. Residence time, expansion toward the equator in the invaded range and native range size matter to climatic niche shifts in non-native species. *Glob. Ecol. Biogeogr.* **23**: 1094–1104.

Liaw, A. and M. Wiener. 2002. Classification and regression by randomForest. *R News* **2**: 18–22.

Locher-Krause, K.E., M. Volk, B. Waske, F. Thonfeld, and S. Lautenbach. 2017. Expanding temporal resolution in landscape transformations: Insights from a landsat-based case study in Southern Chile. *Ecol. Indic.* **75**: 132–144.

Loveland, T.R. and J.L. Dwyer. 2012. Landsat: Building a strong future. *Remote Sens. Environ.* **122**: 22–29.

Markham, B.L. and D.L. Helder. 2012. Forty-year calibrated record of earth-reflected radiance from Landsat: A review. *Remote Sens. Environ.* **122**: 30–40.

Martínez, B., F. Arenas, A. Trilla, R.M. Viejo, and F. Carreño. 2014. Combining physiological threshold knowledge to species distribution models is key to improving forecasts of the future niche for macroalgae. *Glob. Chang. Biol.* **21**: 1422–1433.

Mead, D. 2013. Sustainable management of *Pinus radiata* plantations. *Food and agriculture organization of the United Nations (FAO)* Forestry Paper No. 170.

Meinke, C. 2004. Floristic provinces of sagebrush and associated shrub-steppe habitats in western North America. *Sagemap, U.S. Geological Survey.* Available at: http://sagemap.wr.usgs.gov.

Meinke, C.W., S.T. Knick, D.A. Pyke. 2009. A spatial model to prioritizesagebrush landscapes in the intermountain west (U.S.A.) for restoration. *Restor. Ecol.* **17**: 652–659.

Menne, M.J., I. Durre, R.S. Vose, B.E. Gleason, and T.G. Houston. 2012. An overview of the global historical climatology network-daily database. *J. Atmos. Ocean. Technol.* **29**: 897–910.

Mitchell, A. 2005. The ESRI Guide to GIS Analysis, Volume 2: Spatial Measurements and statistics. *ESRI Press*.

Molina-Montenegro, M.A. and D.E. Naya. 2012. Latitudinal patterns in phenotypic plasticity and fitness-related traits: Assessing the climatic variability hypothesis (CVH) with an invasive plant species. PLoS One 7: e47620.

Moody, M.E., and R.N. Mack. 1988. Controlling the spread of plant invasions: The importance of nascent foci. *Source J. Appl. Ecol. J. Appl. Ecol.* **25**: 1009–1021.

Moritz, C., J.L. Patton, C.J. Conroy, J.L. Parra, G.C. White, and S.R. Beissinger. 2008. Impact of a century of climate change on small-mammal communities in Yosemite National Park, USA. *Science* **322**: 261–264.

Mullican, T.R. and B.L. Keller. 1986. Ecology of the sagebrush vole (*Lemmiscus curtatus*) in southeastern Idaho. *Can. J. Zool.* **64**: 1218–1223.

Mullican, T.R. and B.L. Keller. 1987. Burrows of the sagebrush vole (*Lemmiscus curtatus*) in southeastern Idaho. *Gt. Basin Nat.* **47**: 276–279.

Mundt, J.T., D.R. Streutker, and N.F. Glenn. 2006. Mapping sagebrush distribution using fusion of hyperspectral and Lidar classifications. *Photogramm. Eng. Remote Sens.* **72**: 47–54.

Nahuelhual, L., A. Carmona, L. Antonio, C. Echeverría, and M.E. González. 2012. Land-cover change to forest plantations: Proximate causes and implications for the landscape in south-central Chile. *Landsc. Urban Plan.* **107**: 12–20.

Nielsen, S.E., C.L. Aldridge, S.E. Hanser, M. Leu, and S.T. Knick. 2011. Occurrence of non-native invasive plants: The role of anthropogenic features. - In: Hanser, S.E., M. Leu, S.T. Knick, and C.L. Aldridge (eds), *Sagebrush Ecosystem Conservation and Management: Ecoregional Assessment Tools and Models for the Wyoming Basins.* Allen Press, pp. 357–386.

Nielson, R.P., J.M. Lenihan, D. Bachelet, R.J. Drapek. 2005. Climate change implications for sagebrush ecosystems. Transactions of the 70th North American Wildlife and Natural Resources Conference. p. 145–159.

Nuñez, M.A. and R. Estela. 2007. Afforestation causes changes in post-fire regeneration in native shrubland of Patagonia, Argentina. *J. Veg. Sci.* **18**: 827–834.

Paritsis, J. and M.A. Aizen. 2008. Effects of exotic conifer plantations on the biodiversity of understory plants, epigeal beetles and birds in *Nothofagus dombeyi* forests. *For. Ecol. Manage.* **255**: 1575–1583.

Paritsis, J., J.B. Landesmann, T. Kitzberger, F. Tiribelli, Y. Sasal, C. Quintero, R.D. Dimarco, M.N. Barrios-García, A.L. Iglesias, J.P. Diez, M. Sarasola, and M.A. Nuñez. 2018. Pine plantations and invasion alter fuel structure and potential fire behavior in a Patagonian forest-steppe ecotone. *Forests* **9**: 117-133.

Pauchard, A., A. Escudero, R.A. García, M. de la Cruz, B. Langdon, L.A. Cavieres, and J. Esquivel. 2016. Pine invasions in treeless environments: dispersal overruns microsite heterogeneity. *Ecol. Evol.* **6**: 447–459.

Pearce, J. and S. Ferrier. 2001. The practical value of modelling relative abundance of species for regional conservation planning: a case study. *Biol. Conserv.* **98**: 33–43.

Pearson, R.G., C.J. Raxworthy, M. Nakamura, and A. Townsend Peterson. 2007. Predicting species distributions from small numbers of occurrence records: a test case using cryptic geckos in Madagascar. *J. Biogeogr.* **34**: 102–117.

Peña, E., M. Hidalgo, B. Langdon, and A. Pauchard. 2008. Patterns of spread of *Pinus contorta* Dougl. ex Loud. invasion in a natural reserve in southern South America. *For. Ecol. Manage.* **256**: 1049–1054.

Perry, A.L., P.J. Low, J.R. Ellis, and J.D. Reynolds. 2005. Climate change and distribution shifts in marine fishes. *Science*. **308**: 1912–1915.

Petersen, K.L. and L.B. Best. 1985a. Brewer's Sparrow Nest-Site Characteristics in a Sagebrush Community. *J. F. Ornithol.* **56**: 23–27.

Petersen, K.L. and L.B. Best. 1985b. Nest-Site Selection by Sage Sparrows. *Condor*. **87**: 217-221.

Peterson, E.B. 2006. A map of invasive annual grasses in Nevada derived from multitemporal Landsat 5 TM imagery. *Report for the USDI Bureau of Land Management.* Nevada State Office, Reno, Nevada Natural Heritage Program.

Procheş, Ş., J.R.U. Wilson, D.M. Richardson, and M. Rejmánek. 2012. Native and naturalized range size in Pinus: relative importance of biogeography, introduction effort and species traits. *Glob. Ecol. Biogeogr.* **21**: 513–523.

Pryke, J.S. and M.J. Samways. 2009. Recovery of invertebrate diversity in a rehabilitated city landscape mosaic in the heart of a biodiversity hotspot. *Landsc. Urban Plan.* **93**: 54–62.

QGIS Developmet Team. 2018. QGIS Geographic Information System. - Open Source Geospatial Foundation Project. Available: http://qgis.osgeo.org.

Reeder, S.A. and D.R. Reeder. 2005. Sagebrusg Vole (*Lemmiscus curtatus*). In: *Colorado sagebrush: a conservation assessment and strategy.* Colorado Division of Wildlife, pp. A82–A90.

Renwick, K.M., C.A. Curtis, A.R. Kleinhesselink, D. Schlaepfer, B.A. Bradley, C.L. Aldridge, B. Poulter, and P.B. Adler. 2018. Multi-model comparison highlights consistency in predicted effect of warming on a semi-arid shrub. *Glob. Chang. Biol.* **24**: 424–438.

Reynolds, J.F., R.A. Virginia, P.R. Kemp, A.G. De Soyza, and D.C. Tremmel. 1999. Impact of drought on desert shrubs: effects of seasonality and degree of resource island development. *Ecol. Monogr.* **69**: 69–106.

Rich, T. 1980. Nest placement in Sage thrashers, Sage sparrows, and Brewer's sparrows. *Wilson Bull.* **92**: 362–368.

Richardson, D.M. and W.J. Bond. 1991. Determinants of plant distribution: evidence from pine invasions. *Am. Nat.* **137**: 639–668.

Richardson, D.M., P.A. Williams, R.J. Hobbs. 1994. Pine Invasions in the Southern Hemisphere: Determinants of spread and invadability. *J. Biogeogr.* **21**: 511–527.

Richardson, D.M., B.W. van Wilgen, and M.A. Nunez. 2008. Alien conifer invasions in South America: short fuse burning? *Biol. Invasions* **10**: 573–577.

Richardson, D.M., C. Hui, M.A. Nunez, and A. Pauchard. 2013. Tree invasions: patterns, processes, challenges and opportunities. *Biol. Invasions* **16**: 473–481.

Robson, T.C., A.C. Baker, B.R. Murray. 2009. Differences in leaf-litter invertebrate assemblages between radiata pine plantations and neighboring native eucalypt woodland. *Austral Ecol.* **34**: 368–376.

Rollins, M.G. 2009. LANDFIRE: A nationally consistent vegetation, wildland fire, and fuel assessment. *Int. J. Wildl. Fire* **18**: 235–249.

Roughgarden, J. 1972. Evolution of niche width. *Am. Nat.* **106**: 683–718.

Rowland, M.M., M.J. Wisdom, L.H. Suring, and C.W. Meinke. 2006. Greater sage-grouse as an umbrella species for sagebrush-associated vertebrates. *Biol. Conserv.* **129**: 323–335.

Rowland, M.M., L.H. Suring, M. Leu, S.T. Knick, and M.J. Wisdom. 2011. Sagebrush-associated species of conservation concern. In: Hanser, S.E., M. Leu, S.T. Knick, and C.L. Aldridge (eds), *Sagebrush Ecosystem Conservation and Management: Ecoregional Assessment Tools and Models for the Wyoming Basins.* Allen Press, Lawrence, KS, USA. p. 46–68.

Rupp, D.E., J.T. Abatzoglou, K.C. Hegewisch, and P.W. Mote. 2013. Evaluation of CMIP5 20th century climate simulations for the Pacific Northwest USA. *J Geophys Res Atmos.* **118**: 10884-10906.

Salas, C., P.J. Donoso, R. Vargas, C.A. Arriagada, R. Pedraza, and D.P. Soto. 2016. The Forest Sector in Chile: An Overview and Current Challenges. *J. For.* **114**: 562–571.

Salo, L.F. 2004. Population dynamics of red brome (*Bromus madritensis* subsp. *rubens*): times for concern, opportunities for management. *J. Arid Environ.* **57**: 291–296.

Schlaepfer, D.R., W.K. Lauenroth, and J.B. Bradford. 2012. Effects of ecohydrological variables on current and future ranges, local suitability patterns, and model accuracy in big sagebrush. *Ecography*. **35**: 374–384.

Scholes, M. and T. Nowicki. 1998. Effects of pines on soil properties and processes. In: Richardson, D.M. (ed), Ecology and Biogeography of *Pinus*. Cambridge University Press, pp. 341–350.

Schulz, J.J., L. Cayuela., C. Echeverria, J. Salas, and J.M.R. Benayas. 2010. Monitoring land cover change of the dryland forest landscape of Central Chile (1975–2008). *Appl. Geogr*. **30**: 436–447.

Simberloff, D., M.A. Nunez, N.J. Ledgard, A. Pauchard, D.M. Richardson, A. Sarasola, B.W. Van Wilgen, S.M. Zalba, R.D. Zenni, R. Bustamante, and E. Peña. 2009. Spread and impact of introduced conifers in South America: Lessons from other southern hemisphere regions. *Austral Ecol.* **35**: 489–504.

Soberón, J. 2007. Grinnellian and Eltonian niches and geographic distributions of species. *Ecol. Lett.* **10**: 1115–1123.

Still, S.M. and B.A. Richardson. 2015. Projections of contemporary and future climate niche for Wyoming big sagebrush (*Artemisia tridentata* subsp. *wyomingensis*): A Guide for restoration. *Nat. Areas Assoc.* **35**: 30–43.

Strubbe, D., O. Broennimann, F. Chiron, and E. Matthysen. et al. 2013. Niche conservatism in non-native birds in Europe: Niche unfilling rather than niche expansion. *Glob. Ecol. Biogeogr.* **22**: 962–970.

Suazo, A.A., J.E. Spencer, E.C. Engel, S.R. Abella. 2012. Responses of native and non-native Mojave Desert winter annuals to soil disturbance and water additions. *Biol. Invasions*. **14**: 215–227.

Sunday, J.M., G.T. Pecl, S. Frusher, A.J. Hobday, N. Hill, N.J. Holbrook, G.J. Edgar, R. Stuart-Smith, N. Barrett, T. Wernberg, R.A. Watson. 2015. Species traits and climate velocity explain geographic range shifts in an ocean-warming hotspot. *Ecol. Lett.* **18**: 944–53.

Svenning, J.C. and F. Skov. 2004. Limited filling of the potential range in European tree species. *Ecol. Lett.* **7**: 565–573.

Taylor, K.T., B.D. Maxwell, A. Pauchard, M.A. Nuñez, D.A. Peltzer, A. Terwei, and L.J. Rew. 2015. Drivers of plant invasion vary globally: evidence from pine invasions within six ecoregions. *Glob. Ecol. Biogeogr.* **25**: 96-106.

Thomas, C.D., A. Cameron, R.E. Green, M. Bakkenes, L.J. Beaumont, Y.C. Collingham, B.F.N. Erasmus, M.F. De Siqueira, A. Grainger, L. Hannah, and L. Hughes. 2004. Extinction risk from climate change. *Nature* **427**: 145–8.

Thomson, J.L., T.S. Schaub, N.W. Culver, and P.C. Aengst. 2005. Wildlife at a Crossroads: energy development in western Wyoming. Effects of roads on habitat in the Upper Green River Valley. *The Wilderness Society*, Washington, DC.

Thornton, P.E., S.W. Running, and M.A. White. 1997. Generating surfaces of daily meteorological variables over large regions of complex terrain. *J. Hydrol.* **190**: 214–251.

Thuiller, W., D.M. Richardson, P. Pyšek, G.F. Midgley, G.O. Hughes, and M. Rouget. 2005. Niche-based modelling as a tool for predicting the risk of alien plant invasions at a global scale. *Glob. Chang. Biol.* **11**: 2234–2250.

Tingley, M.W., W.B. Monahan, S.R. Beissinger, and C. Moritz. 2009. Birds track their Grinnellian niche through a century of climate change. *Proc. Natl. Acad. Sci.* **106**: 19637–19643.

Tingley, R., M. Vallinoto, F. Sequeira, and M.R. Kearney. 2014. Realized niche shift during a global biological invasion. *PNAS*. **111**: 10233–10238.

Tomiolo, S., M.A. Harsch, R.P. Duncan, P.E. Hulme. 1960. Influence of climate and regeneration microsites on Pinus contorta invasion into an alpine ecosystem in New Zealand. *AIMS Environ. Sci.* **3**: 525–540.

Torchin, M.E., K.D. Lafferty, A.P. Dobson, V.J. McKenzie, and A.M. Kuris. 2003. Introduced species and their missing parasites. *Nature* **421**: 628–630.

USDA NRCS. 2018. The PLANTS Database (http://plants.usda.gov). National Plant Data Team, Greensboro, NC 27401-4901 USA.

Valladares, F., S. Matesanz, F. Guilhaumon, A.B. Araújo, L. Balaguer, M. Benito-Garazón, W. Cornwell, E. Gianoli, M. van Kleunen, D.E. Naya, and A.B. Nicotra. 2014. The effects of phenotypic plasticity and local adaptation on forecasts of species range shifts under climate change. *Ecol. Lett.* **17**: 1351–1364.

Van Lill, W.S., F.J. Kruger, and D.B. Van Wyk. 1980. The effect of afforestation with *Eucalyptus grandis* Hill ex Maiden and *Pinus patula* Schlecht. et Cham. on streamflow from experimental catchments at Mokobulaan, Transvaal. *J. Hydrol.* **48**: 107–118.

van Wilgen, B.W. and D.M. Richardson. 2012. Three centuries of managing introduced conifers in South Africa: Benefits, impacts, changing perceptions and conflict resolution. *J. Environ. Manage.* **106**: 56–68.

Van Wyk, D.B. 1987. Some effects of afforestation on streamflow in the Western Cape Province, South Africa. *Water SA* **14**: 31–36.

VanDerWal, J., L.P. Shoo, C.N. Johnson, and S.E. Williams. 2009. Abundance and the environmental niche: Environmental suitability estimated from niche models predicts the upper limit of local abundance. *Am. Nat.* **174**: 282–291.

Veblen, T.T., D.H. Ashton, F.M. Schlegel, and A.T. Veblen. 1977. Plant succession in a timberline depressed by vulcanism in South-Central Chile. *J. Biogeogr.* **4**: 275–294.

Veblen, T.T., T. Kitzberger, E. Raffaele, and D.C. Lorenz. 2003. Fire history and vegetation changes in northern Patagonia, Argentina. In: Veblen, T.T., W.L. Baker, G. Montenegro, and T.W. Swetnam (eds), *Fire and Climatic Change in Termperate Ecosystems of the Western Americas.* Springer, New York, NY, USA. p. 265–295.

Villagran, C. and L.F. Hinojosa. 1997. Historia de los bosques del sur de Sudamérica, II: Análisis fitogeográfico. *Rev. Chil. Hist. Nat.* **70**: 241–267.

Walston, L.J., B.L. Cantwell, and J.R. Krummel. 2009. Quantifying spatiotemporal changes in a sagebrush ecosystem in relation to energy development. *Ecography*. **32**: 943–952.

Weber, M.M., R.D. Stevens, J.A.F. Diniz-Filho, and C.E.V. Grelle. 2017. Is there a correlation between abundance and environmental suitability derived from ecological niche modelling? A meta-analysis. *Ecography*. **40**: 817–828.

Weltzin, J.F., M.E. Loik, S. Schwinning, D.G. Williams, P.A. Fay, B.M. Haddad, J. Harte, T.E. Huxman, A.K. Knapp, G. Lin, W.T. Pockmann, R.M. Shaw, E.E. Small, M.D. Smith, S.D. Smith, D.T. Tissue, and J.C. Zak. 2003. Assessing the response of terrestrial ecosystems to potential changes in precipitation. *Bioscience* **53**: 941–952.

Whisenant, S.G. 1990. Changing fire frequencies on Idaho's Snake River plains: ecological and management implications. In: McArthur, E.D., E.M. Romney, and S.D. Smith (eds), *Proceedings Symposium on cheatgrass invasion, shrub die-off, and other aspects of shrub biology and management.* Intermountain Research Station, p. 4–10.

Williams, M.C. and G.M. Wardle. 2005. The invasion of two native Eucalypt forests by *Pinus radiata* in the Blue Mountains, New South Wales, Australia. *Biol. Conserv.* **125**: 55–64.

Wisdom, M.J., M.M. Rowland, L.H. Suring, L. Schueck, C.W. Meinke, and S.T. Knick. 2005. Evaluating species of conservation concern at regional scales. - In: Wisdom, M.J., M.M. Rowland, and L.H. Suring (eds), H*abitat Threats in the Sagebrush Ecosystem: Methods of Regional Assessment and Applications in the Great Basin.* Alliance Communications Group, p. 5–74.

Wisz, M.S., R.J. Hijmans, J. Li, A.T. Peterson, C.H. Graham, and A. Guisan. 2008. Effects of sample size on the performance of species distribution models. *Divers. Distrib.* **14**: 763–773.

Yesson, C., P.W. Brewer, T. Sutton, N. Caithness, J.S. Pahwa, M. Burgess, W.A. Gray, R.J. White, A.C. Jones, F.A. Bisby, and A. Culham. 2007. How global is the global biodiversity information facility? *PLoS One* **2**: e1124.

Young, J.A. and R.A. Evans. 1978. Population dynamics after wildfires in sagebrush grasslands. *J. Range Manag.* **31**: 283-289.

Zamorano-Elgueta, C., J.M.R. Benayas, L. Cayuela, S. Hantsom, and D. Armenteras. 2015. Native forest replacement by exotic plantations in southern Chile (1985–2011) and partial compensation by natural regeneration. *For. Ecol. Manage.* **345**: 10–20.

Zhang, J., S.E. Nielsen, Y. Chen, D. Georges, Y. Qin, S.S. Wang, J.C. Svenning, and W. Thuiller. 2016. Extinction risk of North American seed plants elevated by climate and land-use change. *J. Appl. Ecol*. **54**: 303-312.

Zhu, Z. and C.E. Woodcock. 2014. Continuous Change Detection and Classification of land cover using all available Landsat data. *Remote Sens. Environ.* **144**: 152–171.

Zhu, Z., C.E. Woodcock, and P. Olofsson. 2012. Continuous monitoring of forest disturbance using all available Landsat imagery. *Remote Sens. Environ.* **122**: 75–91.